# A STUDY OF LATERAL CIRCULATION IN AN INLET

by

Neil John Campbell

---

A THESIS SUBMITTED IN PARTIAL FULFILMENT
OF THE REQUIREMENTS FOR THE DEGREE OF
DOCTOR OF PHILOSOPHY

in

PHYSICS

---

We accept this thesis as conforming to
the standard required from candidates
for the degree of DOCTOR OF PHILOSOPHY

Members of the Department of Physics

THE UNIVERSITY OF BRITISH COLUMBIA

December, 1954

ABSTRACT

On the thesis that the lateral frictional stresses should play an important part in determining the horizontal circulation in landlocked bodies of water, a mathematical model of the circulation in an inlet is developed. The circulation is described by a fourth order differential equation

$$\frac{\partial^4 \psi}{\partial x^4} + \frac{\partial^4 \psi}{\partial y^4} = 0$$

where $\psi$ is a stream function.
A solution representing a commonly observed circulation is obtained for a rectangular bay. The significance of Coriolian, frictional, and mass field forces in maintaining such a circulation is discussed.

The theoretical model is tested by means of data available for Burrard Inlet. The data indicate the existence of two net circulations, one at 50 feet which has been attributed to the tides, and the other at the surface which is influenced strongly by the influx of brackish water from the Fraser River. Relaxation methods are introduced to test the current fields for verification of the differential equation.

Despite the more complex boundaries of Burrard Inlet as compared with the rectangular bay investigation, the actual circulation in Burrard Inlet is found to satisfy the fourth order differential equation within the limit of observational error. This agreement suggests that the lateral frictional

stresses do play an important part in the circulation in inlets.

Further applications of relaxation methods are urged for oceanographic studies. Suggestions are made as to where oceanographic observations should be taken for a study of lateral circulations in inlets or bays.

The reasonable agreement of the mathematical model and prototype suggests that lateral effects can be described by the mathematical theory.

THE UNIVERSITY OF BRITISH COLUMBIA

Faculty of Graduate Studies

PROGRAMME OF THE

FINAL ORAL EXAMINATION FOR THE DEGREE

OF DOCTOR OF PHILOSOPHY

of

NEIL JOHN CAMPBELL

B. Sc. (McMaster) 1950
M. Sc. (McMaster) 1951

FRIDAY, JANUARY 7th, 1955 at 3:00 P.M.

IN ROOM 301, PHYSICS BUILDING

COMMITTEE IN CHARGE:
H.F. Angus, Chairman

| | |
|---|---|
| A.R. Clark | W.M. Cameron |
| F.H. Kaempffer | J.R. Mackay |
| G.L. Pickard | M. Kirsch |
| G.M. Shrum | J.L. Robinson |

External Examiner - M. Rattray
University of Washington

# A STUDY OF LATERAL CIRCULATION IN AN INLET


## Abstract

On the thesis that lateral frictional stresses play an important part in determining the horizontal circulation in landlocked bodies of water, a mathematical model of the circulation in an inlet is developed. The circulation is described by a fourth order differential equation. A solution representing a commonly observed circulation is obtained for a rectangular inlet.

The theoretical model is tested by means of data available for Burrard Inlet. The data indicate the existence of two net circulations, one at 50 feet which has been attributed to the tides and the other at the surface which is controlled mainly by the influx of brackish water from the Fraser River.

Relaxation methods are introduced to test the current fields for verification of the differential equation. Despite the complex boundaries of Burrard Inlet as compared with the rectangular model, the actual circulation is found to satisfy the equation. This agreement suggests that the lateral frictional stresses play an important part in the circulation in an inlet.

# GRADUATE STUDIES

Field of Study: Physics

| | |
|---|---|
| Nuclear Physics | M.W. Johns and F. Gulbis |
| Atomic and Molecular Spectroscopy | A.B. McLay |
| Theory of Measurement | A.M. Crooker |
| Quantum Mechanics | A.J. Dekker |
| Dynamic Oceanography | G.L. Pickard |
| Fluid Mechanics | G.L. Pickard |
| Waves and Tides | G.L. Pickard |
| Geophysics | A.R. Clark |

Other Studies:

| | |
|---|---|
| Chemical Oceanography | J.P. Tully |
| Synoptic Oceanography | W.M. Cameron |
| Biological Oceanography | W.M. Cameron |
| Differential Equations | T.E. Hull |

## ACKNOWLEDGMENTS

The author would like to express his gratitude to: Dr. W.A. Clemens for extending the facilities of the Institute of Oceanography and for his sympathetic interest in this work, Dr. G.L. Pickard under whose direction and encouragement this investigation was carried out, Dr. W.A. Cameron for his much helpful advice and criticism during the progress of this work, Mr. R.F. Hooley, Department of Civil Engineering, and to his fellow graduate students, particularly Mr. R.W. Trites, and finally to the Defence Research Board of Canada for the financial assistance which enabled this work to be undertaken.

. . .

TABLE OF CONTENTS

TABLE OF CONTENTS (Continued)



. . .

## LIST OF FIGURES

## LIST OF FIGURES (Continued)

## LIST OF FIGURES (Continued)



. . .

# I. INTRODUCTION

One aspect of oceanographic research which has been particularly active in recent years has been the study of estuarine circulation. An estuary may be defined as a semi-enclosed coastal body of water having a free connection with the open sea and containing a measurable quantity of sea salt (1). Oceanographic investigations on the Canadian West Coast have been focussed primarily on the problems of coastal oceanography. As part of this programme the University of British Columbia has carried out extensive oceanographic surveys of the British Columbia inlets, which are estuaries within the above definition.

In conjunction with the studies of estuarine circulation a number of theoretical models have been proposed to explain some of the physical problems of mixing and dynamics of inlet circulation.

## Classification of Estuaries

Recent studies have brought forth a number of new concepts in estuarine problems. Some of these advances apply to all estuaries, but at the same time many differences have appeared. In order to compare phenomena it is necessary to classify estuaries in terms of fresh water inflow, evaporation, and geomorphology.

Estuaries in which the fresh water drainage exceeds the evaporation have been termed "positive" estuaries. For those in which evaporation exceeds the land drainage and rainfall the term "inverse" estuary has been applied. A third group, termed "neutral estuaries", exists in which neither of the above mentioned processes dominate. Only the "positive type" estuary will be considered further.

Geomorphic differences in structure have led to three further classifications of inlets: coastal plain, fiord, and bar-built estuaries. Coastal plain estuaries characterize most of the larger inlets on the East Coast. They are the result of subsidence of the land or rise of sea level. These estuaries are usually long and shallow and exhibit a dendritic pattern. The glacial cut fiords found in British Columbia and Norway are typified by their extreme length, depth, and steep sides. Bar-built estuaries are formed by the development of an offshore bar with a small channel connecting the basin with the open sea. They are generally located off shore-lines of low relief and shallow water.

Particular attention has been directed toward a study of coastal plain estuaries and the fiords of this continent. The oceanography of Chesapeake Bay, a typical coastal plain estuary, has been described by Pritchard (2), who has stressed the mechanism of a salt balance in that estuary.

Alberni Inlet in Vancouver Island has been described by Tully (3), and recent investigations of several inlets on the British Columbia mainland have been reported by Pick-

ard (4).

Cameron (5) and Stommel (6) have proposed theoretical models of the circulation of a fiord estuary.

## Coastal Plain Estuaries

The oceanographic observations in Chesapeake Bay and its tributary estuaries, carried out by Pritchard, permitted a quantitative study of the physical structure and circulation in the inlet. It is a two layer system; the deep zone of high salinity water has a net motion up the estuary, while the upper zone containing appreciable quantities of fresh water has a net seaward flow. For a steady state the transport of fresh water in the upper zone is equal to the fresh water inflow, and since the salinity of this layer increases to the seaward, a net upward transfer of salt takes place from below.

Pritchard considered the factors controlling the dynamics and salt balance in coastal plain estuaries from a semi-empirical study. He employed as complete a set of equations as possible and used field data to evaluate the significance of the measurable quantities.

He assumed that a steady state existed in regard to a time mean taken over one or more tidal cycles. The instantaneous velocity and salinity terms were replaced by the sum of a mean and random velocity, and mean and random salinity respectively. Terms involving the products of the instantaneous velocities represent the Reynold's or eddy stresses. In oceanography they have been generally replaced by frictional

terms involving an eddy coefficient and the gradient of the mean velocity.

The transverse gradient in salinity and slope of the surface of no net motion suggested that the Coriolis and transverse pressure forces were substantially balanced. Extensive measurements at three cross-sections in the James River estuary indicated that more than 75% of the Coriolis force, related to the mean longitudinal motion, was balanced by the mean transverse pressure gradient. The remaining part of this pressure gradient was associated with the gradient of the lateral component of the eddy stress. The eddy stress components appeared to be related to the tidal velocities.

The entrainment of salt in the upper layer and the processes involved in the exchange of fresh and salt water were also examined by Pritchard. Sufficient measurements were taken to evaluate the significance of the terms involved in these processes.

The mean local change of salt concentration is a function of the mean advection of the mean salt concentration and random flux which is generally termed eddy diffusion in oceanography. Pritchard found that the most important contributions to the control of fresh and salt water distribution arose from the mean longitudinal advection and the vertical random flux of salt. This latter process appeared to be related to the instantaneous tidal velocities rather than to the mean velocities.

## The Fiord Estuaries

The water structure of a fiord differs from that of a coastal plain estuary in that three distinct zones may be recognized rather than two. The upper and middle zones correspond to the upper and lower zones of the two-layered system where exchange processes take place. The deep zone has been considered as playing a relatively inactive role in the dynamics of fiord circulation (3). Recent observations, however, indicate the existence of substantial currents in this zone (4 II).

The dynamics of a typical fiord inlet have been investigated theoretically by Cameron who considered a two dimensional model with lateral homogeneity. He combined the horizontal and vertical components of the equation of motion for a steady state. A particular feature of his study was the retention of the non-linear field acceleration terms. The inclusion of these terms permitted a study of the influence of field accelerations in the circulation and led to the important concept of a critical or upper limiting velocity in an inlet.

The existence of a fresh water source in his model introduces the principle of continuity of fresh water transport and at the same time, the principle of continuity of salt. Both of these principles were satisfied by Cameron's model.

The field acceleration terms are required to maintain a constant fresh water transport. If there is a decrease of fresh water concentration down the inlet then an

acceleration of the surface water is required to assure the constancy of fresh water transport. Since the pressure gradients are associated with the fresh water distribution they have to be just sufficient to accelerate or decelerate the flow, as the case may be, in order to maintain continuity.

Cameron's model closely resembles the mean state in Alberni Inlet. The velocity field was in accordance with the actual mass field in the inlet.

Stommel has also treated a simple two dimensional steady state model of a deep fiord. He considers a two layer system in which the upper layer is brackish water with the density increasing seaward. The lower layer consists of undiluted sea water of constant density throughout the inlet. Exchange processes across the interface are permitted only in the upward direction.

He develops several relationships involving the vertical velocity of mixing of deep water into the upper layer, the thickness of this upper layer, and the density of the two layers.

Stommel's model also predicts a critical velocity at which the model breaks down. He points out that this phenomenon occurs when the velocity of the upper layer is just equal to the velocity of an internal wave at the interface.

The horizontal distribution of density calculated from Stommel's model agrees very closely with that found in Alberni Inlet. His treatment, however, does not take into account the vertical distribution of density as in Cameron's study.

Both models were compared with Alberni Inlet and the agreement found supports the reasonableness of the assumptions. Although basic differences exist between the hypotheses, similar results were obtained. Both solutions led to the novel concept of a limiting velocity at the mouth.

All these investigations have dealt with two dimensional models in the vertical longitudinal plane. Cameron and Stommel were forced to assume lateral homogeneity in their models to avoid mathematical complications. Pritchard's study of a coastal plain estuary involved measurements of salinity and currents in transverse sections. It was designed principally for an investigation of the longitudinal velocity.

Marked lateral differences in mass distribution and currents have been noted in various inlets on the West Coast and elsewhere (2) (5). These observations suggest that the effects of side boundaries, horizontal differences in salinity, and shearing stresses are frequently of such magnitude that they cannot be ignored.

The present thesis is a contribution to the descriptive and theoretical knowledge of estuarine oceanography. It introduces a mathematical model to study some of these lateral effects. It includes a lateral salt balance condition, and employs the use of relaxation methods to test a fourth order differential equation derived from the equations of motion. Two solutions are presented, one representing a solution to the net tidal circulation and another associated with a variation of the mass field.

## II. THE DIFFERENTIAL EQUATIONS OF MOTION

Let the inlet be a semi-enclosed embayment with approximately uniform horizontal dimensions and open to the sea. The origin of the left-handed coordinate system will be taken at the head with the y axis directed seaward along the length and the x axis across the inlet. The z axis will be positive downward and reckoned from a level surface approximating the sea surface.

Consider a steady state condition in which the vertical velocity and the inertial terms are neglected. The motion is then described by the following system of differential equations:

$$\frac{\partial}{\partial x}\left(A_x \frac{\partial u}{\partial x}\right) + \frac{\partial}{\partial y}\left(A_y \frac{\partial u}{\partial y}\right) + \frac{\partial}{\partial z}\left(A_z \frac{\partial u}{\partial z}\right) + c\rho v = \frac{\partial p}{\partial x}, \quad \text{a}$$

and (1)

$$\frac{\partial}{\partial x}\left(A_x \frac{\partial v}{\partial x}\right) + \frac{\partial}{\partial y}\left(A_y \frac{\partial v}{\partial y}\right) + \frac{\partial}{\partial z}\left(A_z \frac{\partial v}{\partial z}\right) - c\rho u = \frac{\partial p}{\partial y}, \quad \text{b}$$

together with the steady state equation of continuity of mass

$$\frac{\partial}{\partial x}(\rho u) + \frac{\partial}{\partial y}(\rho v) = 0. \tag{2}$$

In equations (1a,b) u and v denote the horizontal velocity components in the x and y directions, p is the pressure, $\rho$ is the density, and $c = 2w \sin \upsilon$, the Coriolis parameter, $A_x$, $A_y$, and $A_z$ are the dynamic eddy coefficients

of viscosity associated with the turbulent character of large scale flows. In accordance with the usual practice it will be assumed that the eddy coefficients associated with horizontal shear ($A_x$ and $A_y$) are equal. It will be further assumed that they are independent of position, $A_x$ and $A_y$ will then be replaced by $A_1$. The coefficient associated with the vertical shear, $A_z$, will be assumed to be a function of z.

Integrating these equations vertically from the surface of the sea to a depth h of no motion, where the stresses vanish, and assuming that the hydrostatic equation holds equations (1a,b) become

$$A_1\left(\frac{\partial^2 S_x}{\partial x^2} + \frac{\partial^2 S_x}{\partial y^2}\right) + T_x + c\bar{\rho} S_y = g\frac{\partial Q}{\partial x}, \quad \text{a}$$

and (3)

$$A_1\left(\frac{\partial^2 S_y}{\partial x^2} + \frac{\partial^2 S_y}{\partial y^2}\right) + T_y - c\bar{\rho} S_x = g\frac{\partial Q}{\partial y}, \quad \text{b}$$

where $\bar{\rho}$ is the mean density of the water.

The stresses $\left(A_z\frac{\partial u}{\partial z}\right)_{sfc.}$ and $\left(A_z\frac{\partial v}{\partial z}\right)_{sfc.}$ have been equated to the components $T_x$ and $T_y$ of the wind stress at the surface while $\left(A_z\frac{\partial u}{\partial z}\right)_h$ and $\left(A_z\frac{\partial v}{\partial z}\right)_h$ are zero since h is a depth of no motion.

The quantities $S_x$ and $S_y$ are the components of total volume flow:

$$S_x = \int_{sfc.}^{h} u\,dz \quad \text{and} \quad S_y = \int_{sfc.}^{h} v\,dz, \qquad (4)$$

and the quantity Q is related to the density by the expression

$$Q = \int_{Sfc.}^{h} dz \int_{Sfc.}^{z} \rho \, dz \, . \tag{5}$$

The equation of continuity of mass transport is approximately

$$\frac{\partial}{\partial x}\left(\bar{\rho} S_x\right) + \frac{\partial}{\partial y}\left(\bar{\rho} S_y\right) = 0 . \tag{6}$$

Since the variation of $\bar{\rho}$ is small in the x and y direction as compared with the variations in $S_x$ and $S_y$ then for practical purposes

$$\frac{\partial S_x}{\partial x} + \frac{\partial S_y}{\partial y} = 0 . \tag{7}$$

Eliminating the quantities $\frac{\partial Q}{\partial x}$ and $\frac{\partial Q}{\partial y}$ from equations (3a,b) by cross-differentiation and subtraction, one obtains the equation

$$\left(\frac{\partial^2}{\partial x^2} + \frac{\partial^2}{\partial y^2}\right)\left(\frac{\partial S_y}{\partial x} - \frac{\partial S_x}{\partial y}\right) = -\left(\frac{\partial T_y}{\partial x} - \frac{\partial T_x}{\partial y}\right)\Big/ A_1 . \tag{8}$$

Let $\psi(xy)$ be a transport stream function related to the components of transport by the equations

$$S_x = -\frac{\partial \psi}{\partial y} \qquad \text{and} \qquad S_y = \frac{\partial \psi}{\partial x} . \tag{9}$$

Substituting in equation (8) one obtains

$$\frac{\partial^4 \psi}{\partial x^4} + 2\frac{\partial^4 \psi}{\partial x^2 \partial y^2} + \frac{\partial^4 \psi}{\partial y^4} = -\left(\frac{\partial T_y}{\partial x} - \frac{\partial T_x}{\partial y}\right)\Big/ A_1 , \qquad (10)$$

where the three terms on the left-hand side comprise the biharmonic function; the term on the right-hand side is the vertical component of the curl of the wind stress.

This equation is formally the same as the equation governing the bending of a plate under the action of external forces. It is similar to that derived by Shtokman (7) (8). It was treated by Munk (9) who included the planetary vorticity term or rate of change of the Coriolis parameter with latitude. Munk solved this equation and introduced the actual wind stress for the Atlantic and for the Pacific Oceans. His solution accounted for many of the gross features of the general ocean circulation. However, the treatment did not include a study of the forces associated with the distribution of mass in the ocean. These forces are relatively more important in coastal regions where there is significant dilution of sea water by river discharge.

Another feature of coastal circulation which should be taken into account are the tidal currents which can give rise to a net flow in an inlet.

It is known from physical observations that circulations exist in inlets and bays even in the absence of the wind stress. Assuming also that the middle term of the biharmonic

equation is small, equation (10) then reduces to a homogeneous equation

$$\frac{\partial^4 \psi}{\partial x^4} + \frac{\partial^4 \psi}{\partial y^4} = 0 . \qquad (11)$$

The vertically integrated equations of motion are now of the form:

$$A_l \frac{\partial^2 S_x}{\partial y^2} + c\bar{\rho} S_y = g \frac{\partial Q}{\partial x} \qquad \text{a}$$

and (12)

$$A_l \frac{\partial^2 S_y}{\partial x^2} - c\bar{\rho} S_x = g \frac{\partial Q}{\partial y} , \qquad \text{b}$$

or

$$-A_l \frac{\partial^3 \psi}{\partial y^3} + c\bar{\rho} \frac{\partial \psi}{\partial x} = g \frac{\partial Q}{\partial x} \qquad \text{a}$$

and (13)

$$A_l \frac{\partial^3 \psi}{\partial x^3} + c\bar{\rho} \frac{\partial \psi}{\partial y} = g \frac{\partial Q}{\partial y} . \qquad \text{b}$$

These equations show the relations between the gradients of the mass field and the frictional and Coriolian fields. Differentiating equations (12a) twice with respect to x and (12b) twice with respect to y and substituting in equations (12b) and (12a) one obtains

$$c\bar{\rho} S_y = g\frac{\partial Q}{\partial X} + \frac{A_t g}{c\bar{\rho}}\frac{\partial^3 Q}{\partial y^3} - \frac{A_t}{c\bar{\rho}}\frac{\partial^4 S_y}{\partial x^2 \partial y^2} \qquad \text{a}$$

and (14)

$$c\bar{\rho} S_x = -g\frac{\partial Q}{\partial y} + \frac{A_t g}{c\bar{\rho}}\frac{\partial^3 Q}{\partial x^3} - \frac{A_t^2}{c\bar{\rho}}\frac{\partial^4 S_x}{\partial x^2 \partial y^2} . \qquad \text{b}$$

Cross differentiating equations (14a,b) and combining, it will be seen that the integrated mass field Q also satisfies the reduced biharmonic equation

$$\frac{\partial^4 Q}{\partial x^4} + \frac{\partial^4 Q}{\partial y^4} = 0. \qquad (15)$$

## III. MATHEMATICAL MODEL OF THE CIRCULATION IN A BAY

### The Transport Field

A special case of an inlet is a bay in which there is no fresh water source at the head. The mouth of the bay is presumed to adjoin the sea. The shorelines are assumed to be symmetrically straight and to extend parallel to each other for the full length of the bay. The origin of the coordinate system will be taken at the head of the bay with the y axis directed seaward and the x axis across the bay (figure i).

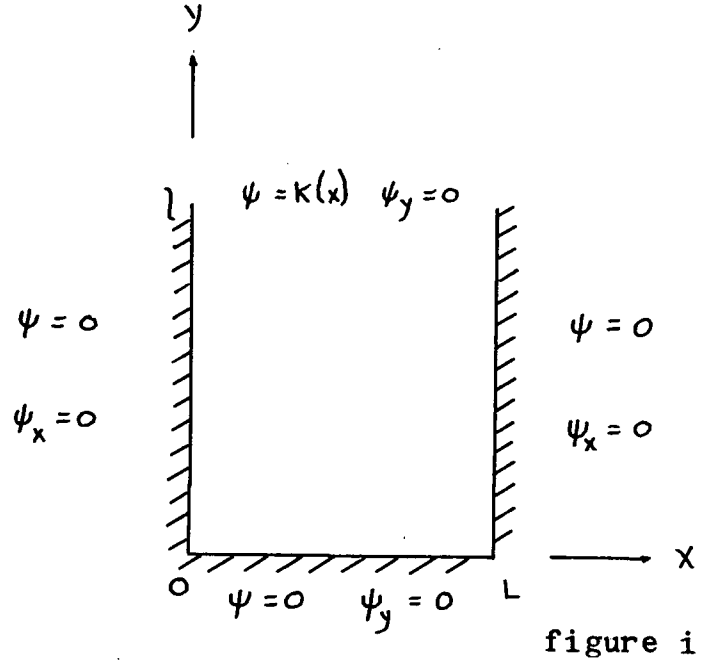


figure i

The equation

$$\frac{\partial^4 \psi}{\partial x^4} + \frac{\partial^4 \psi}{\partial y^4} = 0 \qquad (11)$$

is solvable by Fourier's method if the boundary conditions are known.

The boundary conditions for the sides and head of

the bay are

$$\psi_{bdry} = 0 \quad \text{and} \quad \frac{\partial \psi}{\partial n}_{bdry} = 0 , \tag{16}$$

The first equation states that the boundary itself is a streamline; the second equation states that no slip takes place at the boundary.

The boundary conditions for the figure are

at $x = 0$, $\psi = 0$ at $x = L$, $\psi = 0$

$$\frac{\partial \psi}{\partial x} = \psi_x = 0 , \qquad \frac{\partial \psi}{\partial x} = \psi_x = 0 ,$$

at $y = 0$, $\psi = 0$ and at $y = L$, $\psi = K(x)$

$$\frac{\partial \psi}{\partial y} = \psi_y = 0 , \qquad \frac{\partial \psi}{\partial y} = \psi_y = 0 .$$

The solution to equation (11) is expressed in a product form

$$\psi = X(x)\, Y(y), \tag{17}$$

where X(x) is a function of x alone and Y(y) is a function of y alone.

It can be shown that the product solutions are of the form

$$X_n = \left(\cos\lambda_n x - \cosh\lambda_n x\right)\left(\sin\lambda_n L - \sinh\lambda_n L\right) - \left(\sin\lambda_n x - \sinh\lambda_n x\right)\left(\cos\lambda_n L - \cosh\lambda_n L\right) \quad \text{a}$$

and (18)

$$Y_m = B_m\left(\cos\frac{\lambda_m y}{\sqrt{2}}\sinh\frac{\lambda_m y}{\sqrt{2}} - \sin\frac{\lambda_m y}{\sqrt{2}}\cosh\frac{\lambda_m y}{\sqrt{2}}\right) + C_m \sin\frac{\lambda_m y}{\sqrt{2}}\sinh\frac{\lambda_m y}{\sqrt{2}} , \quad \text{b}$$

where

$$C_m = 2B_m \frac{\sinh \frac{\lambda_m l}{\sqrt{2}}}{\cosh \frac{\lambda_m l}{\sqrt{2}}}, \qquad c$$

and $\lambda_n \simeq \frac{(2n+1)\pi}{2L}$ $n = 1, 2, 3, \cdots$ $\qquad \lambda_m \simeq \frac{(2m+1)\pi}{2L}$ $m = 1, 2, 3, \cdots$ d

Shtokman (8) p. 406.

$B_m$ can be evaluated if the function $\psi = K(x)$ is known at the mouth.

## The Transport Field

Let k(x) at the mouth be

$$K(x) = \left\{\left(\cos\frac{3\pi x}{2L} - \cosh\frac{3\pi x}{2L}\right)\left(\sin\frac{3\pi}{2} - \sinh\frac{3\pi}{2}\right) - \left(\sin\frac{3\pi x}{2L} - \sinh\frac{3\pi x}{2L}\right)\left(\cos\frac{3\pi}{2} - \cosh\frac{3\pi}{2}\right)\right\} \tag{19}$$

$$\left\{-\sin\frac{3\pi}{2\sqrt{2}}\cosh\frac{3\pi}{2\sqrt{2}} + 2\sin\frac{3\pi}{2\sqrt{2}}\sinh\frac{3\pi}{2\sqrt{2}}\right\}$$

which is the first term of the Fourier series of the product solution (11). This simple symmetric function of $\psi$ at the mouth is sufficient to demonstrate the applicability of the model. It yields a circulation which is of particular interest. Other solutions, and hence other circulations, are possible, but they are relatively ponderous and tedious to calculate. The form of $\psi$ and $\frac{\partial \psi}{\partial X}$ as evaluated at the mouth are shown in figures 1a,b. The transport field or circulation evaluated for the bay is shown in figure 2 where the length of the bay 1 has been taken as 1.41 times the width L. This ratio arises from the $\sqrt{2}$ in the denominator of the terms

comprising the Ym part of the product solution. The simplest case is that chosen. Other ratios are possible with correspondingly different values of Bm. However, the length to width ratio should be approximately unity in order to justify the assumption of equal horizontal eddy coefficients.

The direction of flow in figure 2 is determined by the relations

$$\zeta_x = -\frac{\partial \psi}{\partial y} \qquad \text{and} \qquad \zeta_y = \frac{\partial \psi}{\partial x} \tag{9}$$

The direction of flow may be reversed by changing the sign of Bm.

Two circulations are evident in figure 2, a deep penetration of water into the inlet on one side and a similar flow out on the other side. A large back eddy exists deep in the bay which is powered by lateral shear in the region between the two circulations. The largest transports per unit width occur at the mouth of the bay, and these decrease continuously toward the head.

Coriolian and Frictional Fields

From the equations

$$-A_1 \frac{\partial^3 \psi}{\partial y^3} + c\bar{\rho} \frac{\partial \psi}{\partial x} = g \frac{\partial Q}{\partial x} \qquad \text{a}$$

and (20)

$$A_1 \frac{\partial^3 \psi}{\partial x^3} + c\bar{\rho} \frac{\partial \psi}{\partial y} = g \frac{\partial Q}{\partial y} \qquad \text{b}$$

it is possible to determine the lateral distribution of the vertically integrated mass function Q where

$$Q = \int_{sfc.}^{h} dz \int_{sfc}^{z} \rho \, dz . \qquad (5)$$

Integration of either (20a) laterally or (20b) longitudinally will lead to the desired result. In each case two separate fields are obtained, one arising from the frictional term and the other from the Coriolian term. The sum of these fields yields the Q field if the value of the eddy coefficient, $A_1$, is known. Alternately if the Q field and the velocity field are known it is possible to evaluate $A_1$.

The Coriolian Field:

Consider the case of an established transport field defined by $\psi(xy)$ (figure 2). Neglecting the frictional forces, equation (20a) becomes

$$g \int_{o}^{x} \frac{\partial Q}{\partial x} dx = c\bar{\rho} \int_{o}^{x} \frac{\partial \psi}{\partial x} dx . \qquad (21)$$

After integration

$$g(Q - Q_{oy}) = c\bar{\rho}\psi , \qquad \text{a} \qquad (22)$$

and similarly from (20b) $\quad g(Q - Q_{xo}) = c\bar{\rho}\psi . \qquad \text{b}$

The mass field pattern will be similar to the transport field (figure 2). The above relation implies that in the absence of friction flow must take place along the lines of constant property. The $\psi$ field represents the Coriolian field whose direction and magnitude is given by the ascendant of $\psi$.

The Frictional Field:

By defining a function θ such that

$$\frac{\partial \theta}{\partial x} = - A_1 \frac{\partial^3 \psi}{\partial y^3}, \qquad \text{a}$$

and (23)

$$\frac{\partial \theta}{\partial y} = A_1 \frac{\partial^3 \psi}{\partial x^3}, \qquad \text{b}$$

we may plot a field (figure 3) analogous to the Coriolian field which will also describe the direction and magnitude of the frictional forces in the model.

The Coriolian field bears a simple relationship to the velocity, but the frictional field does not bear this simple relationship because the frictional forces can act in the direction of the flow as well as in the opposite direction.

The θ lines (figure 3) have the appearance of rectangular hyperbolae with the origin near the centre of the bay. At the boundary the lines are orthogonal to the streamline $\psi_{bdry} = o$. This characteristic arises from the second boundary condition $\frac{\partial \psi}{\partial n}_{bdry.} = o$ where n is normal to the boundary.

The direction in which the frictional forces are acting is along the ascendants of θ. These forces will be a maximum whose magnitude is determined by the rate of change θ. The frictional forces generally act in the opposite direction to that of the flow, except in the upper region of the gyral where they act in the same direction as the flow.

Thus when the flow is orthogonal to the θ lines

the frictional forces are large and the magnitude of these forces is determined by the rate of change of $\theta$. When the flow is not orthogonal to the $\theta$ lines then the frictional forces are smaller.

The Mass Field:

The mass field can be determined by adding algebraically the Coriolian and frictional fields. The forces associated with a distribution of mass must balance the Coriolian and frictional forces. Since the latter forces are directed along the ascendants of $\psi$ and $\theta$, the mass field forces must be directed along the gradients of Q.

$$g\frac{\partial Q}{\partial x} = c\bar{\rho}\frac{\partial \psi}{\partial x} + \frac{\partial \theta}{\partial x} \qquad \text{a}$$

$$\text{and similarly} \qquad g\frac{\partial Q}{\partial y} = c\bar{\rho}\frac{\partial \psi}{\partial y} + \frac{\partial \theta}{\partial y}, \qquad \text{b} \qquad (24)$$

$$\text{then} \qquad Q = \frac{1}{g}\left(c\bar{\rho}\psi + \theta\right). \qquad (25)$$

To effect the combination of the Coriolian and frictional field the eddy coefficient $A_1$ must be known. The normal practice in oceanography is to determine the mass field first, from which the eddy coefficient is estimated.

Pritchard examined the relationship between the mean transverse pressure force associated with a mass field and the horizontal component of the Coriolis force for three sections of the James River Estuary. His computations showed that the transverse pressure gradient was approximately 75%

of the Coriolis force, the remaining 25% was balanced by the frictional forces.

Assuming that a similar balance of pressure gradients and Coriolian forces could exist for the model, the frictional forces were evaluated to bring about a similar balance of forces. This was achieved by choosing an eddy coefficient $A_1 = 1 \times 10^5$ gm./cm./sec. for a bay of width 6.5 km. The two fields were combined to give the integrated mass field of figure 4. The field does not change significantly by varying the value of the eddy coefficient. The effect of using a slightly larger eddy coefficient, $A_1 = 2 \times 10^5$ gm./cm./sec., is shown in figure (5). (See note 1, page 23.)

The flow with respect to these fields is perpendicular or at some angle to the lines of constant property, the angle of intersection of the streamlines and Q lines increasing with larger values of $A_1$. The prominent features of each mass field are preserved in the two figures (4 and 5) with $A_1 = 1 \times 10^5$ and $2 \times 10^5$ gm./cm./sec. respectively. The central portion of each field has the basic character of the Coriolian field where this term is large. However, the whole field is warped by the presence of the frictional forces which have the effect of forcing the lines of constant property to intersect the boundaries.

The highest values of Q are found at the mouth on the side where the water enters the bay. From this region the field slopes asymmetrically downward to all sides. The flow of water at the mouth is from points of high Q to low Q or

down the sloping sea surface. Large values of Q correspond to regions in which there is a high concentration of brackish water and low values of Q to regions where there is more saline water.

The gyral centred deep in the bay is coupled to the circulation at the mouth by the lateral shearing stresses (per unit area) which are not zero between the two circulations. These forces are proportional to the second derivative of the stream function,

$$\Gamma_x = -A_l \frac{\partial^2 \psi}{\partial y^2} \qquad \text{a}$$

and

$$\Gamma_y = A_l \frac{\partial^2 \psi}{\partial x^2} . \qquad \text{b} \qquad (26)$$

The second of these terms, $\Gamma y$, is zero between the gyrals where v is zero, but $\Gamma x$ remains finite and becomes zero only at the centre of the gyral. The frictional forces (per unit volume), on the other hand, are zero between the two circulations since these forces are proportional to the third derivative of the stream function.

The flow of water in the gyral is down the sloping surfaces of the Q field (figures 4 and 5) and approximately Coriolian, but in order for the water to complete its path it must move up the sloping surfaces of Q at some other point. This movement of water is possible because the forces associated with lateral shear between the two gyrals are large enough to drive the water up the sloping sea surface.

The stream function $\psi$ and its relation to $S_x$ and $S_y$ in the model have been based on the assumption of steady

flow of an incompressible fluid

$$\frac{\partial S_x}{\partial x} + \frac{\partial S_y}{\partial y} = 0 . \qquad (7)$$

This relation considers only the continuity of volume, satisfaction of this condition can be seen from the transport field of figure 2. However, it does not follow that the principle of continuity of mass has been met. This condition will be examined in the next section.

Note 1.

The values of the eddy coefficients $A_1$, $1.0\text{-}2.0 \times 10^5$ gm./cm./sec., calculated for a rectangular inlet corresponding to the dimensions of Burrard Inlet compare favourably with those found in other regions. (Recent investigations of the ratio of $A_1$ to the dimensions of the body of water, McEwen 1950, indicate that this ratio is approximately 0.3-1.0. The ratio calculated for Burrard Inlet agrees with these results.)

McEwen, G.F. 1950. Trans. A.G.U. vol. 31, no. 1, p. 35.

## IV. CONTINUITY OF MASS

For an inlet it is permissible to neglect the influence of the small variation in temperature and to consider the density as simply a function of salinity so that continuity of mass and continuity of salt are synonymous.

The salinity is a function of x, y, z and t. The processes which maintain or tend to alter the distribution of salt in an inlet are advection and diffusion. For a stationary distribution of mass these processes are expressed mathematically by the equation

$$-\left\{\frac{\partial}{\partial x}(\rho u) + \frac{\partial}{\partial y}(\rho v) + \frac{\partial}{\partial z}(\rho w)\right\} - \frac{\partial}{\partial x}\langle\rho' u'\rangle - \frac{\partial}{\partial y}\langle\rho' v'\rangle - \frac{\partial}{\partial z}\langle\rho' w'\rangle = 0, \quad (27)$$

where $\rho$ and u, v, and w are the mean density and mean velocities; $\rho'$ and u', v', and w' are the variations from the mean. The products of the terms $\langle\rho' u'\rangle$ etc., are the eddy diffusion terms.

Integrating equation (27) first with respect to x across the inlet, the lateral diffusion and advection terms will drop out since there can be no diffusion or advection through the side boundaries. Similarly, the vertical diffusion and advection terms can be removed by integration from the surface (z = s) to the bottom (z = h), on the assumption that no vertical diffusion or advection takes place through the surface or the bottom.

Equation (27) becomes

$$-\int_{Sfc}^{h}\int_{o}^{L}\frac{\partial}{\partial y}(\rho v)\,dx\,dz \;-\int_{Sfc.}^{h}\int_{o}^{L}\frac{\partial}{\partial y}\langle\rho' v'\rangle\,dx\,dz = 0. \qquad (28)$$

This is an equation for the longitudinal advection and diffusion of salt. Let us first consider this equation at the mouth of the inlet and examine the mass transport through a transverse vertical section, assuming that in this region the longitudinal diffusion of salt is small.

Then at the mouth

$$\int_{Sfc.}^{h}\int_{o}^{L}\rho v\,dx\,dz = 0. \qquad (29)$$

Let the density $\rho$ be in the form

$$\rho = \rho_o + \Delta\rho, \qquad (30)$$

where $\rho_o$ is a constant and $\Delta\rho$ is an anomaly which may be a function of x, y and z. Equation (29) becomes

$$\rho_o\int_{Sfc}^{h}\int_{o}^{L}v\,dx\,dz + \int_{Sfc}^{h}\int_{o}^{L}\Delta\rho\, v\,dx\,dz = 0. \qquad (31)$$

Equating the first term of this equation to zero we have the continuity of volume equation which was considered in the circulation of a bay (section III). The second term equated to zero is the equation of continuity of mass anomaly. It remains to show that this equation can be satisfied

for the circulation in a bay.

Variations of density, along the length and width of an inlet, give rise to a system of forces capable of maintaining a lateral circulation. The magnitudes of these forces depend on the relative differences in density and are particularly large in the upper zone where appreciable quantities of brackish water exist owing to river run-off. The lateral differences in density can be studied by considering the non-integrated equations of motion.

The equations of horizontal motion including the assumptions made in section II, and still assuming that the hydrostatic equation holds, are

$$0 = -\frac{\partial p}{\partial x} + c\bar{\rho}v + A_l \frac{\partial^2 u}{\partial y^2}, \qquad \text{a}$$

$$0 = -\frac{\partial p}{\partial y} - c\bar{\rho}u + A_l \frac{\partial^2 v}{\partial x^2}, \qquad \text{b} \quad (32)$$

and

$$0 = -\frac{1}{\rho}\frac{\partial p}{\partial z} + g. \qquad \text{c}$$

where the effects of vertical stress are not being considered. To these must be added the equation of continuity of mass for a steady state.

$$\frac{\partial}{\partial x}(\rho u) + \frac{\partial}{\partial y}(\rho v) = 0. \qquad (33)$$

For an incompressible fluid

$$\frac{\partial u}{\partial x} + \frac{\partial v}{\partial y} = 0, \qquad (34)$$

and it is possible to define a stream function

$$u = -\frac{\partial \Psi}{\partial y} \quad \text{and} \quad v = \frac{\partial \Psi}{\partial x}. \tag{35 a,b}$$

The assumption of incompressibility requires that in equation (31) the term

$$\rho_o \int_{Sfc}^{h} \int_{o}^{L} v \, dx \, dz = 0, \tag{36}$$

and it remains to prove that

$$\int_{Sfc}^{h} \int_{o}^{L} \Delta\rho \, v \, dx \, dz = 0 \tag{37}$$

for a salt balance.

Cross-differentiating equations (32a,b) with respect to x and y, subtracting, and using equation (34) along with the relations (35a,b) we obtain

$$\frac{\partial^4 \Psi}{\partial x^4} + \frac{\partial^4 \Psi}{\partial y^4} = 0, \tag{38}$$

which is the same form as the equation derived in (section II). The solution will be of the form

$$\Psi = xy. \tag{39}$$

Using equations (30) and (35a,b) and differentiating (32a) with respect to z and (32c) with respect to x and bearing in mind that the product terms involving v and the derivative

of $\rho$ are small, then (32a) becomes

$$g\frac{\partial \Delta\rho}{\partial x} = c\bar{\rho}\frac{\partial^2 \Psi}{\partial x \partial z} - A_1\frac{\partial^4 \Psi}{\partial y^3 \partial z}, \tag{40}$$

$\Psi$ must also be a function of z. Let $\Psi$ be in the form of a product solution

$$\Psi = x\,y\,z, \tag{41}$$

satisfying equation (38).

Integrating equation (40) laterally one obtains

$$g(\Delta\rho - \Delta\rho_o) = c\bar{\rho}\frac{\partial \Psi}{\partial z} - A_1\int_o^x \frac{\partial^4 \Psi}{\partial y^3 \partial z}\,dx, \tag{42}$$

and equation (37) becomes

$$\int_{Sfc}^{h}\int_o^L \left\{\frac{c\bar{\rho}}{g}\frac{\partial \Psi}{\partial z} - \frac{A_1}{g}\int_o^x \frac{\partial^4 \Psi}{\partial y^3 \partial z}\,dx\right\} v\,dx\,dz = o, \tag{43}$$

or in terms of the product solution of (38) equation (43) becomes

$$\frac{c\bar{\rho}}{g}y^2\int_{Sfc.}^{h} z\,z'\,dz\int_o^L x\,x'\,dx - \frac{A_1}{g}y'''y\int_{Sfc.}^{h} z\,z'\,dz\int_o^L x'\,dx\int_o^x x\,dx = o. \tag{44}$$

This form of the steady state continuity of mass equation which is maintained by advective processes can be made zero by imposing restrictions on the vertically integrated term common to both parts of the equation.

Thus if

$$\int_{Sfc}^{h} Z Z' dz = 0 \qquad (45)$$

equation (44) has been satisfied. $\Delta\rho$ is a function of $Z'$ and the velocity is a function of $Z$. Then from equation (35b)

$$V = X' Y Z \qquad \text{a}$$

and from (40) (46)

$$\Delta\rho = X Y Z'. \qquad \text{b}$$

$X'Y$ and $XY$ are constant at any point in the inlet and for all practical purposes we can write

$$V = K_1 Z \qquad \text{a}$$

and

$$\Delta\rho = K_2 Z, \qquad \text{b} \qquad (47)$$

or

$$\Delta\rho = \frac{K_2}{K_1}\frac{\partial V}{\partial Z}, \qquad \text{c}$$

then (45) becomes

$$\frac{1}{K_1^2}\int_{Sfc}^{h} \frac{\partial V}{\partial Z} V dz = \frac{1}{2} V^2 \Big|_{Sfc}^{h} = 0, \qquad (48)$$

or

$$V_h^2 - V_{Sfc}^2 = 0.$$

This restriction on the velocities at the surface and the bottom appears too unreal and contributes no further limitation on the mass distribution.

The solution obtained for the mathematical model of a bay (section III) satisfied the principle of volume

continuity, but it did not necessarily follow that the solution would indicate a mass distribution maintained in the steady state by advective processes alone. The reason why this condition was not met follows from an examination of equation (44). The first term of this equation is zero since

$$\int_0^L XX' \, dx = \frac{X^2}{2}\Big|_0^L = 0, \tag{49}$$

where $X = 0$ on the lateral boundaries.

However, the second term of equation (44) is not identically zero. If this were the case then either $Y'''$ or $\int_0^L X' dx \int_0^x X dx$ would have to be zero everywhere. This would reduce the problem to a simple study of Coriolian flow.

A lateral salt balance for the model was achieved by incorporating the condition for a salt balance in one of the kinematic boundary conditions at the mouth. Thus if one assumes no friction at the mouth $Y'''$ is zero and a lateral salt balance exists through this cross-section. Elsewhere in the bay continuity demands that eddy diffusion participates in the maintenance of a salt balance. The assumption made to obtain continuity of salt is not unreal. Cameron's investigation of the dynamics of inlet circulations showed that the existence of a critical velocity at the mouth represented a solution to the equation of motion in the absence of friction satisfying the condition of a constant fresh water transport.

In this respect both theoretical models are similar although in this thesis the condition of no friction at the mouth must be introduced in the form of a boundary condition. It appears then that a more complete solution would have been realized if the field accelerative terms had been included in the initial equations (1a,b).

The assumption of no friction at the mouth implying Coriolian flow is based upon a study of Portland Canal by Cameron (10). He found that the mean transverse pressure distribution approximated that required for Coriolian flow. Therefore Coriolian flow at the mouth of the model inlet implies that a lateral salt balance exists.

## Transport and Mass Fields with a Salt Balance

Previously the boundary conditions assigned at the mouth were $\psi = K(x)$ and $\psi_y = 0$ which implies no cross-inlet flow (figure 2). The product solutions for the first term of the Fourier's series are

$$X = \left(\cos\lambda_1 x - \cosh\lambda_1 x\right)\left(\sin\lambda_1 L - \sinh\lambda_1 L\right) - \left(\sin\lambda_1 x - \sinh\lambda_1 x\right)\left(\cos\lambda_1 L - \cosh\lambda_1 L\right), \quad \text{a}$$

and (50)

$$Y = B_1\left(\cos\frac{\lambda_1 y}{\sqrt{2}}\sinh\frac{\lambda_1 y}{\sqrt{2}} - \sin\frac{\lambda_1 y}{\sqrt{2}}\cosh\frac{\lambda_1 y}{\sqrt{2}}\right) + C_1 \sin\frac{\lambda_1 y}{\sqrt{2}}\sinh\frac{\lambda_1 y}{\sqrt{2}}, \quad \text{b}$$

$$\text{where} \qquad C_1 = 2B_1 \frac{\sinh\frac{\lambda_1 l}{\sqrt{2}}}{\cosh\frac{\lambda_1 l}{\sqrt{2}}} . \quad \text{c}$$

With the salt balance condition $\frac{\partial^3 \Psi}{\partial y^3} = 0$ at the mouth the Y term becomes

$$Y_i = B_i \left( \cos\frac{\lambda_i y}{\sqrt{2}} \sinh\frac{\lambda_i y}{\sqrt{2}} - \sin\frac{\lambda_i y}{\sqrt{2}} \cosh\frac{\lambda_i y}{\sqrt{2}} \right). \qquad (51)$$

Evaluating these terms for the inlet, a solution representing the circulation in the bay was obtained (figure 6). The transport field (figure 6) thus satisfies the principles of volume continuity and mass continuity. It differs slightly from that first derived (figure 2). The depth of penetration into the bay is much less than in the previous case. At the same time the whole pattern of the circulation has contracted towards the mouth of the bay. Cross inlet flow can now exist at the mouth since $\frac{\partial \Psi}{\partial y} \neq 0$.

The frictional field (figure 7) satisfies the condition that it must be zero at the mouth. Consequently the $\theta$ lines intersect the side boundaries rather than cross the boundary at the mouth. High and low values of $\theta$ are therefore found inside the bay and near the boundaries.

The two frictional fields (figure 3 and figure 7) have several differences. The pattern of the frictional field associated with a salt balance is shifted slightly toward the head of the bay. The region where this field is a minimum is not between the two circulations as in the previous example, but rather is near the lower tip of the gyral.

Comparing the direction of the friction force with the direction of flow into the bay the frictional forces first

oppose the motion and then reverse. This effect is evident from figure 7 because the frictional forces are directed along the ascendants of $\theta$. The magnitude of the forces is determined by the rate of change of $\theta$.

The frictional forces also act in the same direction as the flow along the upper end of the gyral. Elsewhere in the circulation of the gyral they oppose the motion.

The circulation of the gyral (figure 6) is more pronounced than in the previous case (figure 2) indicating that the lateral stresses are more effective in maintaining the circulation.

The resultant mass field which is obtained by combining the Coriolian and frictional fields is shown in figure 8. The value of the eddy coefficient calculated for this example is $1.5 \times 10^5$ gm./cm./sec.

An interesting balance of the forces involved in the system is seen by considering the flow with respect to the mass field. The flow at the mouth is predominately Coriolian or along the lines of constant property. Elsewhere the flow is across the isopleths of the mass field. The distinction in these flows arises from the relative magnitudes of the Coriolian and frictional forces in balance with the pressure gradients. Cross isobaric flow occurs in regions where the frictional forces are dominant. This flow is generally down the sloping sea surfaces; the frictional forces are thus directed up the slopes. The only exception to this type of flow is in the gyral near the mouth where the flow

and direction of the frictional forces are the same.

There are regions in the mass field (figure 8) and the other two fields (figures 4, 5) where the Coriolian and frictional forces are in balance. Consequently the field is divided into regions where either one of the two forces dominates. The frictional forces are most conspicuous near the boundaries while the Coriolian force is dominant in the central area.

Summary from the Study of the Mathematical Models

The two simple models demonstrate how a lateral circulation can be maintained by a distribution of mass and the associated forces which balance the Coriolian and frictional forces. The mass fields require a source of fresh water at the mouth to maintain the proper pressure gradients needed for such circulations.

Commonly the inflow of fresh water occurs at the head of an inlet, and therefore, boundary conditions describing the discharge of a river would be required. This problem was considered for an inlet, but an additional complication arises with the boundary conditions at the head. Mathematically there is a wide choice of such functions describing a river flow, but these functions must represent physically acceptable flow conditions. This would require that the model also satisfy the principles of volume and salt continuity. Consequently, some relation must exist between the functions describing the circulation at the head and at the

mouth. In practice it would be necessary to determine these functions by physical measurements.

The development of the theory is sufficient to permit a comparison of the theoretical model with field observations in an appropriate inlet. Sufficient data for the fiord type of inlet are not yet available, but current observations and oceanographic data are available for Burrard Inlet. The inlet is approximately rectangular in shape (figures 9 and 10) corresponding to the mathematical model.

The place of the river at the head is taken by the First Narrows through which saline water flows periodically. This periodic flow results from the tide, the effects of which cause intense mixing of surface and deep water. The Fraser River supplies a large amount of fresh water at the mouth of the inlet.

Before a comparison can be made a study of the field data is necessary. These data will be considered in the next section.

## V. THE OCEANOGRAPHY OF BURRARD INLET

If the theoretical development and discussion of the mathematical model is to represent natural events in an inlet it is necessary to relate the unknown functions to the velocity measurements, and to compare the theoretical mass field with the actual distribution of salinity. The oceanographic observations would normally be carried out with a view to satisfying as many of these conditions as possible. The measurements, however, are frequently influenced by external factors, the most important of which are wind, tide, and river run-off.

During the Fall of 1949 and continuing until the early Spring of 1951 an extensive oceanographic survey of the Fraser River estuary was undertaken by the Pacific Oceanographic Group, Nanaimo, B.C. Their cruises included observations in Vancouver Harbour, Burrard Inlet, False Creek, and the Strait of Georgia from just south of Pt. Roberts to Bowen Island (figure 9). In 1950, in conjunction with these observations, the Canadian Hydrographic Service carried out a three months summer programme of current measurements in Burrard Inlet and Vancouver Harbour. Aerial photographic surveys of the inlet were made by the British Columbia Lands and Forests Department on June 1 and June 10, 1950. The photographs show marked differences in colour between the Fraser River water and Georgia Strait water.

The programme of investigation was stimulated by the Vancouver and Districts Joint Sewerage and Drainage Board to guide their proposed expansion of the sewage disposal system of Greater Vancouver. The current measurement phase was intended for the preparation of hourly current charts as an aid to mariners (11). The entire project was arranged so that seasonal changes in the circulation and the influence of the Fraser River could be examined in Burrard Inlet.

Oceanographic Observations

Twelve oceanographic stations were established by the Pacific Oceanographic Group in Burrard Inlet, where complete oceanographic observations were taken at different times of the year. Each station was occupied on opposite phases of the tide whenever possible.

A complete oceanographic station consisted of meteorological observations, vertical measurements of salinity, temperature, and sometimes oxygen. The discussion of this aspect of the oceanography of Burrard Inlet will be confined to the salinity observations.

Each of the current observation stations established by the Canadian Hydrographic Service (figure 14) was occupied for a complete tidal cycle of twenty-five hours on two occasions. Gurley-Price current meters were used at all the anchor stations for measurements of speed. The current direction was observed, by one of three methods depending on the

situation namely, (1) a captive drift pole buoy, twelve feet in length, used for surface observations, or (2) metal vanes attached by a light line to a captive buoy and set for specific depths, or (3) the metal vanes and line were secured directly to a winch on board the ship (12).

## Factors Influencing the Oceanography

Oceanographic observations are affected by wind, tide, and river run-off, all of which are variable. Quite frequently it is impossible to estimate their effects on the observations. A true comparison of the physical parameters with the proposed mathematical model requires that the data be reduced to a steady state. A true steady state does not exist in the presence of the oscillatory tidal currents, but a mean or net state can be described from the data. The influence of wind, tide, and fresh water on the circulation must be considered first.

### Tides:

The diurnal inequality in time and height of the tide (figure ii) in this region is controlled predominantly by the moon's declination north or south of the equator. The diurnal variation in height of the tide will be distinguished by the range of the tide between high water and low water, since the terms "neap" and "spring" tides are not applicable in the usual sense.

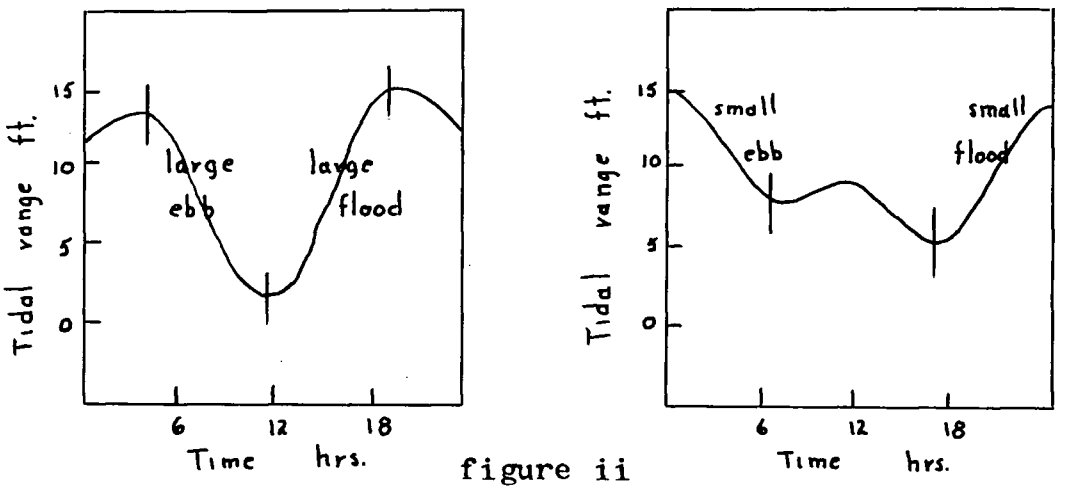


figure ii

The tidal currents vary in a similar manner as the tides. However, at the surface the effects of wind and fresh water drainage are superimposed and sometimes prevail.

Wind:

Reliable current measurements can be made only during periods of light wind, consequently the observations were restricted to these occasions. Therefore, the effects of wind on the present current observations are assumed negligible.

Fresh Water:

It will be demonstrated that the effects of fresh water are confined largely to the surface layers of the inlet where vertical and lateral mixing of saline water with the surface water produce large horizontal variations in salinity and hence pressure gradients.

The intrusion and mixing of muddy Fraser River water in Burrard Inlet is visible in the surface waters (figures 11,12). Although the discharge of the river varies appreciably during the summer months there is always sufficient discoloration to identify the water.

The monthly mean discharge of the river during 1950, metered at Hope, B.C., varied from a low of 23,600 cfs. in March to a high of 314,000 cfs. in June (13). During the period of freshet the discharge rate can increase by as much as 30,000 cfs. per day. The maximum discharge recorded was 440,000 cfs. on June 20, 1950.

The occurrence of the freshet in May, June or July is governed principally by the amount of snow cover and meteorological conditions existing in the interior of the Province. The heavy annual rainfall and large drainage area west of Hope add considerably to the total discharge of the Fraser, increasing it by an average of approximately 40% at New Westminster (14).

The river discharges into the Strait of Georgia through three main branches: the North, Middle, and South Arms. During the freshet period the distribution of muddy river water extends well over the Strait (figure 13). The major portion of the discharge takes place through the South Arm, but approximately 6% of the total discharge occurs from the North Arm (15).

## Current Measurements in Burrard Inlet

Burrard Inlet is considered as the region bounded by the North Shore, Stanley Park, and Vancouver City including English Bay. The west and east boundaries are shown in figure 10.

Hourly current measurements were taken at all stations (figure 14) at depths of 5, 18 and 50 feet by the Hydrographic Service. A few measurements were made at 25 feet on three stations, but the observations there have been included with the remainder at 18 feet.

During the period of these observations the Fraser River run-off exceeded a discharge of 170,000 cfs. except when station 2 was occupied; the discharge at this time was 135,000 cfs..

The current velocities on the flood and ebb phases of the tides were averaged separately for the large and small ranges of height to give four mean pictures of flood and ebb velocities in the inlet. The net circulation was obtained by averaging all the data for the 50 hour period of observation.

The mean circulations for the various phases of the tide are presented to point out the characteristic features of the currents in the inlet. The net circulation is related to these features and is included to show further detail of the tidal and surface circulations.

## Current Distribution

### Large Ebb:

At all depths, 5, 18, and 50 feet, (figures 15, 16, 17) the ebb pictures show the existence of a strong narrow jet which extends from the First Narrows to Pt. Atkinson. The central core of the stream lies offshore except in the region between Reardon Pt. and the First Narrows. The highest velocities of the stream occur close to shore between these two points. The jet stream broadens out along its path and narrows again at Pt. Atkinson.

South of the jet, and west of Stanley Park, a large counter-clockwise gyral exists. It is clearly defined at 50 feet (figure 17) by stations 17, 12, 13, and 15, but at 18 feet (figure 16) the gyral is noticeably more elongated. This effect appears to be associated with the higher average ebb velocities of the jet recorded at this depth. The eddy does not sweep the shore of Kitsilano beach, because a return circulation lies between the gyral and the shore. Some of the water from this gyral is returned to the jet stream while part, when sweeping southward, is deflected outward just north of Jericho Beach and Spanish Banks adding to the return circulation from Kitsilano and False Creek. This broad flow parallels Spanish Banks and moves out in a westerly direction.

Ebb waters south of Pt. Grey and in the Strait of Georgia flow northward while the ebb from Howe Sound is southward. The three broad streams from Pt. Grey, Howe Sound, and

Burrard Inlet meet west of the outer boundary and flow out into the Strait as one stream.

Small Ebb:

The current direction during the small ebb (figures 18, 19, 20) exhibits most of the gross features found for the large ebb. The jet persists along the North shore, but with reduced average velocities. The back eddy off Stanley Park is less well defined than that of the large ebb. The westward movement of water north of Spanish Banks follows the same path as the ebb from the larger tide. Off Pt. Grey the water fans out from the mouth of the Fraser. The direction of flow off Pt. Atkinson, however, is reversed on this ebb as compared with that of the large ebb.

Large Flood:

The flood waters move into the inlet from the north, south, and west (figures 21, 22, 23). The three streams join at the mouth and flow into the inlet. The main body of the water sets towards the Narrows, while the water at the lateral extremities of the streams fans shoreward. At the surface a large back eddy forms along the North Shore, but at 18 feet and 50 feet this eddy is not maintained, and a resultant return circulation takes its place. A similar situation occurs in English Bay on a smaller scale. A return circulation develops west of Kitsilano Beach and extends along Spanish Banks. This movement generally takes place during the last stages of

flood and is not very pronounced.

The large flood tidal range can temporarily seal off the river, preventing any further discharge at the mouth. However, for discharges of the order of 200,000 cfs. or more, there is some discharge of the river into the Strait. This phenomenon is quite small compared with the effect on smaller flood tides.

Small flood:

The situation for the flood on the small tide is similar to that of the large flood. The main part of this circulation is again directed towards the Narrows with the weak circulation along the south shore still persisting. A return circulation along the North shore from Sandy and Pilot Coves and out by Pt. Atkinson is evident at all depths. The circulation around Pt. Atkinson is directed up Howe Sound on this flood, while for the large flood the direction of flow is from Howe Sound into the inlet. A strong southerly current is observed at station 1 similar to that on the small ebb. Both the flood and ebb currents off Pt. Grey (stations 1, 3 and 16), show a divergent flow of water. The smaller range of the flood is insufficient to contain the river, and hence the brackish and muddy water spreads out into the Strait.

Summary of the Circulation:

The aerial photographs (figures 11, 12, 13) show that the surface movement of brackish water can be traced visually. However, the current measurements are necessary to

yield quantitative information.

The direction of ebb remains essentially the same as at other depths, but the ebb flows are more nearly uniform over the whole inlet as opposed to the streaming nature in the deeper waters. Ebb velocities in the jet are greater at 18 feet than at the surface. Off Pt. Grey in the vicinity of the Fraser River, the surface velocities are affected by the fresh water discharge and are two and three times as large as the deeper velocities. At station 14 west of Pt. Atkinson, where there is little brackish water the average velocity is nearly the same at all depths.

The combined effects of flood tide and Fraser discharge give rise to much higher speeds along Pt. Grey, Spanish Banks, and the northern reaches of English Bay. The stations which are swept by fresh water exhibit continually higher hourly surface speeds than those at 18 feet.

The Net Circulation:

The flood and ebb circulations differ at each depth of measurement and reveal the existence of two net circulations in the inlet. Characteristic circulations appear for both the upper and lower depths of Burrard Inlet (figures 27, 28, 29).

The net velocities at each station were obtained from the vector sum of all the hourly flood and ebb velocities taken during the periods of observation. The magnitudes of the velocities of the net circulation are approximately 10% of the maximum velocities recorded at the current metering

stations.

The jet stream which is a marked characteristic on the ebb tide is still evident in the net circulation. The counter-clockwise gyral off Stanley Park remains as part of the deep circulation. The gyral at 18 feet is more extensive and relatively more dominant than that at 50 feet. This is probably associated with the higher average velocities and larger lateral shearing forces at 18 feet.

The flow of the deeper water (figure 29) from Pt. Grey into the inlet divides into two streams, one branch following around Spanish Banks and flowing towards the Narrows between the gyral and the shore-line, and the other sweeping across the mouth and joining the jet stream south of Pt. Atkinson. The region in the immediate vicinity of station 10 exhibits little character because of the opposing flows.

The surface circulation shows an entirely different appearance. The back eddy off Stanley Park has completely disappeared because the main flow from Pt. Grey sweeps directly into the Narrows and the jet stream (figure 27). The circulation centred in English Bay is either in the form of an eddy or a return circulation close along the shore. The observations are too few in this area to establish definitely the nature of flow. Visual observations and photographs from Mt. Hollyburn and West Point Grey indicate that the basic circulation in English Bay is in the form of a gyral, but that it can extend westwards as far as the Inner Beacon on Spanish Banks.

The difference between the circulation at the surface

(figure 27) and at 18 and 50 feet (figures 28, 29) appears to be associated with the large quantities of brackish water flowing into the inlet in the upper 10 feet. The circulation at 50 feet is attributed to the mean pressure field associated with the tides, since the fresh water pressure gradients acting at this depth are small (see Mean Salinity Distribution). Bearing in mind that the side boundaries are essentially the same for both circulations, the differences in circulation must be due to different forcing functions present at the seaward boundary and the First Narrows. The current distribution at 50 feet can be considered as representing the net tidal circulation of the inlet while the surface circulation represents the combined circulation related to the fresh water field and the tides.

The relative differences in the distribution of mass at the surface and 50 feet become apparent from the oceanographic observations. The inferred movement of water from these observations adds more detail to the progressive changes of the direction of flow taking place during a flood or ebb tide and will be considered next.

## Distribution of Salinity in Burrard Inlet

The oceanographic observations that were carried out by the Pacific Oceanographic Group from 1949-1951 included locations other than those in Burrard Inlet (16). Unfortunately, some of these surveys in the adjacent areas did not overlap with all the stations in the inlet (figures 30, 34).

A synoptic picture could not be determined from these surveys primarily because of the different relative tidal times of observations and the daily changes in the Fraser River discharge. However, data from four oceanographic surveys taken during 1950 and 1951 in Burrard Inlet yield representative salinity distributions for river discharges ranging from approximately 24,000 cfs. in February to 200,000 cfs. in June.

Survey N 28/ii/51 (Figures 30, 31 and 32 a,b,c)

This survey was carried out over a three hour period between the times of high water and maximum ebb on a large ebb tide (inset figure 31). The average discharge of the Fraser River was 24,500 cfs. The lack of fresh water is partly responsible for the simple salinity distributions (figures 32a,b,c).

The surface isohalines (figure 32a) along the North Shore extend parallel to the shore from the Narrows to Pt. Atkinson in the corresponding region of the jet (figure 15). The average ebb velocity of 1.2 knots in the jet is sufficient for a particle of water to be transported from Reardon Pt. to Pt. Atkinson in three to four hours. The flow becomes parallel to the isohalines after this time. In the region off Stanley Park the distribution of salinity indicates that the water pushes out into the inlet as a continually expanding cloud or eddy. The current measurements (figure 15) confirm this deduction, since the movement of water is largely circulatory. The eddy gradually expands and moves westwards with the circulatory motion of its boundaries decaying. North of Spanish Banks the isohalines become tangent to the Banks in

the direction of flow. The flow eventually crosses the isohalines near the west boundary of the inlet.

A similar picture is evident at 6 feet (figure 32b) except that the isohalines appear as tongues along the North Shore. At 18 feet (figure 32c) the difference is more pronounced. These changes are caused partly by the initial time lag between the ebb at the surface and the deeper water. The ebb velocities at 18 feet are less than those at the surface for the first hour of ebb and they do not become larger until the second hour. The salinity picture at 18 feet shows part of the structure from the preceding flood north of Spanish Banks, while the distribution of salinity from the Narrows is just beginning to follow a similar pattern to that at 6 feet.

The character of the water masses below 15 feet is plotted in a T-S diagram (figure 31). The remnants of the previous flood from Pt. Grey are distinguished by the warm water mass at stations 11, 15, 18 and 17, while the colder ebb water from the Narrows is shown at stations 8, 12, 13, and 16. The high velocities and turbulent conditions existing in the Narrows cause vertical mixing of the warm surface water with the deeper colder water. The resulting water is well mixed and colder. The surface T-S relations for stations 8, 10, 13, and 16 are related to those of the mixed cold water from the Narrows.

Survey K 20-27/vii/50 (Figures 33a,b,c)

This survey is represented in terms of the average

distribution of salinity for a period of one week. The observations were taken over a three hour interval between the times of maximum ebb and low water on a large ebb tide. The average discharge of the Fraser was 110,000 cfs. for the period of observations.

The surface isohalines which extended from Jericho Beach to Pt. Ferguson as indicated in survey N (figures 32a, b,c) do not move appreciably until the later stages of ebb when they begin to bulge out into the central section of the inlet as shown in figures 33b,c of survey K. The water from English Bay is the last large mass of water to move in the inlet during the ebb tide. It flows northward into the middle section of the inlet and turns southward off Spanish Banks. However, it is not always completely flushed out of the inlet during a single ebb, and is frequently returned to the inlet on the following flood appearing as a large mass of water on the tip of the intruding tongue which floods in around Spanish Banks.

Survey G 31/v/50 (Figures 34,35, and 36,a,b,c) 1/vi/50 (Figures 37, 38, and 39a,b,c)

These two sets of observations were taken on successive days: the first on 31/v/50 during the period between low water and maximum flood (inset figure 35), and the second on 1/vi/50 between high water and maximum ebb (inset figure 38). The average Fraser River discharge for these two days was 200,000 cfs.

The surface isohalines (figure 36a) along the North Shore have a similar distribution to those of Survey N (figure 32a) indicating that during a long ebb this pattern becomes characteristic and possibly approximates a steady state distribution. This distribution is not immediately destroyed by the first stages of flood. The direction of flow as shown by the current measurements (figure 15) would have been along these lines of constant property. The flood is first apparent near Spanish Banks as shown in figure 36a.

This movement of water takes place early in the flood before any appreciable changes occur in the northern sections of the inlet. (The hourly current measurements at stations 5, 9, and 16, and 11, 17, and 21, show that ebb currents persist along the North Shore until at least one hour after the time of low water, while flood currents are observed in the south almost immediately after the change of tide).

The low salinity water at the tip of the tongue (figure 36a) is probably a cloud of brackish water discharged from the North Arm of the Fraser, while the remainder of the tongue is mixed water from Sturgeon Banks and the South Arm of the river (17) (18).

The north side of this large tongue presses over to the North Shore while the south side wedges into English Bay (figure 36a) pushing water westwards along Kitsilano Beach and Spanish Banks and also northwards past Stanley Park. Once the brackish flood water has moved over Spanish Banks and has reached the Narrows the small secondary tongues along

the shore-lines begin to recede. This effect is represented partly by the isohalines extending from Jericho Beach to Stanley Park which are so characteristic of English Bay.

The same overall pattern of the distribution of salinity is observed at 6 feet and 18 feet. The isohalines at 6 feet along the North Shore have shifted southward from Pt. Atkinson and shrunk to Reardon Pt. (figure 36b), and those at 18 feet to Sandy Cove (figure 36c).

The ebb characteristics on survey G 1/vi/50 (figures 39 a,b) reveal several interesting features. The eddy of brackish water which formerly appeared close to the Narrows (figure 36a). appears to have been transported along the North Shore during the time of the half tides. It is indicated by the circular salinity pattern at the surface, 6 feet, and 18 feet.

The T-S relations (figure 35) for 31/v/50 show the distinction between the high salinity cold water of the jet at stations 30, 35, and 36 and the warm less saline water in the central and southern regions. Almost the same T-S characteristics exist on 1/vi/50 (figure 38) as on the previous day except that there is no indication of the presence of cold saline water along the North Shore. Nearly all the water in the inlet appears to be flood water from the previous day.

The T-S diagrams for station 37 on 31/v/50 identify what is probably the North Arm water. The same T-S relationship occurs at station 35 on 1/vi/50, indicating perhaps that this mass of water did actually move along the North Shore.

Survey M 27/ix/50 (Figures 40, 41, and 42a,b,c)

This survey (figures 42a,b,c) was conducted during the small flood of a half tide and shows the situation for a Fraser River discharge of 60,000 cfs. as compared with the other observations taken during higher river discharges of 110,000 and 200,000 cfs.

In place of the single intruding tongue of fresh water, two tongues are present, one relatively fresh and the other more saline. This difference in the character of the flood as compared with that of survey G is related to the much smaller discharge of the Fraser. For run-offs of the order of 200,000 cfs. the tidal rise is insufficient to prevent some discharge of the river even at high water, and brackish water flows around Pt. Grey (figure 36a). For lower discharges of the river it is sealed off by a flood tide and saline water moves around Pt. Grey close to the shore (figure 42b). The brackish water which originally extended far out from the mouth of the river on the previous ebb is cut-off by the incoming tide and moves into the inlet as a cloud or tongue next to the saline tongue at Pt. Grey.

Remnants of the previous flood and ebb are still noticeable near the Narrows. The large eddy of brackish water (figures 42a,b), situated near English Bay, began its northward movement on the previous ebb but did not complete its westward movement, because of the short duration of this ebb. This eddy has the same T-S characteristics (figure 41) as the brackish flood water. Probably it was brought in on the pre-

vious large flood tide and settled in English Bay. The water lying just offshore from Pt. Grey and Spanish Banks is much colder and more saline, and is definitely not associated with Fraser River water.

Summary of the Salinity Distributions:

The circulations inferred from the salinity distribution are in agreement with the current observations. The isohalines are approximately parallel to the North Shore in the region of the jet, their southward displacement (survey K) follows the movement of water in this direction late in the ebb (11). The same general features are also shown at 6 feet and 18 feet.

The large tongues of saline water which extend from the Narrows are associated with the back eddy developed on the ebb tide, while the tongue-like distributions of saline water across English Bay are features of both flood and ebb tides. The change of position of these isohalines during the tides indicates some of the stages of the water movements which are obscured by considering only the average velocities over a full ebb or flood. The flood movement of brackish water through the inlet is also indicated by the large tongues of low salinity water, particularly in the region off Spanish Banks.

Mean Salinity Distribution:

An approximate mean surface salinity distribution (figure 43) related to a high river discharge was obtained by considering the gross features of the salinity patterns for

flood and ebb stages of the tide on surveys G and K.

Survey G (figure 36a) shows the distribution of salinity off Pt. Grey during flood tide, while survey K (figure 33a) shows the distribution of salinity from the Narrows during ebb tide. The tongues of brackish water near Pt. Grey and Spanish Banks indicate flow in the directions of the North Shore, the Narrows, and English Bay. In English Bay the isohalines generally extend across from Jericho Beach to Ferguson Pt. for both the average flood and ebb distribution of salinity. The salinity distribution of the jet stream along the North Shore is slightly distorted by the tongues of intruding brackish water off Spanish Banks (figure 43).

The tidal analyses of the oceanographic observations have revealed the general features of flow in the inlet. If one assumes that the tongues of saline water along the southern boundary indicate flow towards the Narrows and that the parallel isohalines along the North Shore indicate flow along the lines of constant property from the Narrows to Pt. Atkinson, then this interpreted current field agrees basically with the net surface circulation (figure 27) obtained from the current measurements.

The flow in and out of the inlet across the mouth is generally along the lines of constant salinity. This phenomenon agrees with the theoretical assumption (section iv) that flow must be along the lines of constant property at the mouth in order that a salt balance be maintained.

At 50 feet the average lateral difference of salinity for surveys G and K is only $1^{o}/oo$ while the surface difference across the mouth is $14^{o}/oo$. The net circulation at 50 feet also differs from the net circulation at the surface. The pressure gradients associated with the distribution of mass at the surface decrease vertically downwards and disappear at some depth. At 50 feet they are small compared with the pressure gradients developed by the oscillatory sea surface. The circulation at 50 feet is more likely to be associated with the mean tidal pressure field, while that at the surface is influenced strongly by the large local pressure forces which arise from the larger differences in salinity and higher concentration of fresh water.

# VI. VECTOR AND SCALAR FIELDS OF CIRCULATION IN BURRARD INLET

A formal solution by Fourier series to the mathematical model of a rectangular inlet is possible if $\Psi(xy)$ and one of its derivatives are known at the river and seaward boundaries. This would require current measurements at the head and mouth of a suitably selected inlet which has symmetrical boundaries. However, most inlets are not rectangular, and not even regular in shape. Solutions for these conditions are not practical by formal methods.

Formal rules for approximating irregular boundaries by regular functions have not been worked out but, knowing the current distribution, it will be shown that solutions can be obtained by numerical means.

The current observations in Burrard Inlet illustrate the essential features of flow which take place during flood and ebb tides. The analysis of the data indicate different mean vector current fields at the surface and at 50 feet. On the assumption of no net discharge or flow through the First Narrows (see appendix) a field of $\Psi(xy)$ representing the circulation in terms of streamlines has been obtained from the vector fields. Two fields have been derived in this manner: one at 50 feet, which it will be assumed shows the net tidal circulation, and the other at the surface which represents the combined net tidal and fresh water circulation.

The scalar fields have been examined by numerical methods to determine how accurately they satisfy the fourth

order differential equation

$$\frac{\partial^4 \Psi}{\partial x^4} + \frac{\partial^4 \Psi}{\partial y^4} = 0, \qquad (38)$$

which was derived earlier.

In order to preserve the natural shape of the inlet and still employ the data available (section v), a numerical method of solution is offered which is still applicable to irregular boundaries and has all the advantages of the Fourier method. The use of relaxation methods (19) (20) has provided an analytic method for testing the scalar fields for verification of equation (38) within the limits of accuracy of the observations. By expressing the differential equation in the form of finite-difference equations a numerical operator can be derived. This operator is used for testing the field.

The network of anchor stations (figure 14) establishes a grid of observation points in the inlet. The net vector velocities at each of these stations is sufficient to indicate the general features of flow, but a quantitative vector field is required for an analytical study. By reducing the grid size to a finer mesh and interpolating vector velocities at each intersection or node of the network a more detailed field satisfying the principle of volume continuity was developed.

Since the flow is assumed to be incompressible, a stream function $\Psi(xy)$ may be related to the velocity field by the relations.

$$u = -\frac{\partial \Psi}{\partial y} \qquad \text{and} \qquad v = \frac{\partial \Psi}{\partial x}, \tag{52}$$

so that

$$\Psi(xy) - \Psi(ab) = \int_{ab}^{xy} (v\,dx - u\,dy). \tag{53}$$

The vectors are given at the points of intersection or nodes of the grid. The x and y components of the velocity are u(x,y) and v(x,y). At the solid boundaries $\Psi = 0$ and $\frac{\partial \Psi}{\partial n} = 0$ where n is the normal to the boundary.

Equation (53) was solved for the stream function $\Psi(xy)$ in the inlet by carrying out a numerical integration over the grid. Scalar fields at both 5 and 50 feet were evolved from the vector interpolations and integrations. These fields were then contoured for $\Psi(xy)$ (figures 44, 46) and checked for satisfaction of the differential equation by relaxation methods.

## The Verification of a Scalar Field with a Fourth Order Differential Equation

The two terms of the differential equation expressed in the form of a finite-difference approximation for square nets are (19)

$$h^4 \left(\frac{\partial^4 \Psi}{\partial x^4}\right)_0 = \Psi_9 - 4\Psi_1 + 6\Psi_0 - 4\Psi_3 + \Psi_{11}, \quad \text{(a)}$$

and (54)

$$h^4 \left(\frac{\partial^4 \Psi}{\partial y^4}\right)_0 = \Psi_{10} - 4\Psi_2 + 6\Psi_0 - 4\Psi_4 + \Psi_{12}, \quad \text{(b)}$$

where the coordinates of these points are the numbered intersections of the net (figure iii). The point o may be any point remote from a boundary, but for convenience let it be the origin of the system.

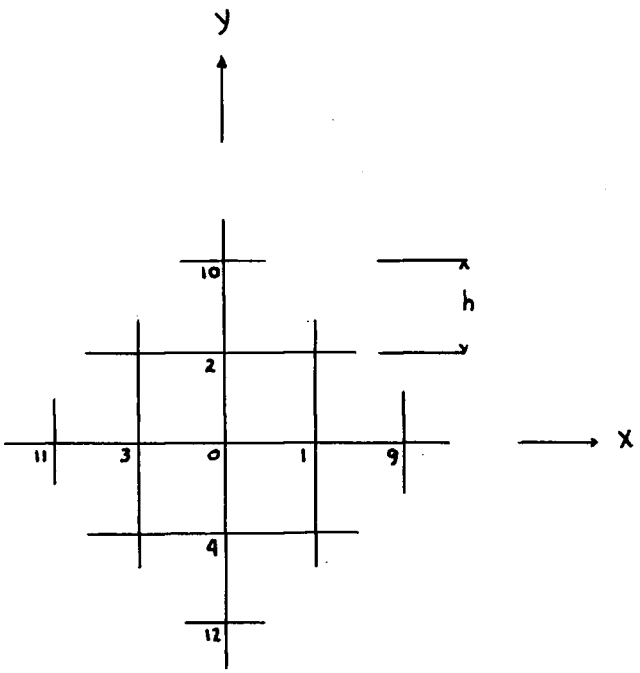


figure iii

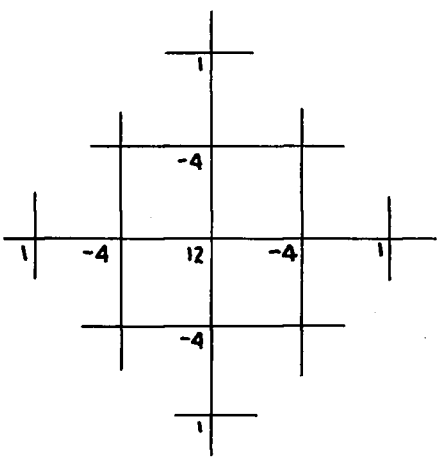


figure iv

The differential equation in the form of a unit operation operator for points remote from a boundary is represented in figure iv. For points near a boundary standard methods are used to check the boundary conditions $\Psi = \frac{\partial \Psi}{\partial n} = 0$ (19). The simplest method is to approximate each section of the boundary by a straight line of the network.

By applying the operator to each grid point of the field, the field may be tested for verification of the differential equation. Since the equation is homogeneous, the sums and differences of the products taken around the central node should be zero (figure iii). Generally a residual will remain which can be liquidated by slight adjustments of the values of the scalar quantity at one of the nine points.

For the two scalar fields of $\Psi$ examined, positive and negative residuals were found, indicating that the fields did not satisfy the differential equation identically. The residuals were liquidated or reduced to a minimum by relaxing the field at some of the grid points. Each change of $\Psi$ at a grid point affects the residuals at eight other points, consequently there is a continual wash-back of residuals while the field is being altered. The goal is to reduce the residuals to a minimum without destroying the original field. The effort involved in these operations is considerable if the unit relaxation operator (figure iv) is used exclusively. It is a matter of personal choice, somewhat dependent on the distribution of the residuals, how to ease this laborious process. Point and line relaxation operators were the easiest to employ for relaxation near the boundaries, while simple block operators were more successful in the central area. In this connection a certain amount of discretion is required because the field itself has already been established independently from other sources. Thus the relaxed field satisfying the equation must still retain the basic character of the scalar field from

which it is derived.

A critical feature of this method is the proper choice of grid size. For ease of operation it is best to choose as coarse a grid as possible. It will contain fewer nodes and the liquidation processes will be correspondingly easier. Relaxation of the field can always be advanced to a finer net by simply halving the network. A finer net was found to be necessary in regions where the most rapid changes of $\psi$ occurred, in particular, areas adjacent to the North Shore, Stanley Park, and Spanish Banks. In these areas the behavior of $\psi$ was studied in closer detail.

It is difficult to assess the possible error of the final fields because there is one error which arises through incomplete liquidation of the residuals and a second which arises from neglect of higher order terms in the finite-difference expressions. An arbitrary residual limit was set at $\pm$ 10% of the value of $\psi_o$ for any grid point with approximately equal distribution of positive and negative values throughout the field.

Results:

The scalar fields (figures 44, 46) derived by integrating the current fields were successfully relaxed to satisfy the differential equation and boundary conditions within the 10% limit of accuracy. Further relaxation carried out to reduce the residuals another 5% resulted in an overall change of less than 1% of the values of $\psi$ . Since there exists an

inherent error of approximately 10% in the current observations and one equally as large for the interpolation of the vector field, further liquidation of the residuals was not considered to be significant.

The final relaxed fields satisfying the theoretical assumptions and physical measurements are shown in figures 45 and 47. The extent of distortion introduced by relaxation has been confined to a smoothing effect of the $\psi$ function. The character of the vector field is still preserved, and the general flow pattern has become more apparent; a feature which is frequently lost when only the directional qualities of the vectors are used.

The above tests were carried out using the reduced biharmonic equation

$$\frac{\partial^4 \Psi}{\partial x^4} + \frac{\partial^4 \Psi}{\partial y^4} = 0.$$

In addition both the scalar fields were tested with the full biharmonic operation operator derived from the equation

$$\frac{\partial^4 \Psi}{\partial x^4} + 2\frac{\partial^4 \Psi}{\partial x^2 \partial y^2} + \frac{\partial^4 \Psi}{\partial y^4} = 0. \qquad (55)$$

The values of the residuals found in using this operator were within the 10% limit of accuracy set for the reduced biharmonic equation. However, relaxation employing the full biharmonic operator is much more tedious to perform, since it is more slowly convergent than the reduced form. The contribution of the middle term to the field does not appear to be

significant within the limits of accuracy of the current measurements and the interpolated vector field.

Discussion:

The net current distributions at the surface and 50 feet (figures 27, 29) were considered in section (V). The scalar fields (figures 44, 46) representing these circulations provide further details which were not originally apparent in the vector field. The streamlines are crowded towards the shores while in the middle regions they are generally widely separated. This crowding of the streamlines and the associated high velocities near a boundary are common features of coastal circulations.

The jet stream is clearly defined by the streamlines at the surface and 50 feet.

The deep circulation is characterized by the back eddy west of the Narrows and the shallow penetration of the water at the mouth. The streamlines around Pt. Grey and Spanish Banks are deflected southward into English Bay before turning towards the First Narrows. The central region now appears as a stagnation point in the inlet.

The surface pattern of streamlines exhibits crowding along the North Shore while the streamlines from Pt. Grey extend directly into the Narrows with some turning northwards and adding to the jet stream. The large but weak back eddy shown in English Bay is merely indicated since the magnitude of the $\Psi$ terms are small compared with those in the

remainder of the field. English Bay may be considered as another bay off the main inlet delineated by a line from Spanish Banks to Prospect Pt. The circulation in this area closely approximates that previously discussed in the mathematical model with a salt balance. A similar type of circulation might be expected in Pilot and Sandy Coves.

The difference between the circulations at 50 feet and the surface implies that different boundary conditions exist at the Narrows and the mouth for the two depths. Any change of the forces acting in the inlet will reflect on these boundary conditions at the open ends.

The end boundary conditions at the Narrows are not well defined owing to the lack of observational data in this region. The form of $\Psi$ and its first derivative here, will affect the values and distribution of $\Psi$ elsewhere in the inlet. However, it is felt that reasonable estimates of the velocities and hence of the $\Psi$ functions have been made which fit the overall current distribution of the inlet. The necessity for doing this serves to emphasize the importance of detailed measurements across the open boundaries of an inlet.

The brackish water is generally limited to the upper ten feet and it is not surprising that marked gradients of salinity exist. The variation in this mass field produces relatively large forces; forces which, averaged over a period of time, are large enough to override the mean pressure gradient forces associated with the tides. A characteristic sur-

face circulation is maintained by the influx of fresh water and the fresh water field.

The extent of penetration of water into the inlet from the seaward boundary depends on the size of the eddy off the First Narrows (figures 46, 47). The shallow sweep of water at the mouth is confined to this region by the eddy, the effects of which are reflected on the boundary conditions at the mouth. If the eddy shrinks towards the Narrows, more water will flow into the inlet. The eddy may extend to the surface, but its size appears to be controlled by the boundary conditions at the mouth which change as the amount of brackish water flowing into the inlet varies.

The scalar fields of $\Psi(xy)$ represent two possible solutions to the linear homogeneous differential equation. The difference of these two solutions must also be a solution. If the tidal circulation remains essentially the same at all depths and is the fundamental circulation of the inlet, then it should be possible to study changes of the surface circulation when other forces become effective. The surface circulation studied in the present thesis represents a temporary mean state of water movement existing during high Fraser River discharge. Assuming that the fresh water effect for lower discharges of the Fraser also satisfies the same differential equation then it should be possible to correlate the surface circulation with other mean discharges of the Fraser. In this way seasonal differences in circulation, controlled by the discharge of the Fraser, can be predicated from the observa-

tions gathered on a single concentrated oceanographic survey.

Reference has been made to the full biharmonic equation, equation (55), which governs the bending of a flat plate. The similar equation describing the bending of a plate and the circulation in the fluid model suggests that an inexpensive and practical plate model of the inlet could be built to assist in the field observations and interpretation of the data (21). Boundary conditions can be simulated by clamping and loading the plate. The advantage of this technique would be that the solution is directly revealed by the deflection of the plate. The contours of the deflection could then be related to the current pattern in the inlet. Another advantage is that the middle term of the biharmonic equation is taken into account in the bent-plate model.

However, the magnitude of this term was evaluated and found to be insignificant except in regions where marked curvature of the streamlines exists particularly at the solid boundaries.

This was done by evaluating the residuals $R_1$ and $R_2$ from both equations 38 and 55.

$$\frac{\partial^4\Psi}{\partial X^4} + \frac{\partial^4\Psi}{\partial Y^4} = R_1 \qquad (38)$$

$$\frac{\partial^4\Psi}{\partial X^4} + 2\frac{\partial^4\Psi}{\partial X^2 \partial Y^2} + \frac{\partial^4\Psi}{\partial Y^4} = R_2 \qquad (55)$$

The magnitude of the middle term is of the order of $\left|(R_1 - R_2)\right|$ and was found to be less than 5% of either $\left|\frac{\partial^4\Psi}{\partial X^4}\right|$ or $\left|\frac{\partial^4\Psi}{\partial Y^4}\right|$.

Thus the contribution of the longitudinal frictional forces to the circulation in Burrard Inlet is small compared with that of the lateral frictional forces.

# VII. SUMMARY AND CONCLUSIONS

Theoretical and practical examples of lateral circulations have been presented and related to frictional forces, and forces associated with pressure gradients in an inhomogeneous medium. The presentation of these examples has required theoretical and numerical solutions to the boundary-value problem of the circulation in an inlet. Both methods of solution were required to study critical phases of the circulation.

The Fourier type solution affords a practical means of studying some of the characteristics of the Coriolian and frictional fields as well as the integrated mass fields. It is only useful for symmetrically shaped models with uniform side boundaries. On the other hand, the numerical method is applicable to natural boundaries, and is more practical from the oceanographic point of view.

Without the introduction of a salt balance the model would lack physical reality. The inclusion of this principle in the boundary conditions has made a study of the circulation possible. Although the mass field is undefined by virtue of the vertical integration, it is possible to study the relative significance of either the Coriolian or frictional forces.

The mass field may be described by a function Q which is related to the density by the equation

$$Q = \int_{sfc.}^{h} dz \int_{sfc}^{z} \rho \, dz . \qquad (5)$$

The horizontal variation of Q is expressed by the equation

$$\frac{\partial^4 Q}{\partial x^4} + \frac{\partial^4 Q}{\partial y^4} = 0. \qquad (15)$$

Calculating the values of Q from oceanographic data the field could be developed and tested by relaxation methods in a similar manner to that of the current field. Knowing this field and the velocity field it would be possible to evaluate the eddy coefficient, $A_1$. This method has the disadvantage that it would require a long series of oceanographic observations to establish the mean mass field. In this respect direct current observations have the advantage of yielding the velocity field directly, from which scalar fields of the stream functions can be developed and tested. The Coriolian and frictional fields could then be determined, and hence the mass field. This field could be compared with that of the inlet for further verification of the model.

The introduction of relaxation methods has provided an excellent method of bridging the gap between observational data and theory. The question of dealing with asymmetric boundaries in nature and symmetric theoretical boundaries has been answered by this numerical approach.

The two solutions to the differential equation describing the circulations at 50 feet and at the surface have been attributed to the forces associated with a mass field.

The surface circulation is primarily controlled by the influx of fresh water from the Fraser establishing a large pressure field which in turn influences the mean tidal pressure field at the surface. At 50 feet this phenomenon is small and the circulation appears to be associated only with the mean tidal pressure field. The two solutions can be combined to give the net circulation associated with the inhomogeneity of the fluid. The surface circulation is controlled largely by the discharge of the Fraser. The discharge varies seasonally, and it would be expected that some change would occur in the surface circulation of Burrard Inlet. This effect may be studied by considering the two solutions. A proportionate change of the solution at the surface combined with that of the tide should correlate the seasonal changes of the circulation with the discharge of the Fraser.

Both the theoretical and numerical solutions provide an indication of the observational data which would be required for inlet studies. The field observations should include current measurements across the mouth and river (if there is one) and for purposes of checking the model also along the longitudinal axis of the inlet. If a detailed study of the circulation is desired the effects of boundary configuration on the flow must be included in the planning of an oceanographic survey.

Another problem in physical oceanography is that the ships and manpower available are never adequate for an exhaustive survey. It is always necessary to decide whether it is better to distribute the effort over all the inlet and

be satisfied with the gross features of the circulation, or to concentrate in limited regions in order to obtain a detailed picture of the circulation. On the basis of this study a number of suggestions are offered for field investigations of lateral circulations. A preliminary survey of the area is desirable to establish an approximate field of flow so that a coarse grid of the stream function can be obtained. Relaxation of such a field would involve a minimum of effort and still prove valuable for indicating the most significant regions for further field observations. These data may be included in the approximate field by reducing the grid size. By repeating these theoretical and observational studies, the circulation could be well established with a minimum of effort.

It would seem feasible to investigate the practicability of elastic plate models for the study of lateral circulations. The biharmonic equation developed for the fluid model (equation 55) also governs the bending of an elastic plate. By stressing the plate the vertical deflection can be contoured and related to the flow pattern in the fluid prototype. The differential equation is satisfied without relaxation, and the plate would show the complete scalar field. The information obtainable from such a model is directly applicable to the problem of locating stations for oceanographic observations.

In the present study wind effects were neglected for the purpose of studying the influence of fresh water and

tides. However, the possibility still exists that the wind stress could be included in a study of this type. By calculating the value of the wind stress at each oceanographic station and interpolating over the grid pattern of the model, the value of the curl of the wind stress would be known. The relaxation residuals of the current field would have to be related to these values of the curl of the wind stress. In this manner wind effects may be considered in the circulation of an inlet.

The agreement between the mathematical model and the oceanographic observations in Burrard Inlet indicates that lateral circulations can be described by the differential equation

$$\frac{\partial^4 \psi}{\partial x^4} + \frac{\partial^4 \psi}{\partial y^4} = 0 . \qquad (11)$$

The success which has been achieved by describing the circulation in Burrard Inlet demonstrates that the theoretical considerations are physically sound and reasonable enough to consider further the problems of lateral circulation in other estuaries.

. . .

# REFERENCES


1. Pritchard, D.W. (1952). Estuarine hydrography. Advances in Geophysics, vol. 1, 243-280. Academic Press Inc. New York, N.Y..

2. Pritchard, D.W. (1950). A review of our present knowledge of the dynamics and flushing of estuaries. Tech. Rept. 4. Ref. 52-7. Chesapeake Bay Institute, John Hopkins University.

3. Tully, J.P. (1949). Oceanography and prediction of pulp mill pollution in Alberni Inlet. Fish. Res. Board, Canada. Bull. 83. 169 pp.

4. Pickard, G.L. (1953, 1954). Oceanography of British Columbia mainland inlets I, II, III, IV. Fish. Res. Board, Canada. Progress Reports of Pacific Coast Stations, 96, 97, 98, 99.

5. Cameron, W.M. (1950). On the dynamics of inlet circulation. Doctoral dissertation. Scripps Institution of Oceanography. University of California, La Jolla, Calif., 1951.

6. Stommel, H. (1951) Recent studies in the study of tidal estuaries. Tech. Rept. Ref. 51-33. Woods Hole Oceanographic Institution.

7. Shtokman, V.B. (1948). Equations for a field of total flow induced by the wind in a non-homogeneous sea. Comptes Rendus (Doklady) de l'Academcie des Sciences de l'URSS. vol. LIV, no. 5, 403-406.

8. Shtokman, V.B. (1948). Relationships between the wind-field the transport-field and the mean mass-field in a non-homogeneous ocean. Dok. Akad. Nauk SSSR vol. 59, no. 4, 675-678. Manuscript translation T 56R. Defence Scientific Information Service, DRB. Canada, 1952.

9. Munk, W.H. (1950). On the wind-driven ocean circulation. Journal of Meteorology, vol. 7, no. 2, 79-93.

10. Cameron, W.M. (1951). On the transverse forces in a British Columbia inlet. Trans. Roy. Soc. Canada., vol. XLV, series iii, 1-8.

11. Canadian Hydrographic Service. Tidal Current Charts, Vancouver Harbour, British Columbia. Department of Mines and Technical Surveys, Ottawa. Tidal Publication no. 22. 1950.

12. La Croix, G.W. (1950). MS. Report on current investigation, Burrard Inlet. Hydrographic Survey, Victoria, B.C.

13. Unpublished data (subject to revision) Dominion Water and Power Bureau, Vancouver Office.

14. Sewerage and Drainage of the Greater Vancouver Area, British Columbia, 1953. Sewerage Board, Vancouver, B.C. p. 126.

15. Ibid. p. 125.

16. Data Record. MS. Fraser River Estuary Project, 1950. Pacific Oceanographic Group, Nanaimo, B.C..

17. Fjarlie, R.L.D. (1950). MS. Fraser River estuary project Pacific Oceanographic Group, Nanaimo, B.C..

18. Fjarlie, R.L.D. (1950). MS. The oceanographic phase of the Vancouver sewage problem. Pacific Oceanographic Group, Nanaimo, B.C.

19. Shaw, F.S. (1953). An Introduction to Relaxation Methods. Dover Publications Inc. New York, N.Y.. 395 pp.

20. Arthur, D.W. de G. (1954). Relaxation Methods. McGraw-Hill Book Company Inc. New York, N.Y.. 256 pp.

21. Hidaka, K. and Koizumi, M. (1950). Vertical circulation due to winds as inferred from the buckling experiments of elastic plates. Geophysical Notes, vol. 3, no. 3, 1-9. Geophysical Institute, Tokyo, Japan.

22. Surface Water Supply of Canada (1941-1942). Pacific Drainage, 94. Department of Mines and Resources. Ottawa. 1946.

. . .

# A P P E N D I X

# APPENDIX

The influence of the Narrows on the circulation in Burrard Inlet has been seen from the oceanographic observations. The current fields were developed on the assumption of no net discharge through the Narrows and that the flow was asymmetric.

Estimates of the net discharge have been made from the total discharge on flood and ebb tides. These data were supplied by the office of the Vancouver Harbour Model Project. Discharge figures were calculated by the method of cubature, and supplemented by current measurements taken by the Water Resources Board.

This information on the circulation and discharge through the Narrows is presented to supplement the current fields of Burrard Inlet.

Discharge through the Narrows:

The volume discharge through the Narrows depends on the tidal range of flood and ebb. The average volume transport on May 4, 5, 1954, (when measurements were carried out) was approximately $7.7 \times 10^9$ cu. ft. on flood and $7.2 \times 10^9$ cu. ft. on ebb for an average range of 14 feet. The difference in volume discharge is related to the differences of tidal range which was approximately 1 foot for the large tides of May 4 and 5, 1954. Any net transport of water through the Narrows

is temporary and dependent on the tides. It is too small to consider over a long time average of the tides. This assumption presumes that the volume of fresh water draining into the inlet is not significant. This effect will be considered later.

Current Measurements:

Figures 44 and 46 indicate an inward movement of water through the First Narrows along Stanley Park and an outward movement along the North Shore. Current measurements along transverse sections, situated east and west of the Lions Gate Bridge, indicate that the flow has this asymmetric pattern. The flood movement of water flows past the Stanley Park side of the Narrows and crosses the Narrows striking the shore east of the bridge. The magnitudes of the flood velocities are large, and give rise to net inward components of velocity west of the bridge on the south side, and east of the bridge on the north side. The ebb movement of water is partly from Stanley Park east of the bridge across to the North Shore on the west side of the bridge. This flow together with the ebb along the North Shore produces a net outward flow along the North Shore west of the bridge. East of the bridge the direction of the net flows is reversed with respect to those west of the bridge. Part of this effect inside the Bridge may be the result of large back eddies formed along both shores on flood and ebb tides.

Fresh Water Drainage:

A study of Burrard Inlet and the First Narrows is not complete without some mention of the fresh water drainage into the area. There are a great many small streams draining into the inlet, particularly along the north side and Indian Arm. The discharge of these streams is insufficient to warrant continuous stream measurements. Four major rivers are located along the North Shore namely, the Capilano, Seymour, Indian, and Lynn. Daily discharge measurements are taken only on the Capilano and Seymour Rivers. The Indian River system was metered for a period of 8 years from 1912-1920. There are no discharge figures for the Lynn Creek.

The variation of daily discharge of these rivers from season to season is large. Some idea of the extremes of discharge for the Capilano, Seymour and the Fraser may be gained from Table I (22).

| River | Discharge cfs. | | Drainage Area |
|---|---|---|---|
| | Maximum | Minimum | Sq. Miles |
| Capilano | 20,800 | 6.5 | 76 |
| Seymour | 17,200 | 9.3 | 68 |
| Fraser | 536,000 | 12,000 | 85,600 |

Table I.

One stream which is of a size comparable with the others is the Lynn. The only satisfactory means of estimating its discharge is to consider the mean annual distribution of rainfall over the drainage basin of the river (figure 48).

This can be done by considering the whole Howe Sound-Burrard Inlet and Greater Vancouver area where there are a number of rainfall stations (figure 48).

From the distribution of rainfall an estimate of 160 cfs. for the mean discharge of the Lynn was deduced. This figure was calculated for a yearly cycle. Similar calculations for the Capilano, Seymour, and Indian Rivers were made and compared with the metered values of discharge for these rivers (Table II).

| River | Metered Discharge (yearly mean) cfs. | Estimated Discharge (yearly mean) cfs. |
|---|---|---|
| Capilano | 702 | 704 |
| Seymour | 552 | 607 |
| Indian | 654 | 638 |
| Lynn | -- | 160 |

TABLE II

The estimated and actual values of discharge agree very closely for the Capilano, Seymour, and Indian Rivers. On this basis the discharge of the Lynn was incorporated into the figures for fresh water drainage into Burrard Inlet. The total mean yearly discharge for the four rivers is approximately 2080 cfs. and for the inlet slopes outside these drainage areas 575 cfs.

The total contribution of the fresh water draining into the inlet for an averaged tidal time of 7.6 hours for flood and ebb is approximately $7.4 \times 10^7$ cu. ft. If all this water passed through the Narrows on ebb it would account for less than $1^o/o$ of the discharge. This small contribution can be neglected compared with the total discharge through the Narrows. The assumption of no net transport through the Narrows is still valid.

. . .

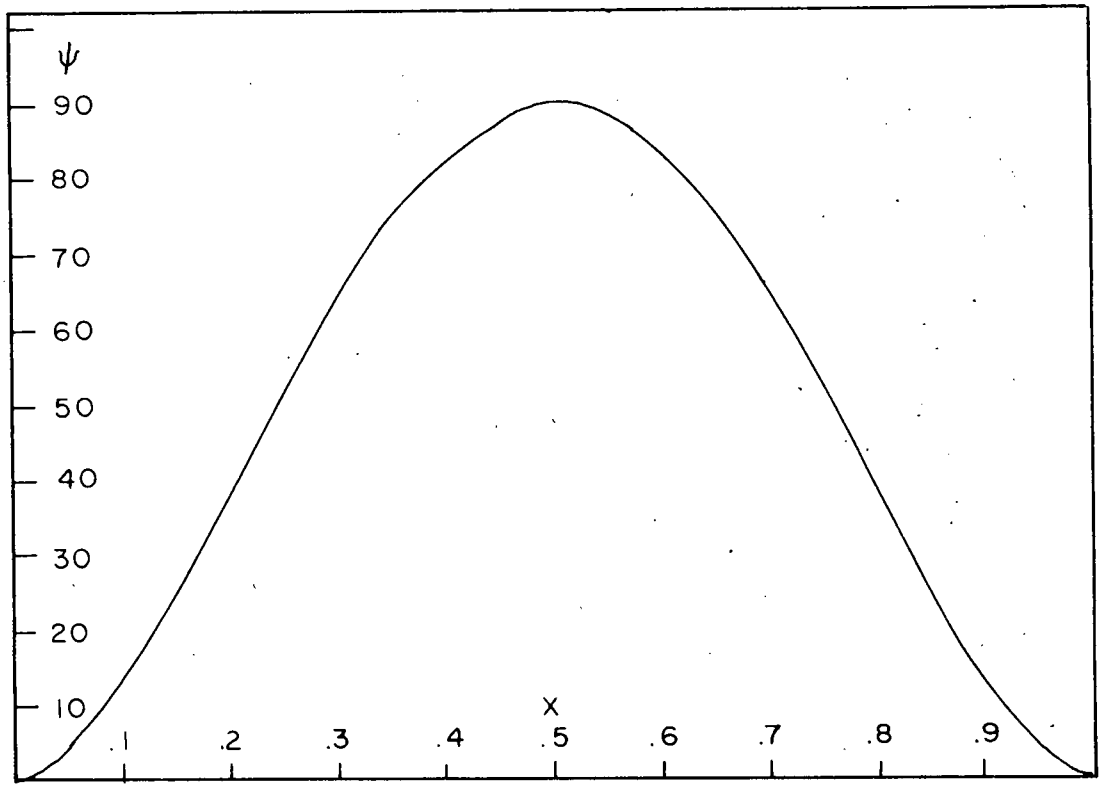


(a) $\psi$ evaluated at the mouth of the bay

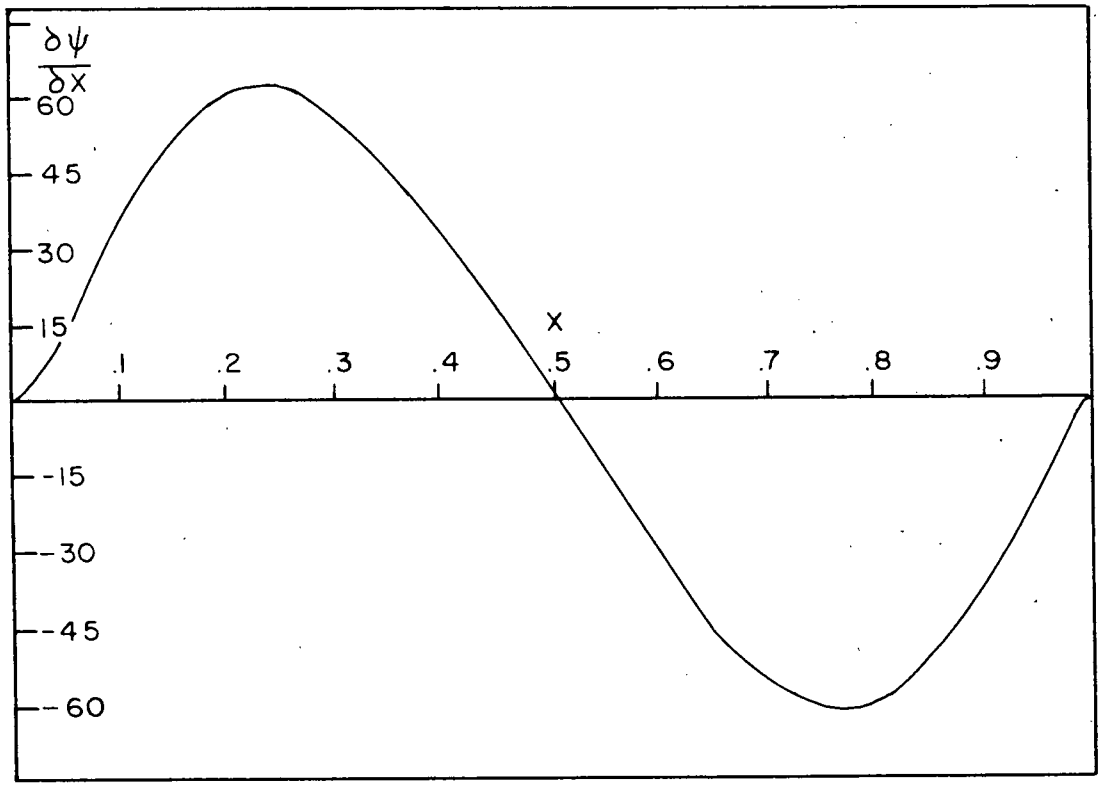


(b) $\frac{\delta \psi}{\delta X}$ evaluated at the mouth of the bay

Figure 1.

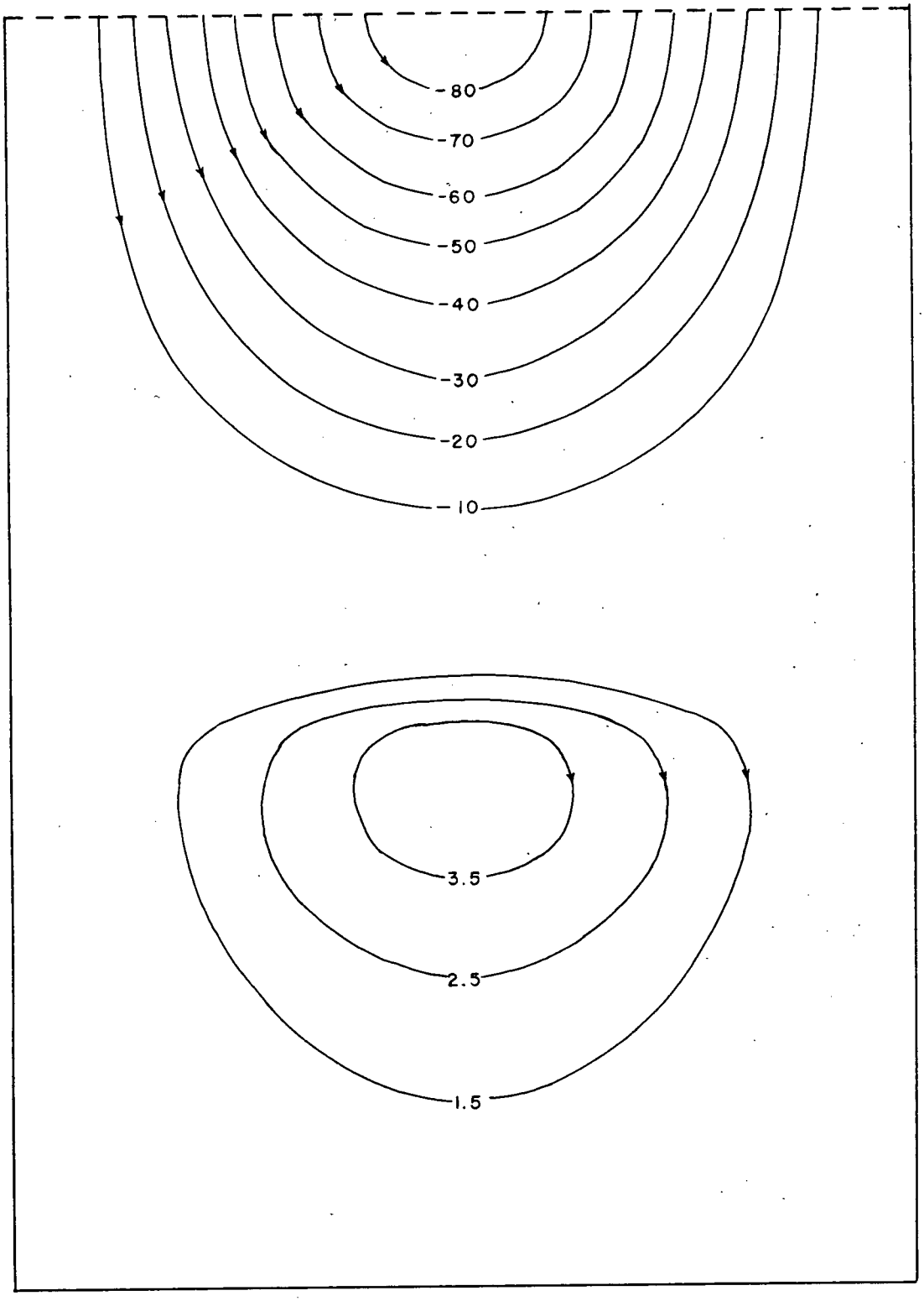


Transport or Coriolian field for the bay

Figure 2.

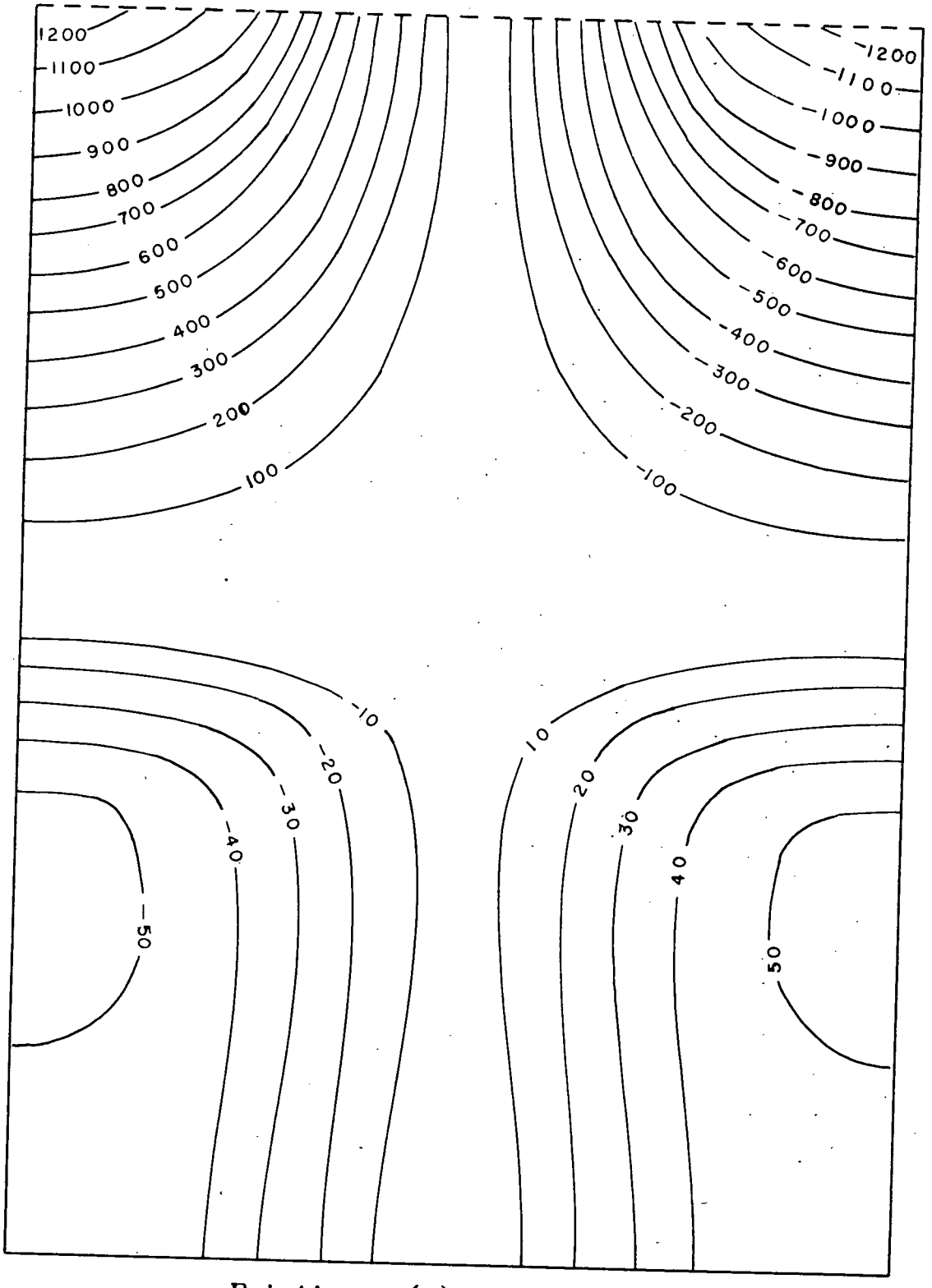


Frictional (θ) field for the bay

Figure 3.

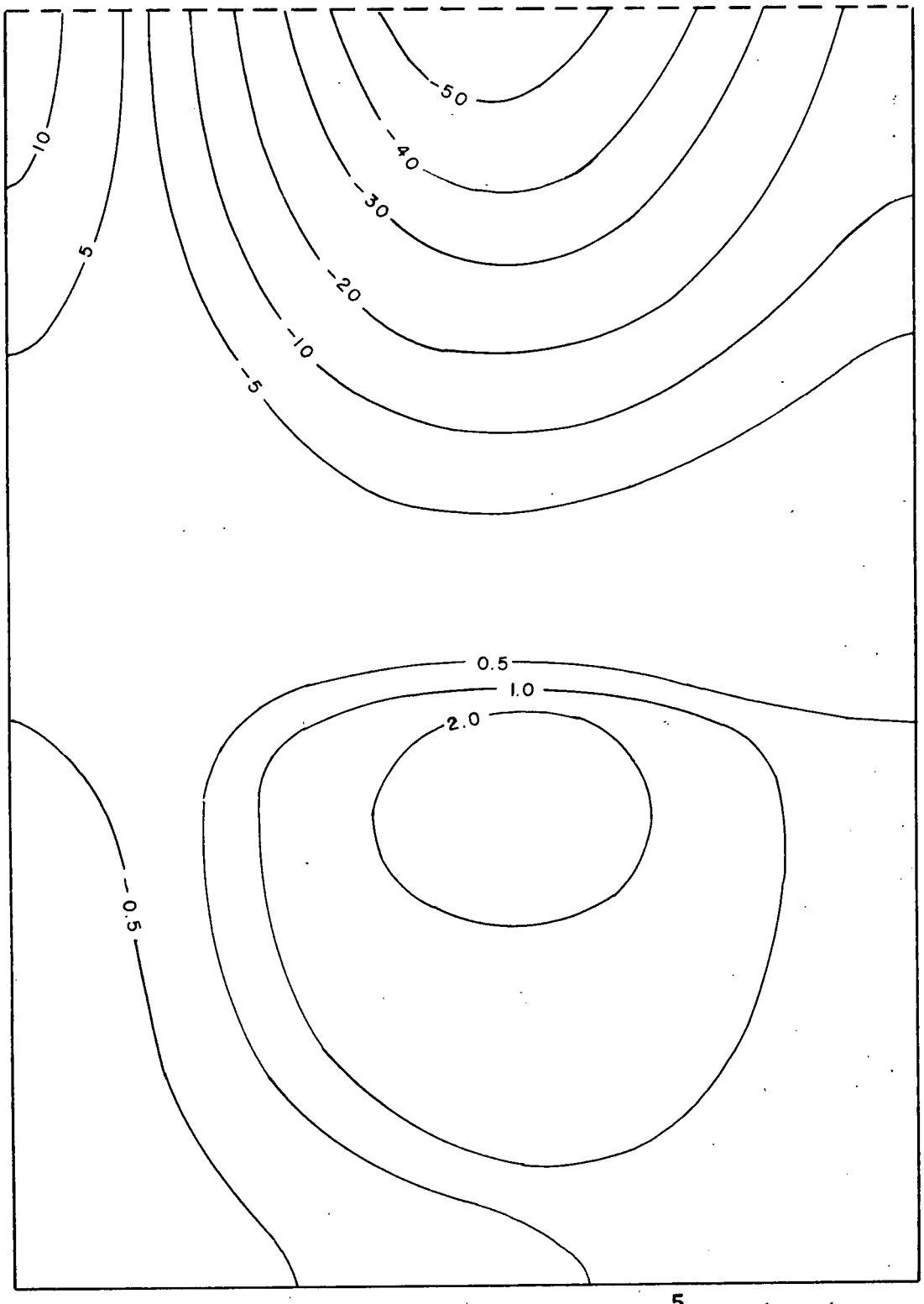


Mass field with $A_1 = 1.0 \times 10^5$ gm./cm./sec..

Figure 4.

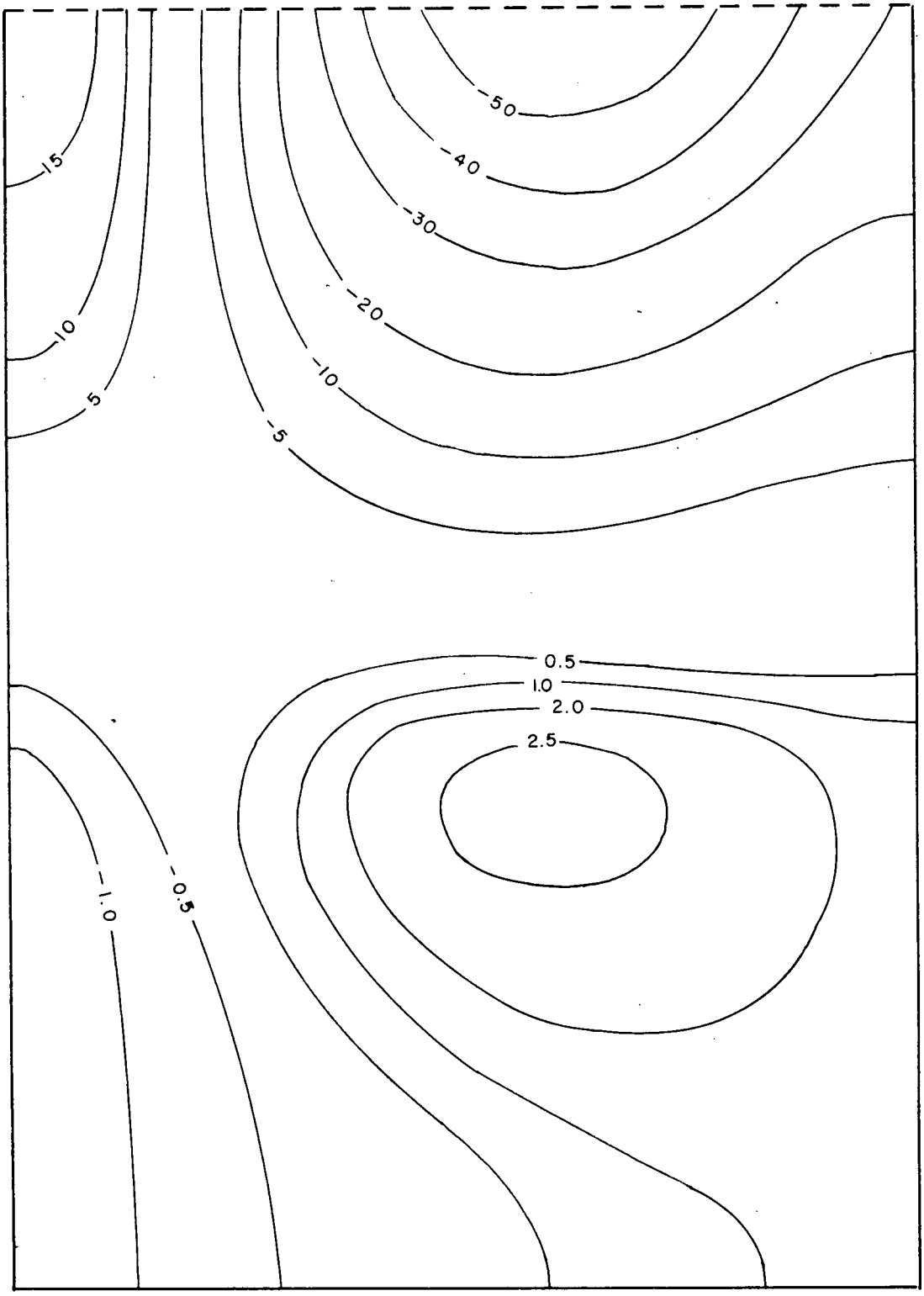


Mass field with $A_1 = 2.0 \times 10^5$ gm./cm./sec..

Figure 5.

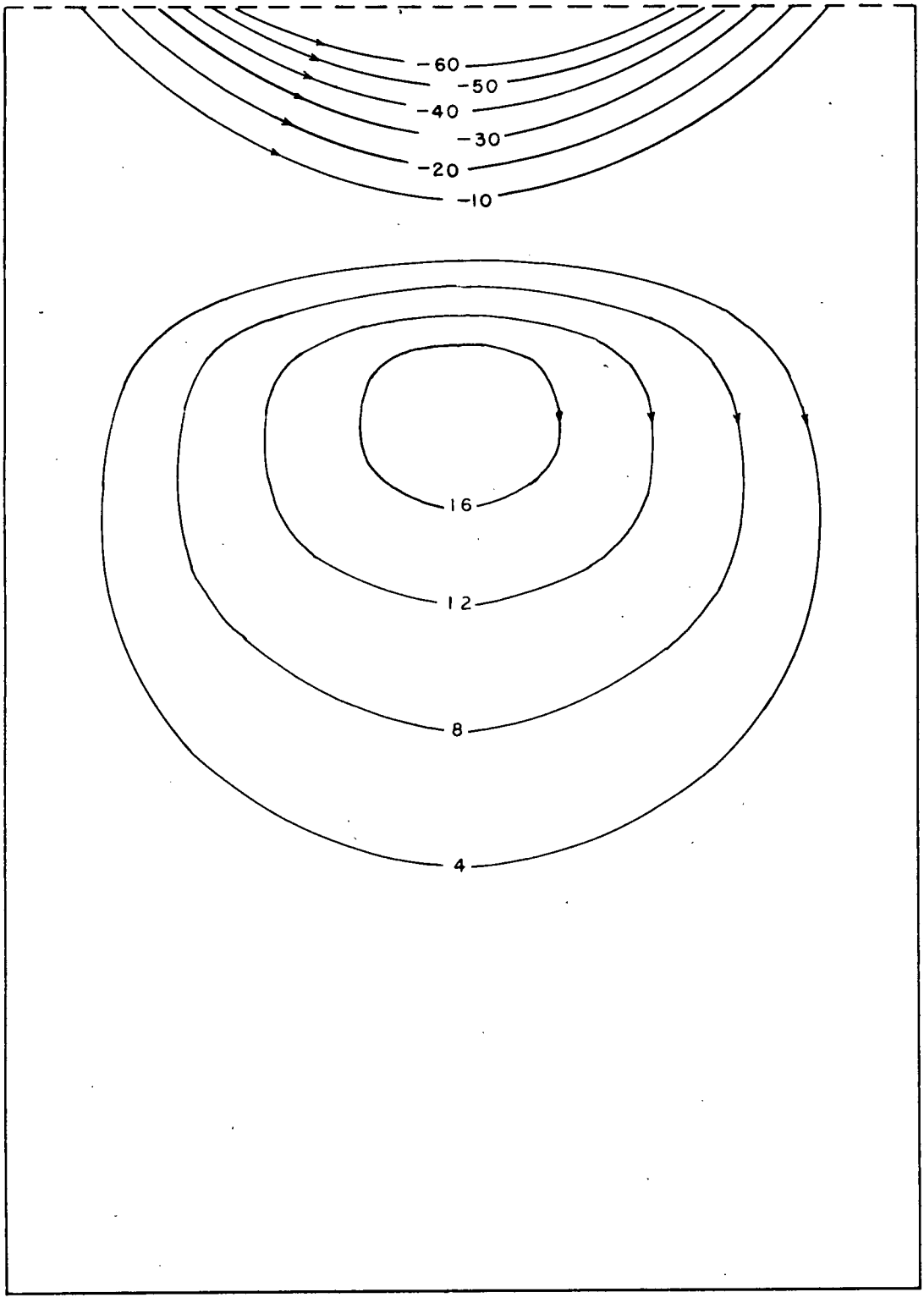


Transport or Coriolian field
which satisfies a lateral salt balance.

Figure 6.

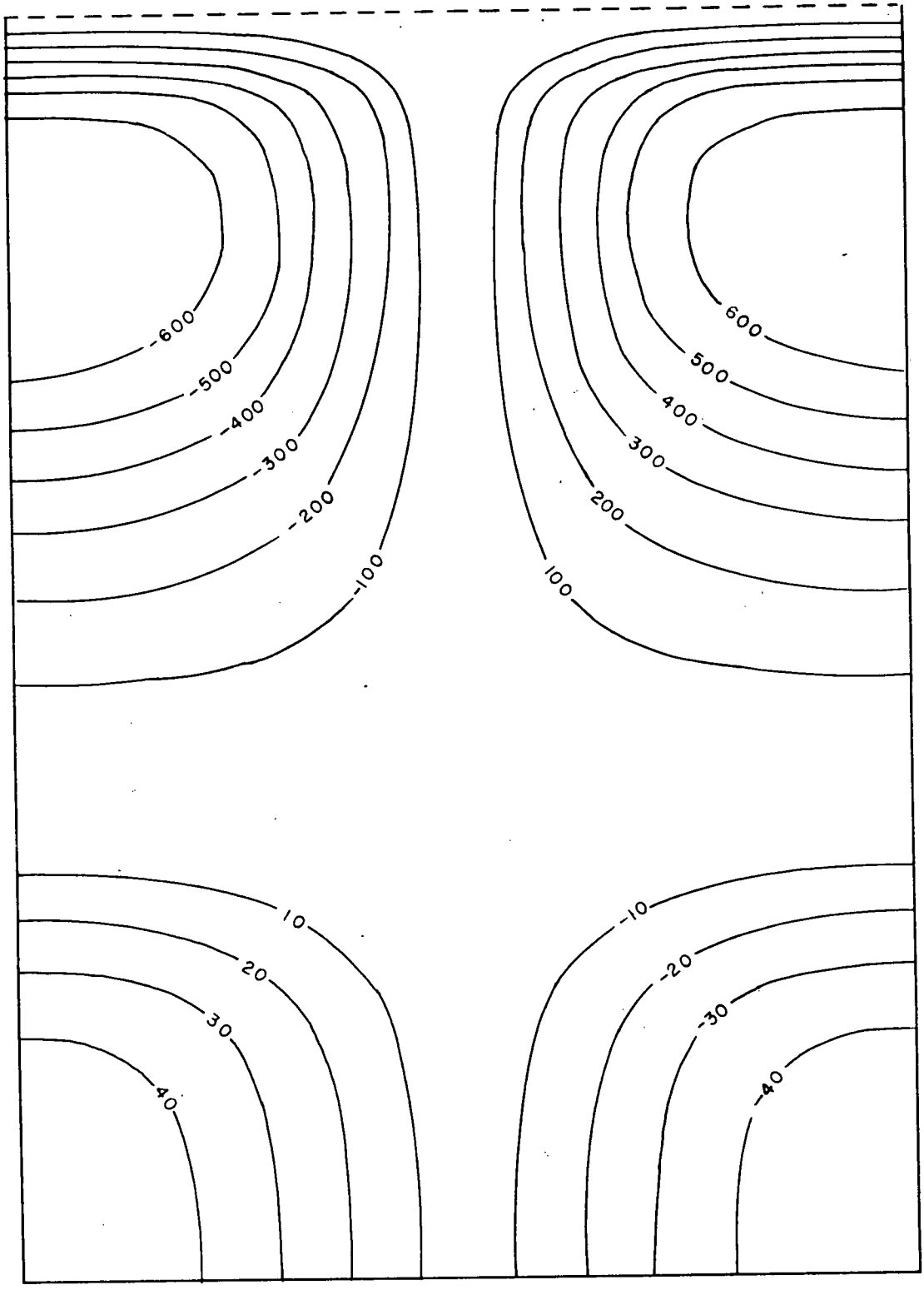


Frictional field which satisfies
a lateral salt balance

Figure 7.

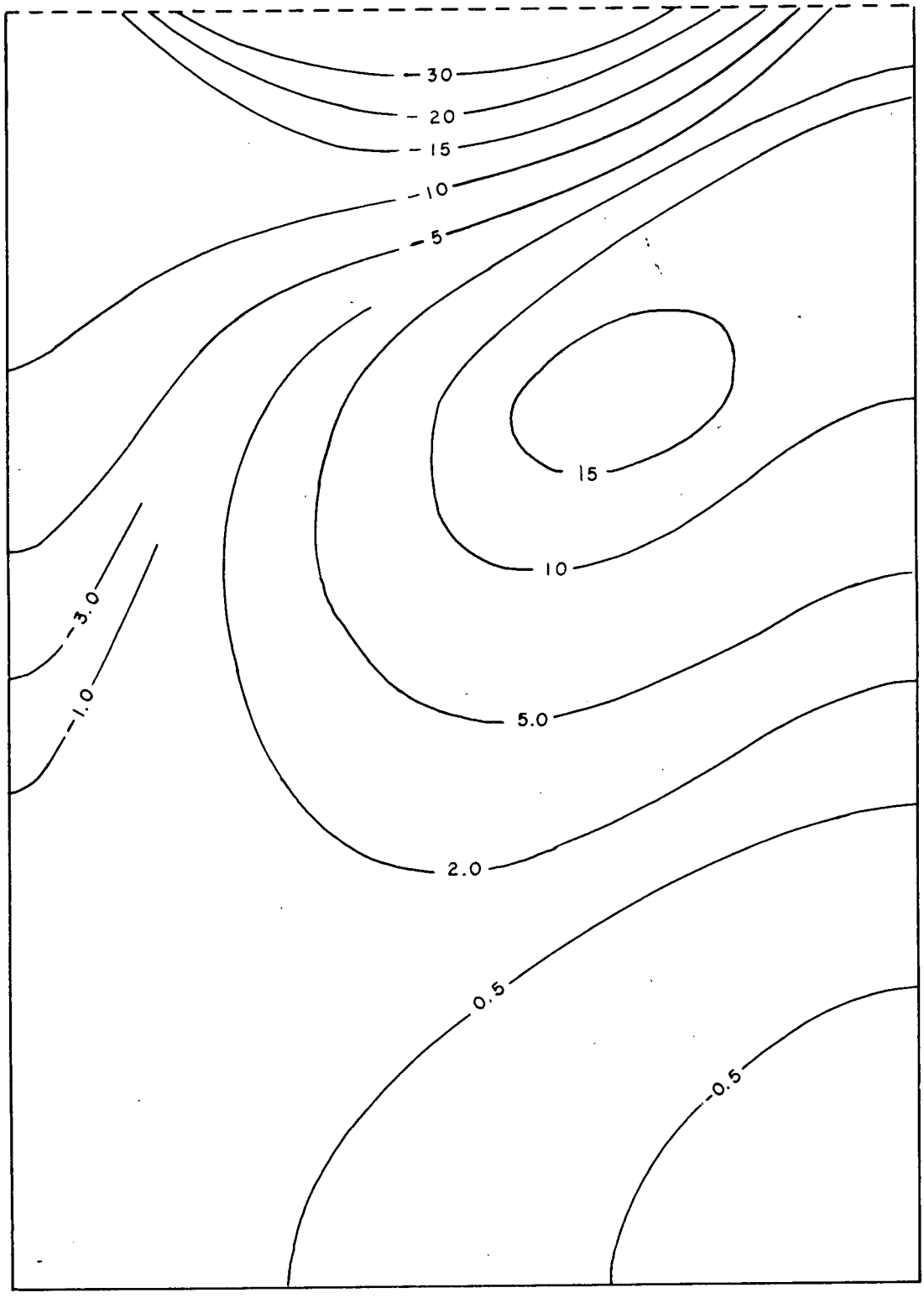


Mass field which satisfies a lateral salt balance

Figure 8.

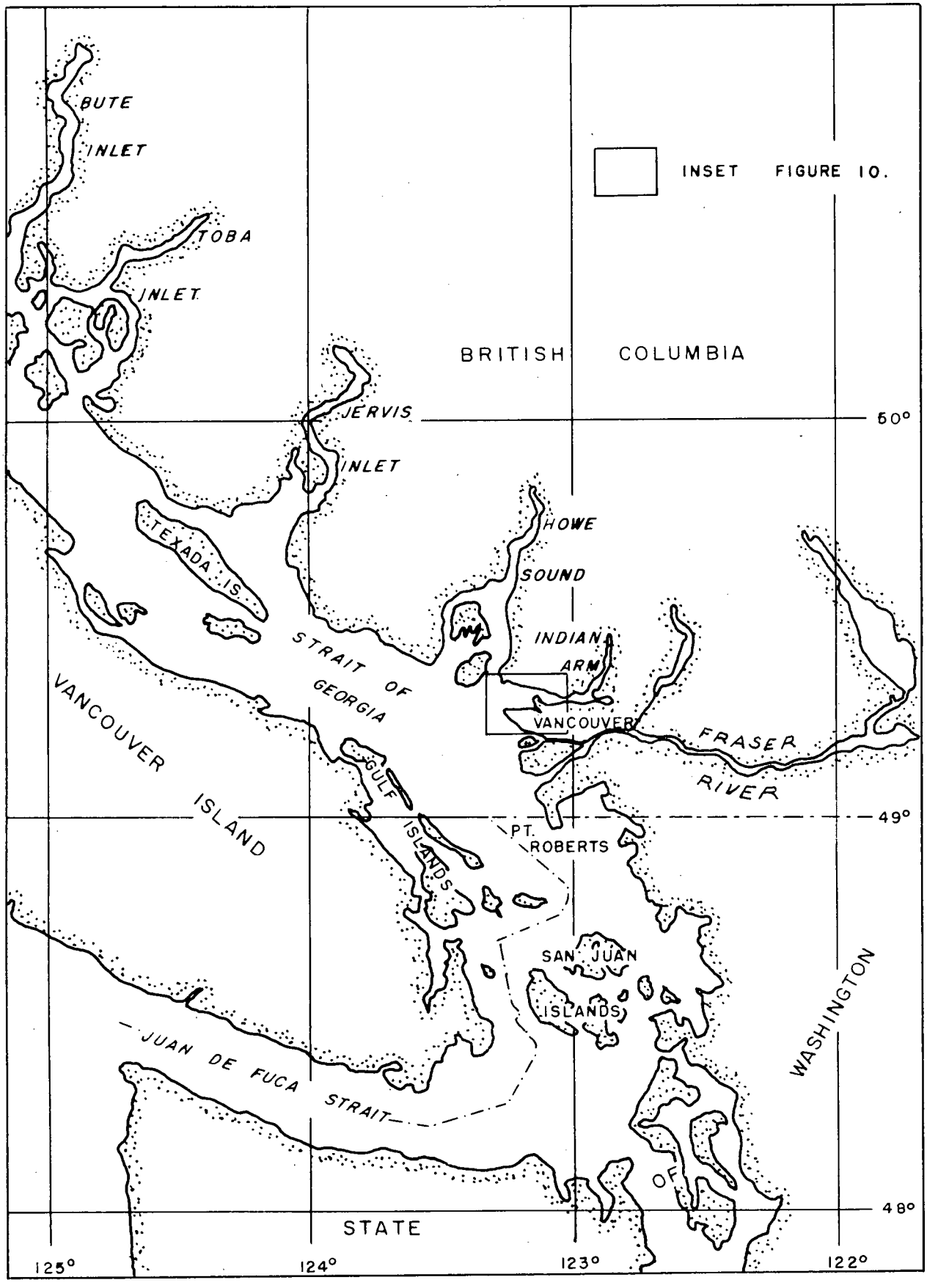


Lower Mainland of British Columbia

Figure 9.

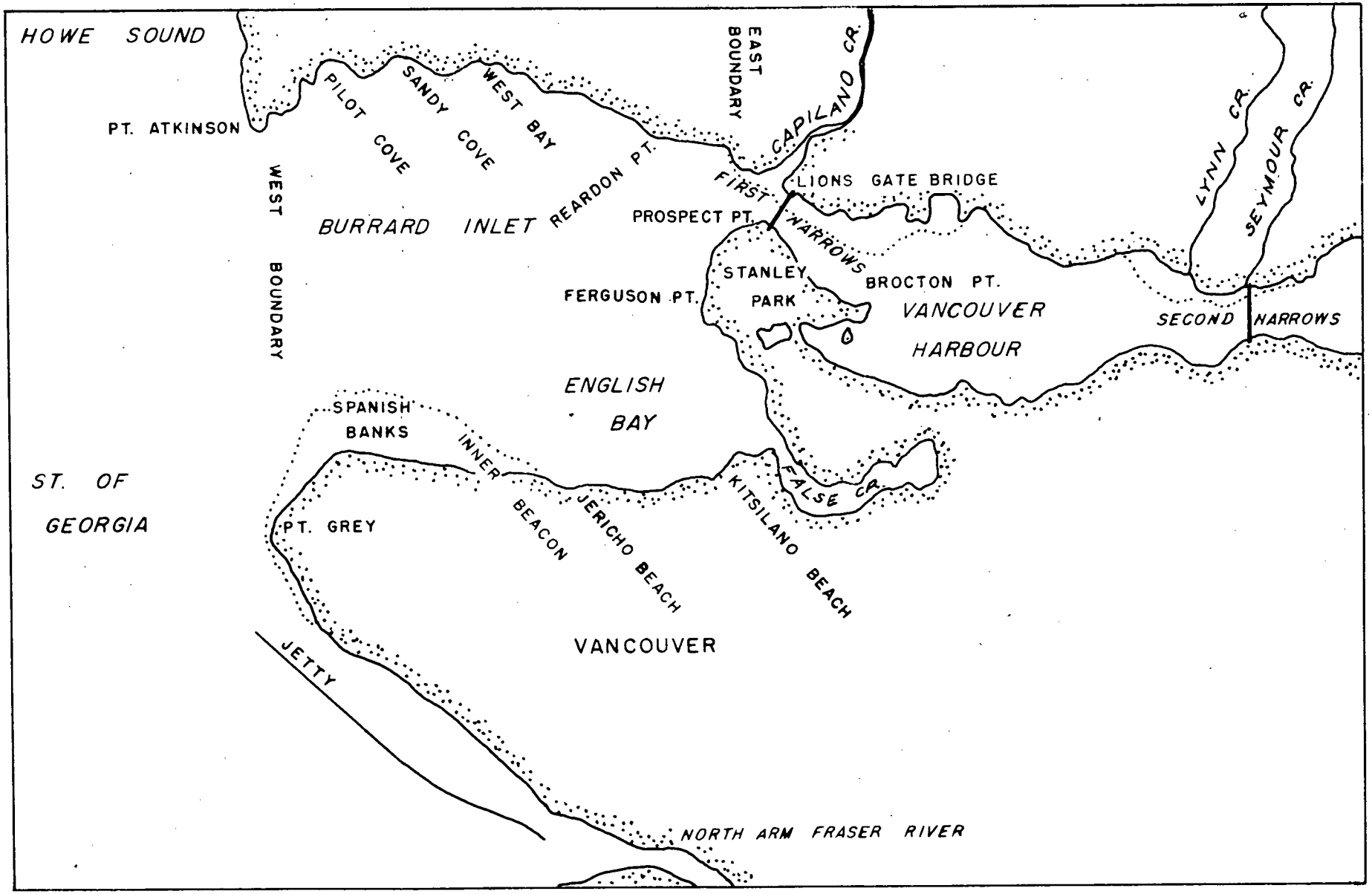


Figure 10. Burrard Inlet


Cloud of Fraser River water intruding
into Burrard Inlet

B.C. Government Photograph

Figure 11.

Cloud of Fraser River water
entering First Narrows

B.C. Government Photograph

Figure 12.


Clouds of muddy Fraser River
water in the Strait of Georgia

B.C. Government Photograph

Figure 13.

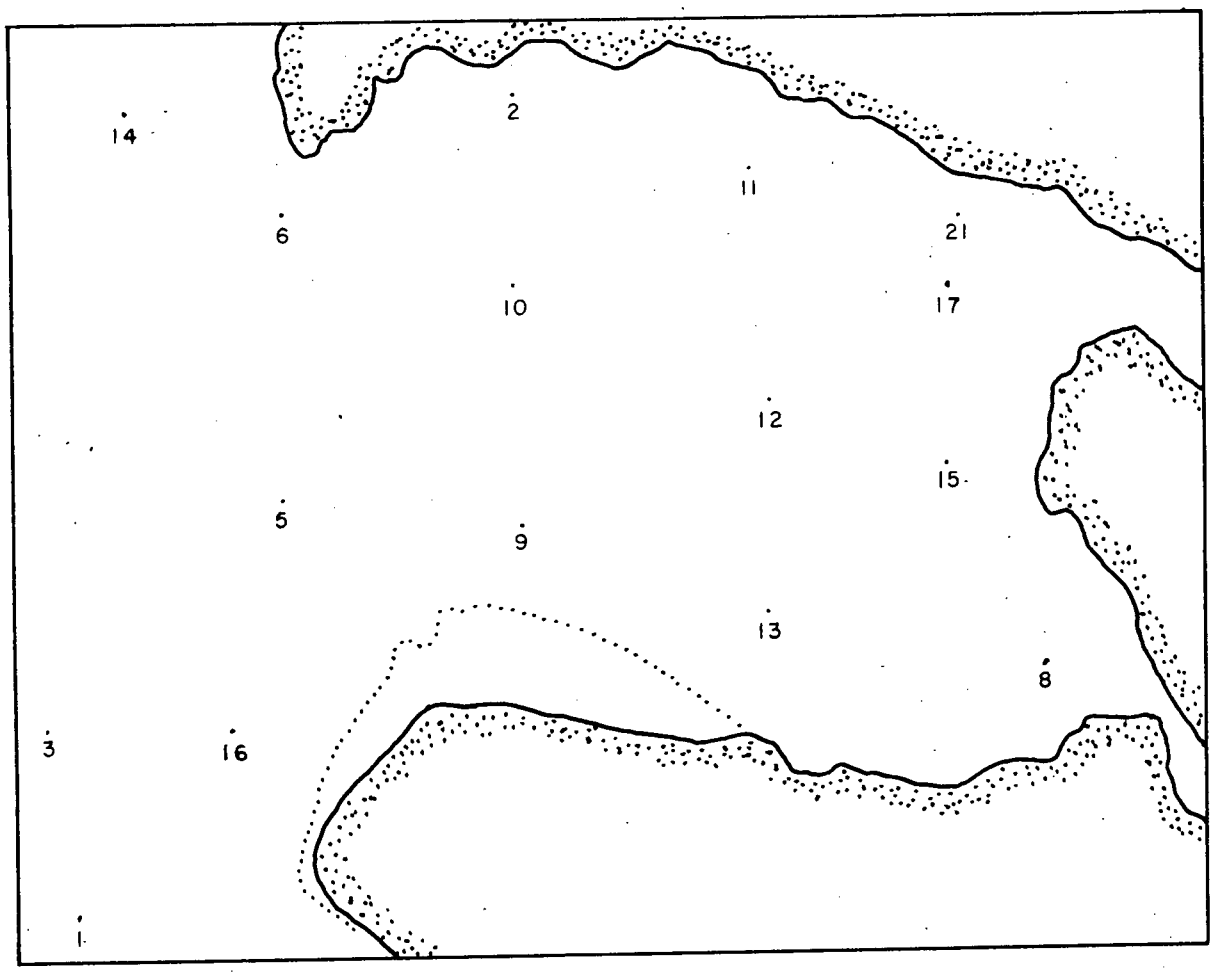


Current metering stations
Burrard Inlet

Figure 14.

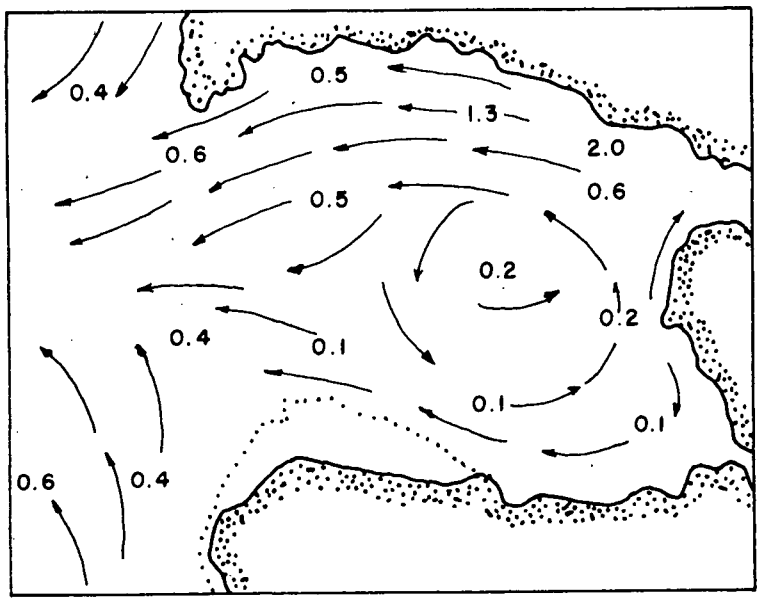


Current distribution
Large ebb
5 feet

Figure 15.

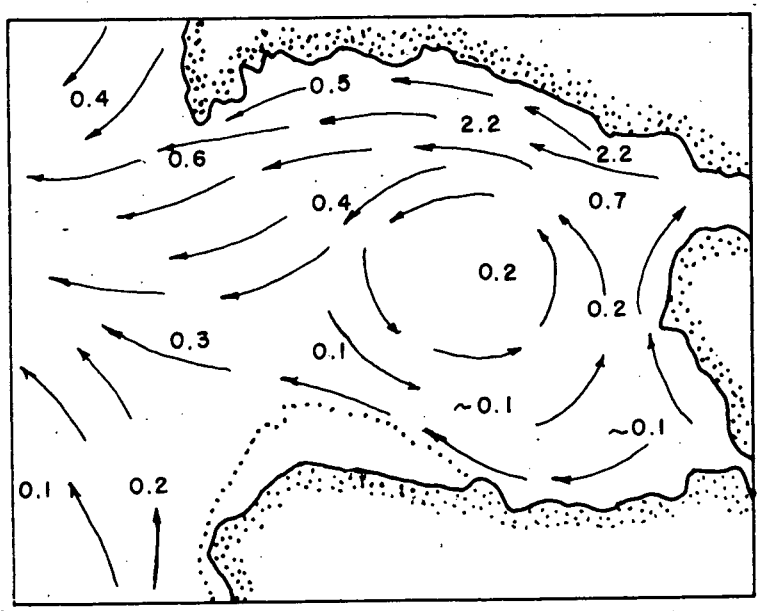


Current distribution
Large ebb
18 feet

Figure 16.

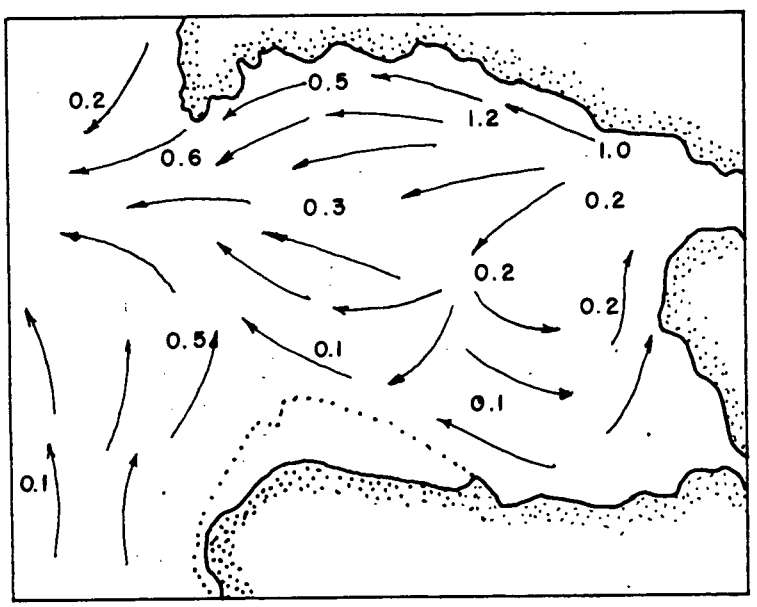


Current distribution
Large ebb
50 feet

Figure 17.

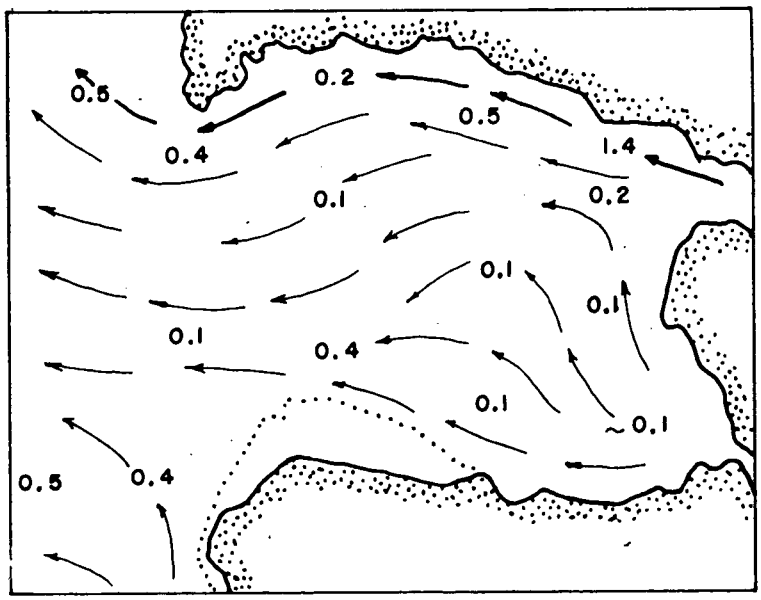


Current distribution
Small ebb
5 feet

Figure 18.

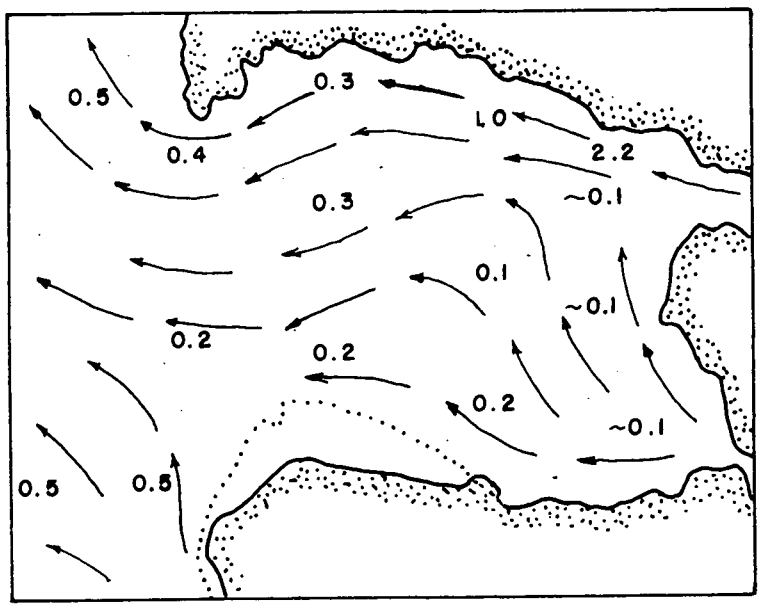


Current distribution
Small ebb
18 feet

Figure 19.

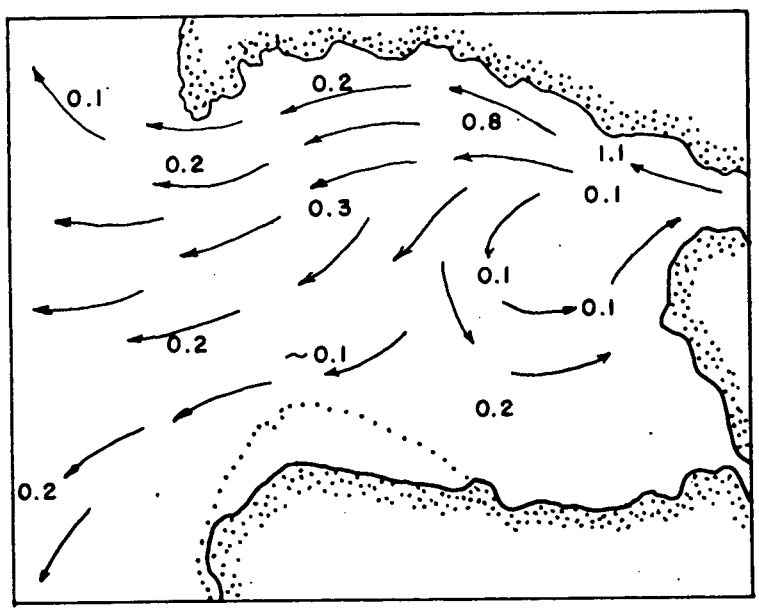


Current distribution
Small ebb
50 feet

Figure 20.

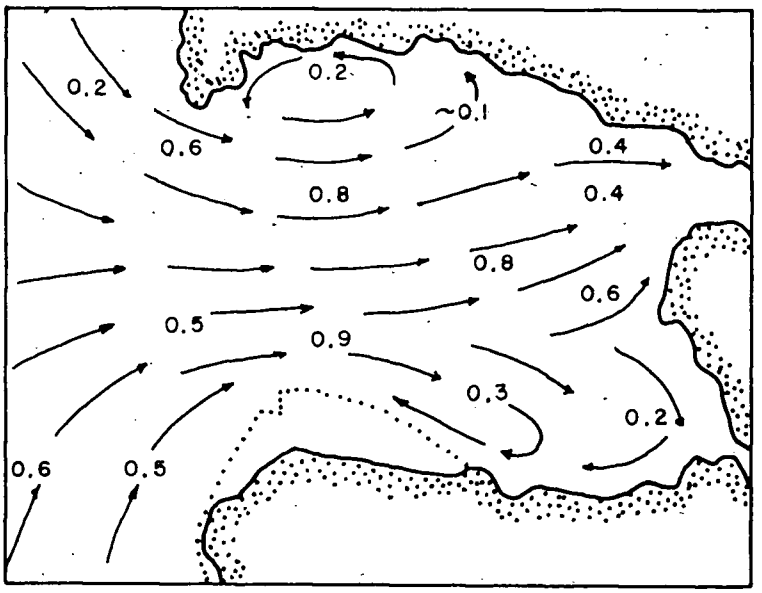


Current distribution
Large flood
5 feet

Figure 21.

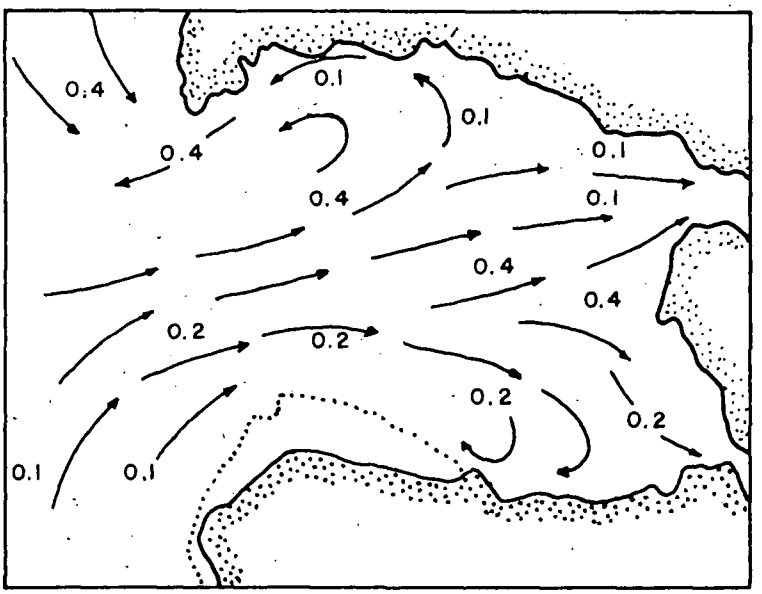


Current Distribution
Large flood
18 feet

Figure 22.

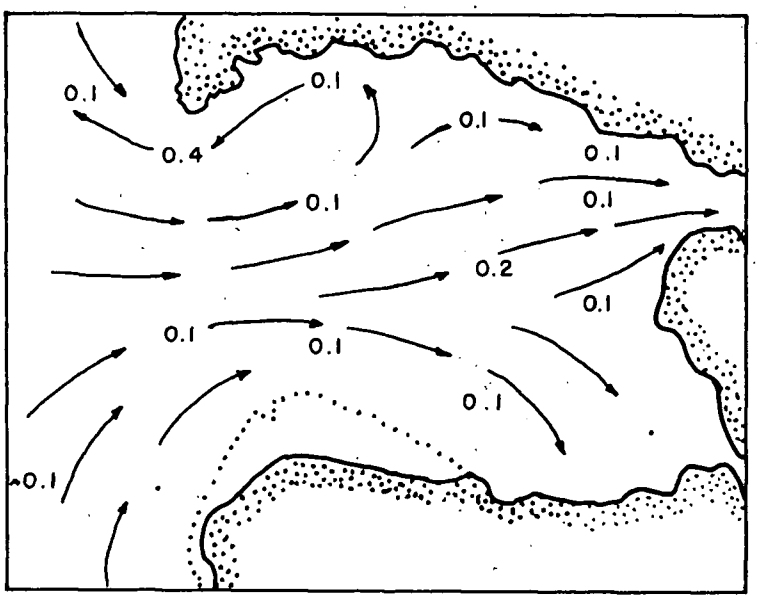


Current distribution
Large flood
50 feet

Figure 23.

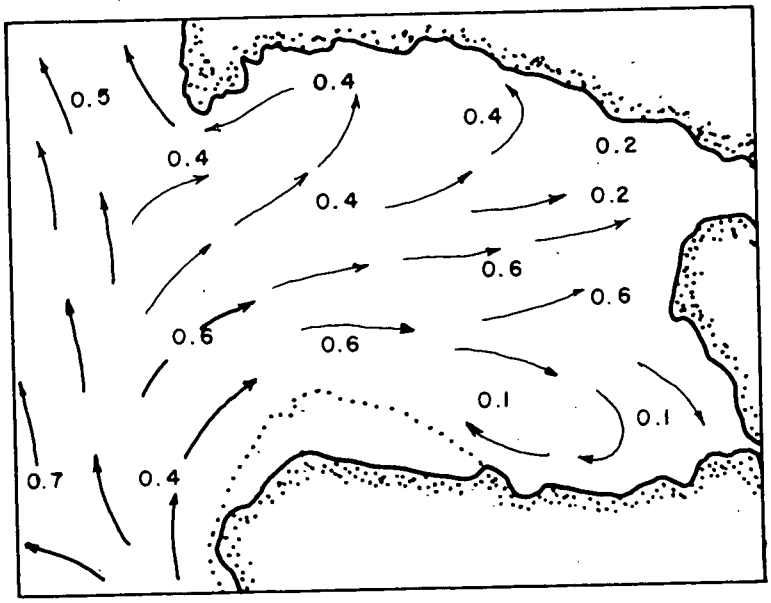


Current distribution
Small flood
5 feet

Figure 24.

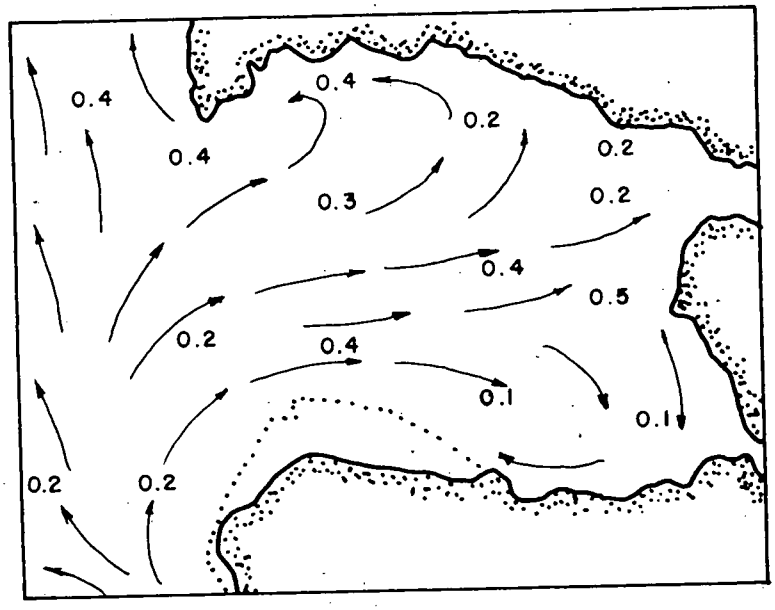


Current distribution
Small flood
18 feet

Figure 25.

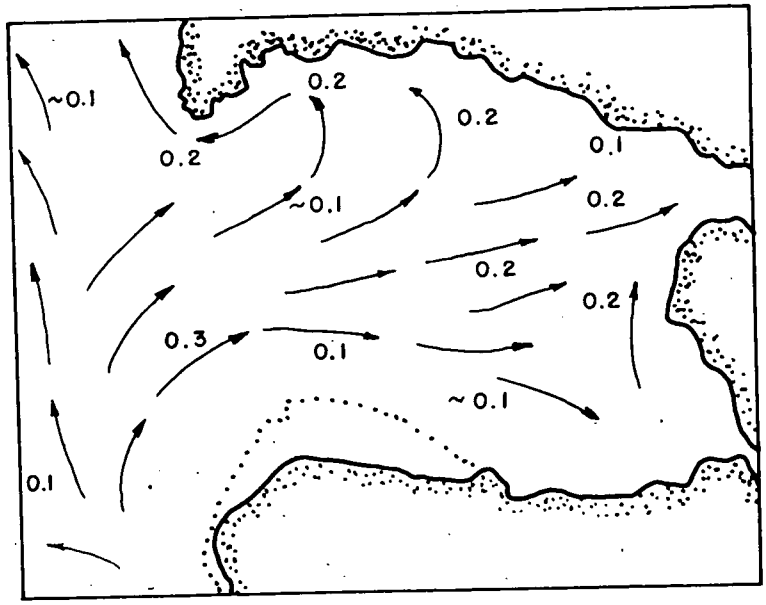


Current distribution
Small flood
50 feet

Figure 26.

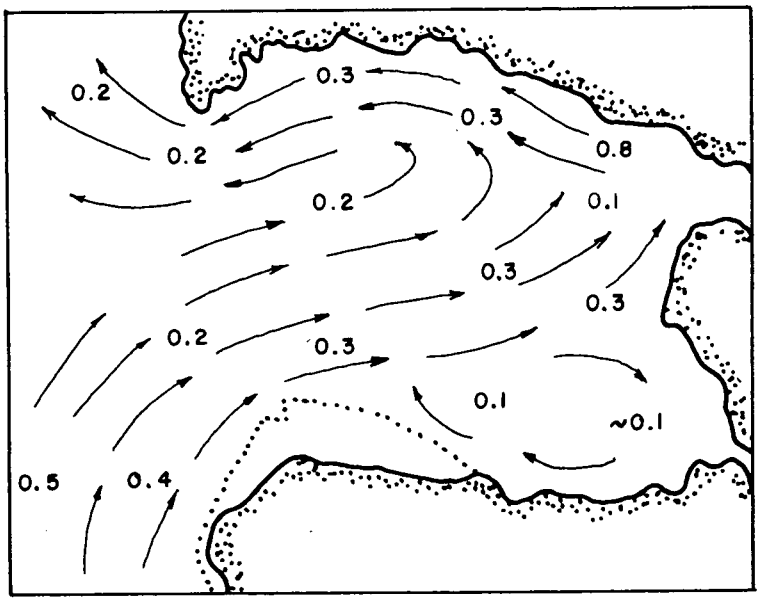


Net circulation
5 feet

Figure 27.

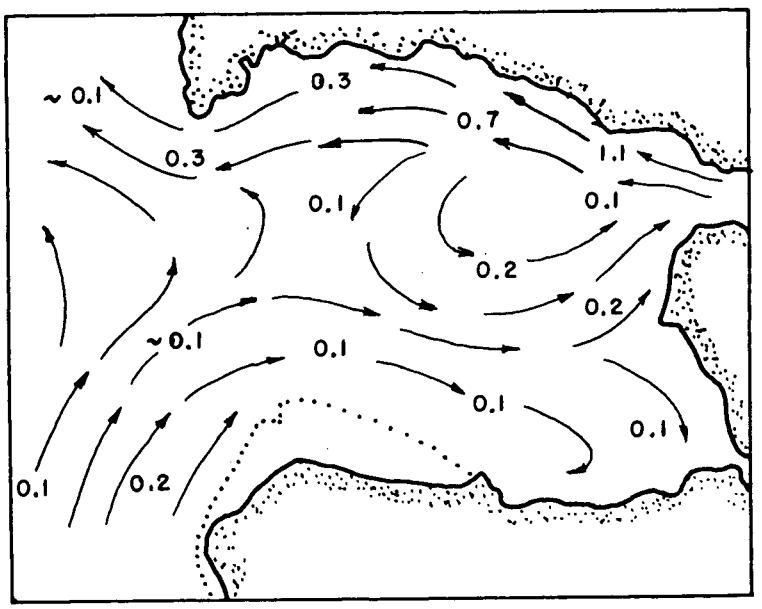


Net circulation
18 feet

Figure 28.

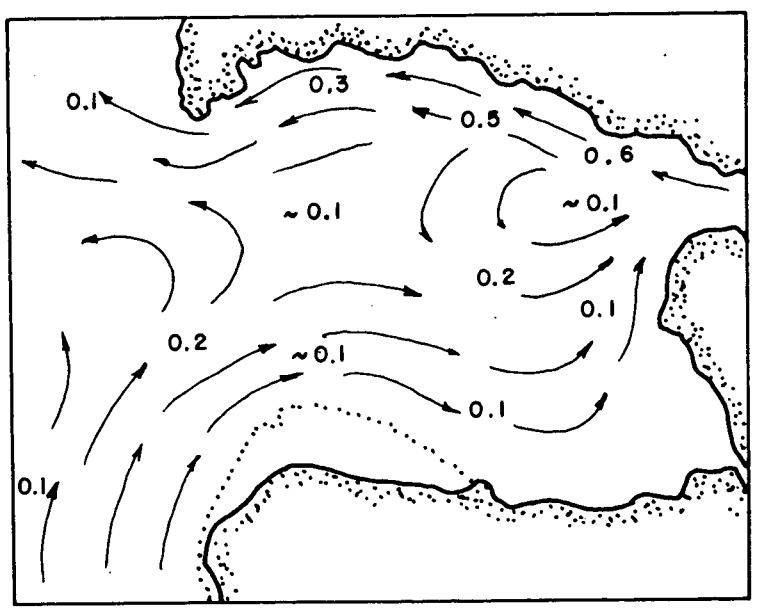


Net circulation
50 feet

Figure 29.

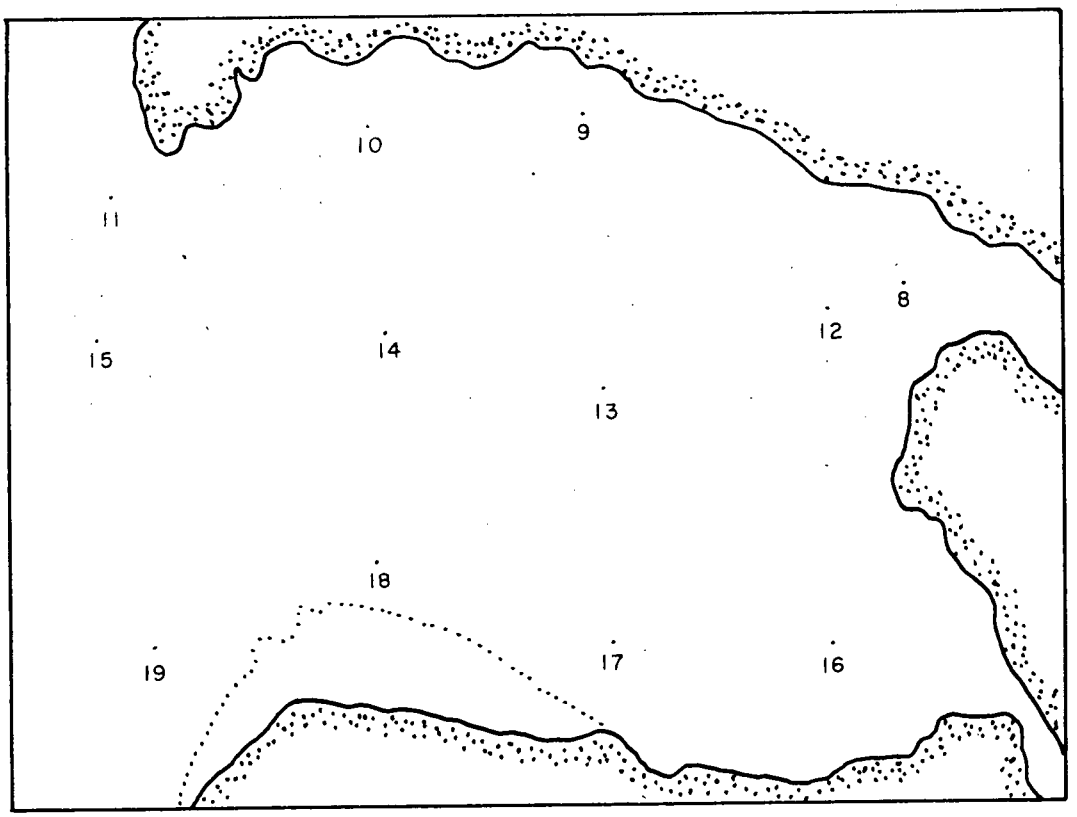


Figure 30. Oceanographic stations
Survey N. 28/ii/51

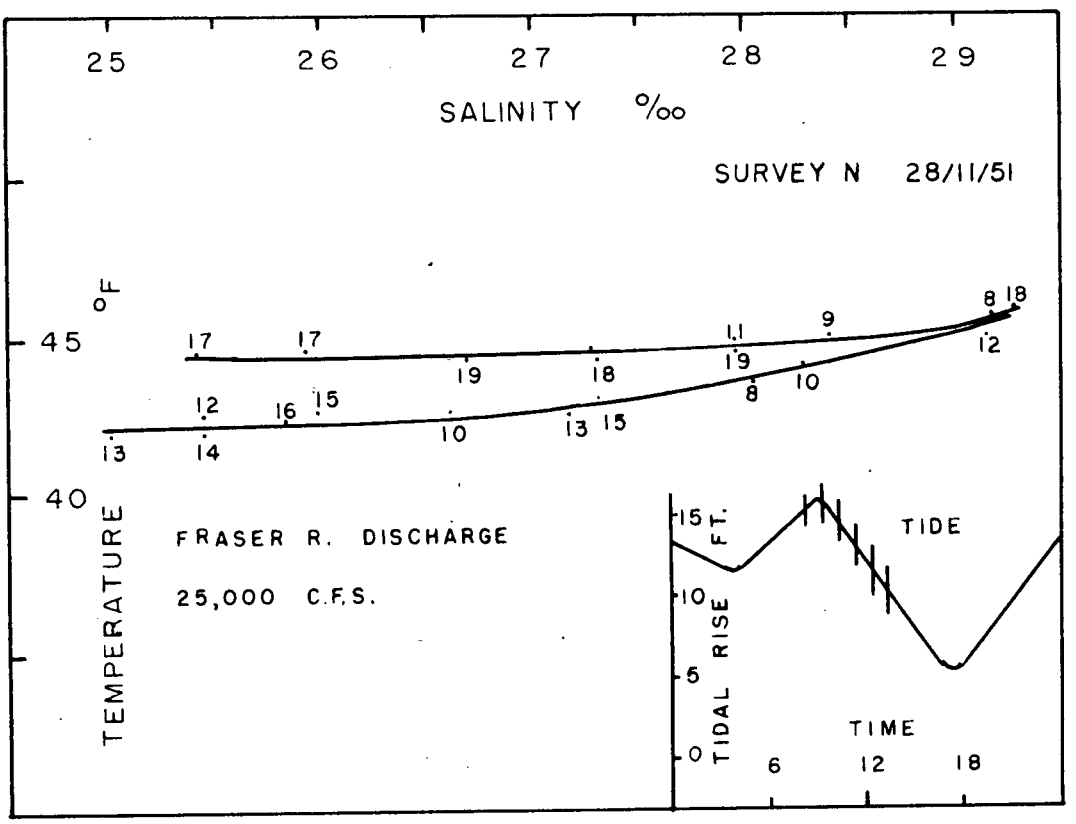


Figure 31. T-S relationships

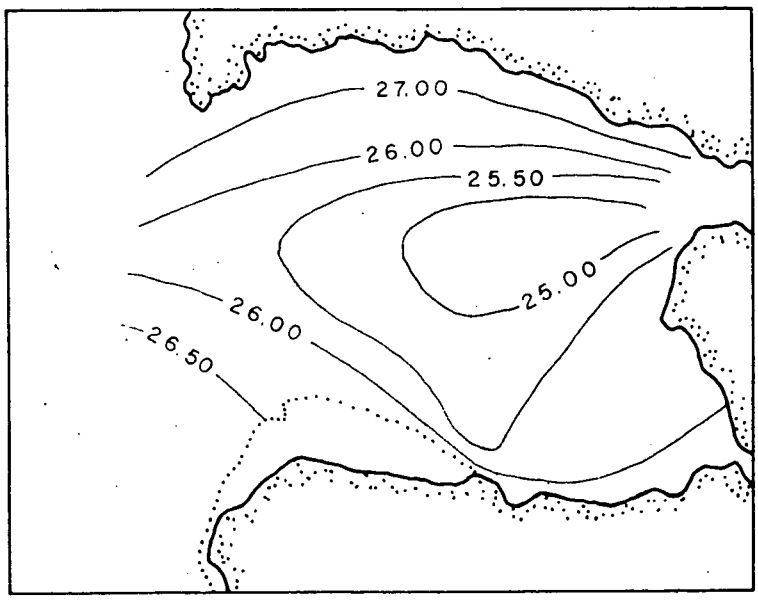


SURVEY N
28/ii/51

Salinity distribution

Surface

Figure 32a.

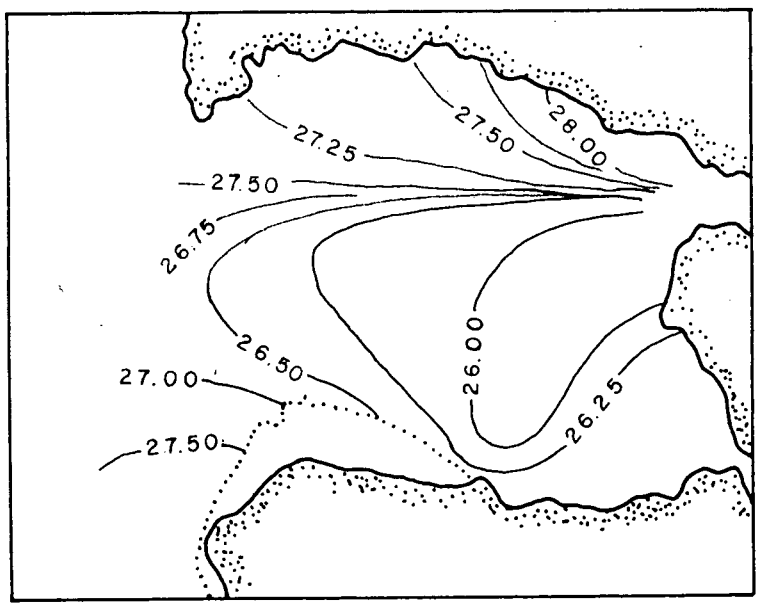


Salinity distribution

6 feet

Figure 32b.

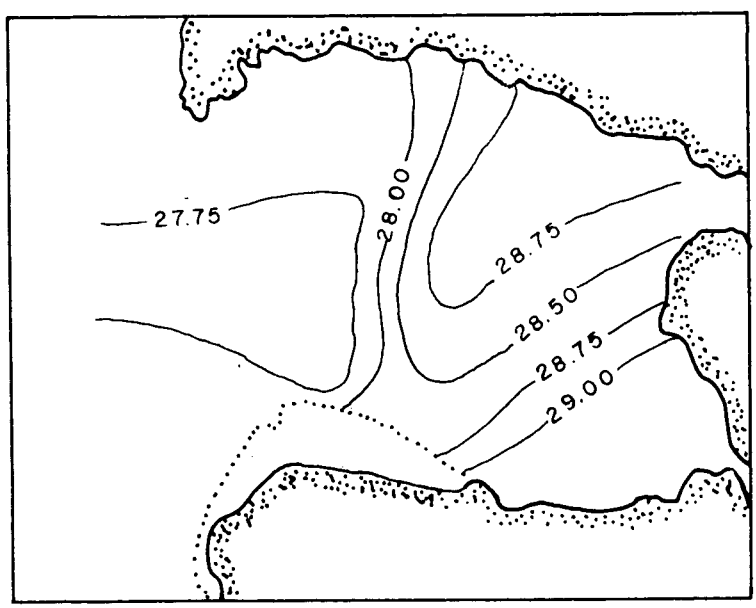


Salinity distribution

18 feet

Figure 32c.

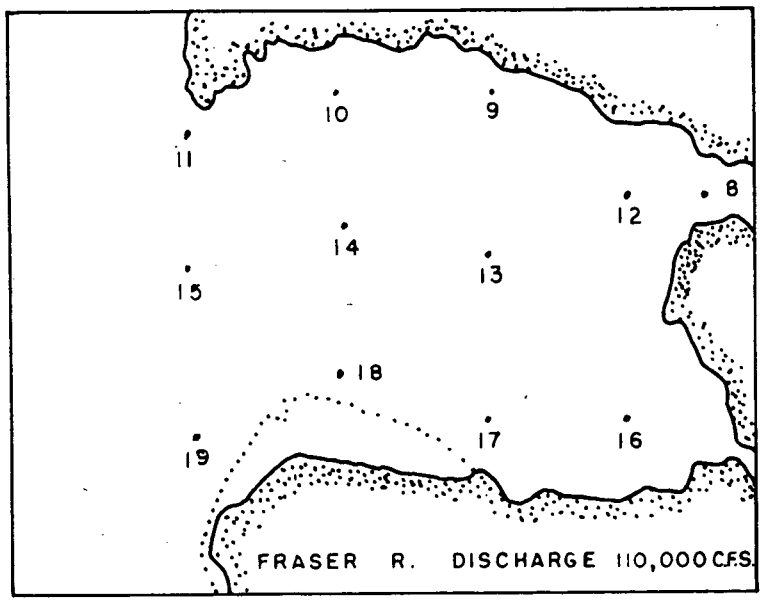


SURVEY K
20-27/vii/50

Oceanographic stations

Figure 33a.

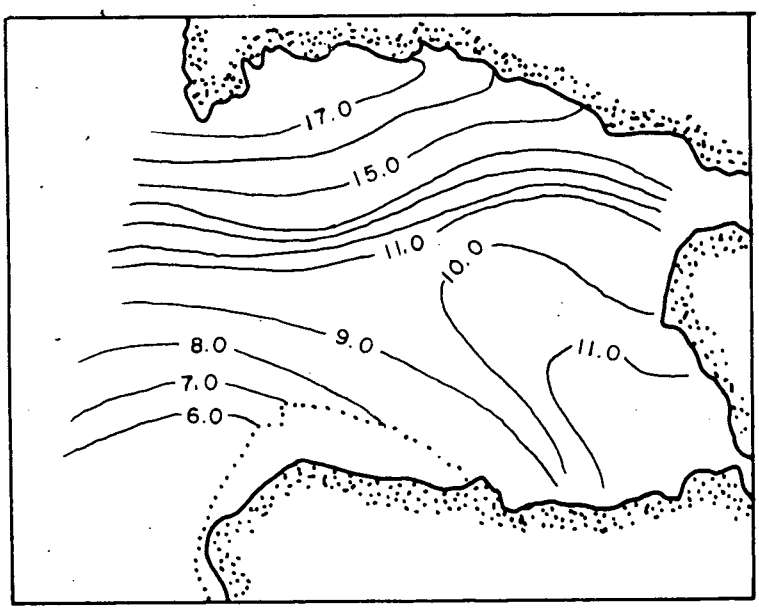


Salinity distribution
Surface

Figure 33b.

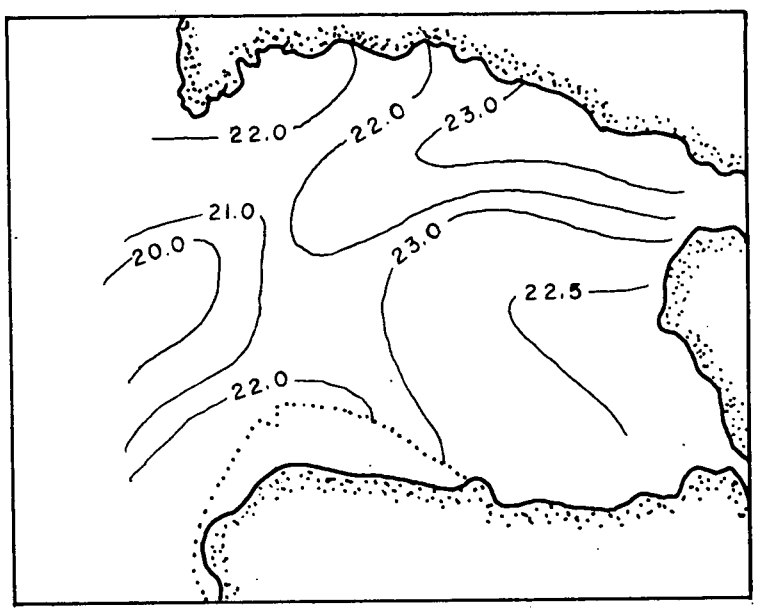


Salinity distribution
6 feet

Figure 33c.

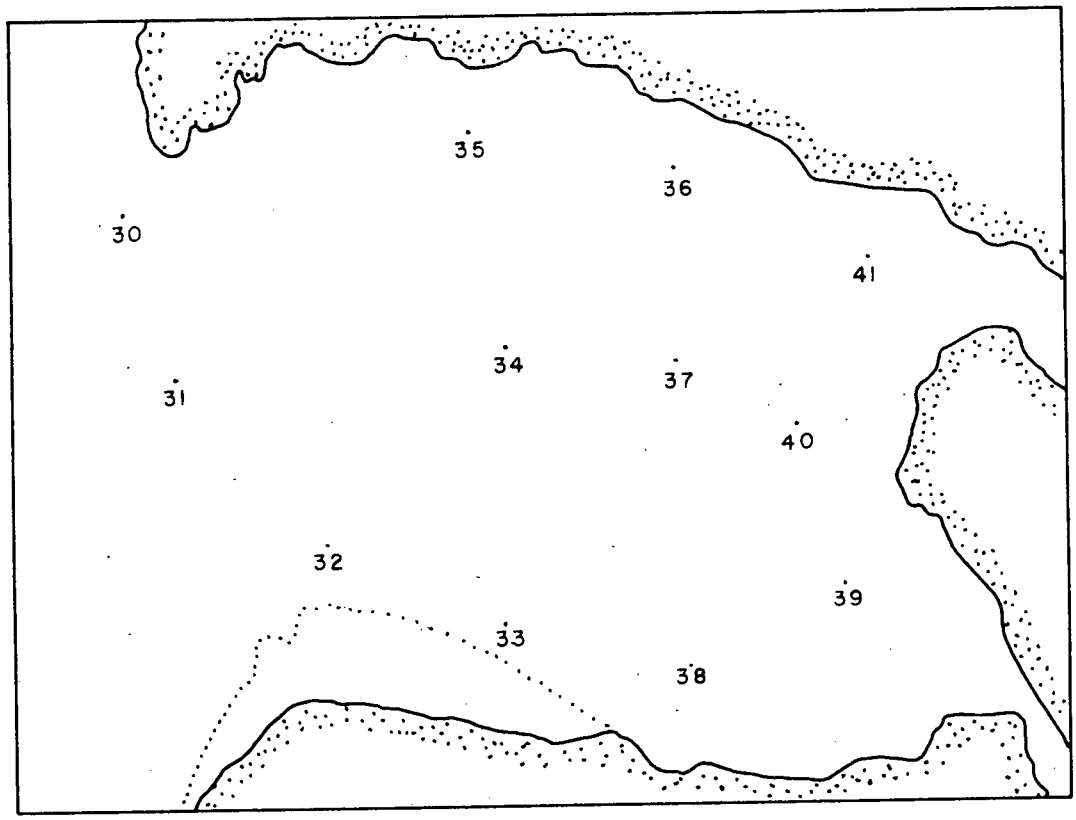


Figure 34. Oceanographic stations
Survey G. 31/v/50

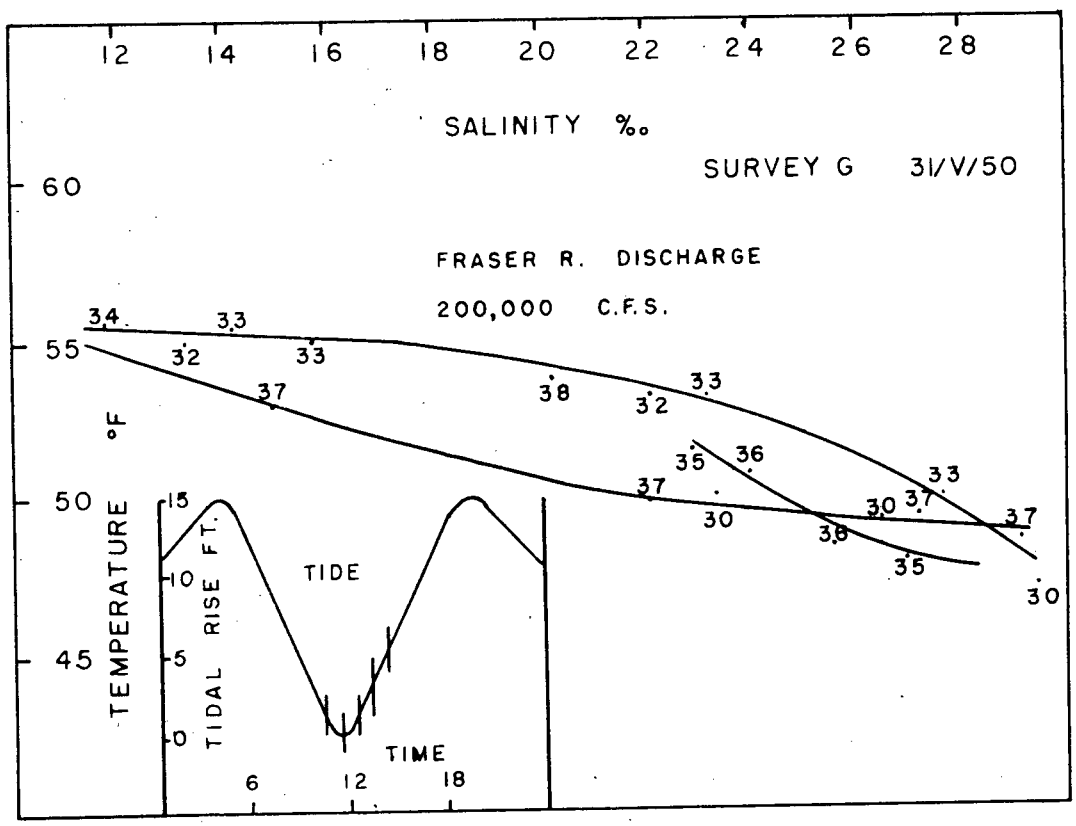


Figure 35. T-S relationships

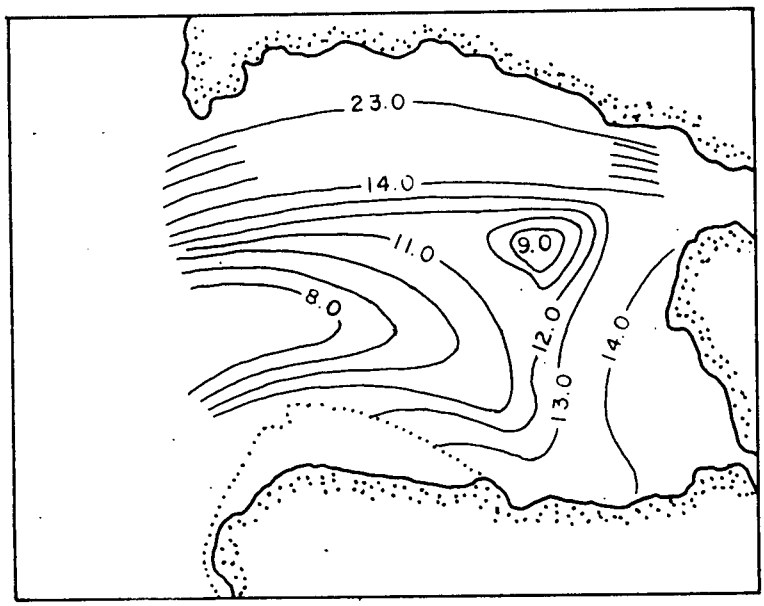


SURVEY G
31/v/50

Salinity distribution
Surface

Figure 36a.

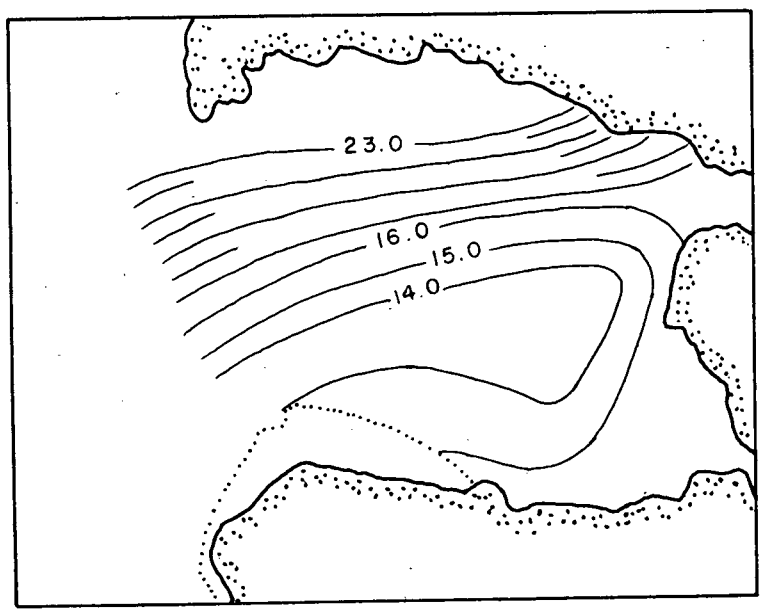


Salinity distribution
6 feet

Figure 36b.

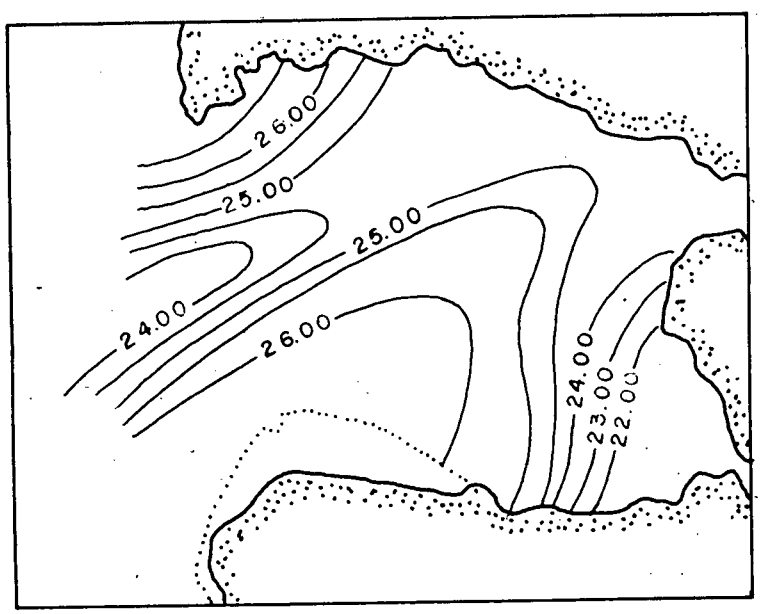


Salinity distribution
18 feet

Figure 36c.

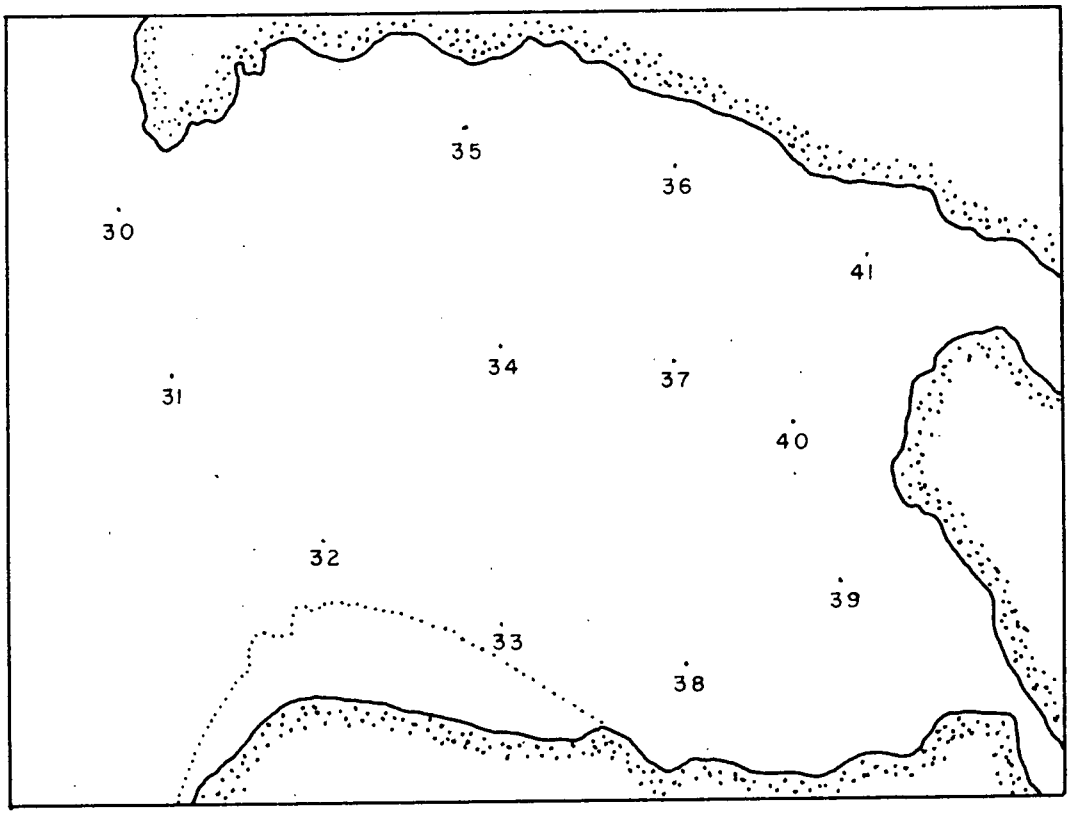


Figure 37. Oceanographic stations
Survey G. 1/vi/50

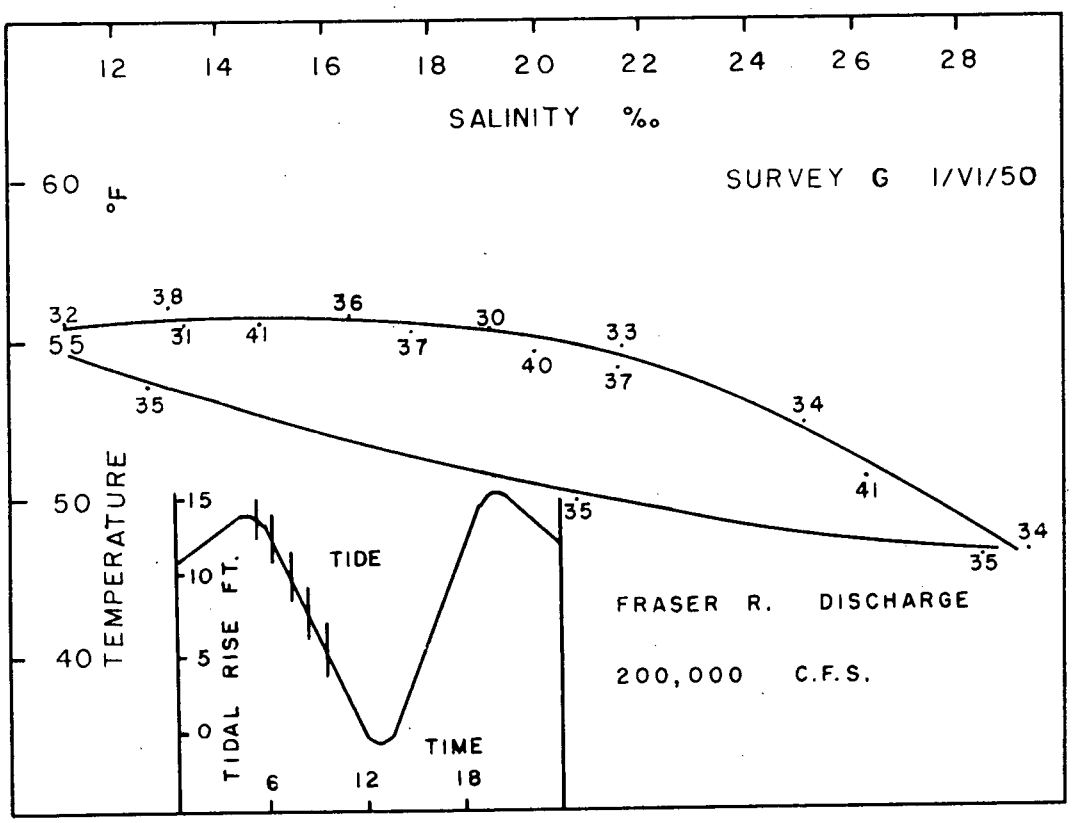


Figure 38. T-S relationships

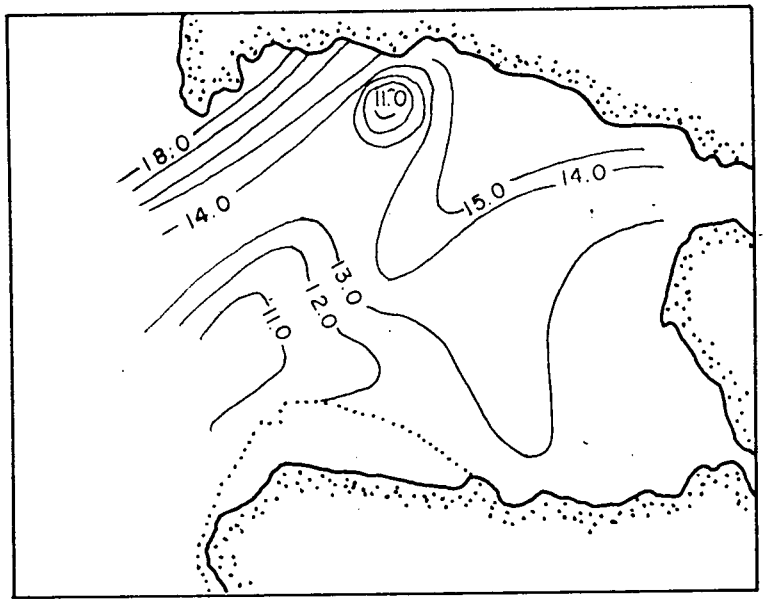


SURVEY G
1/vi/50

Salinity distribution
Surface

Figure 39a.

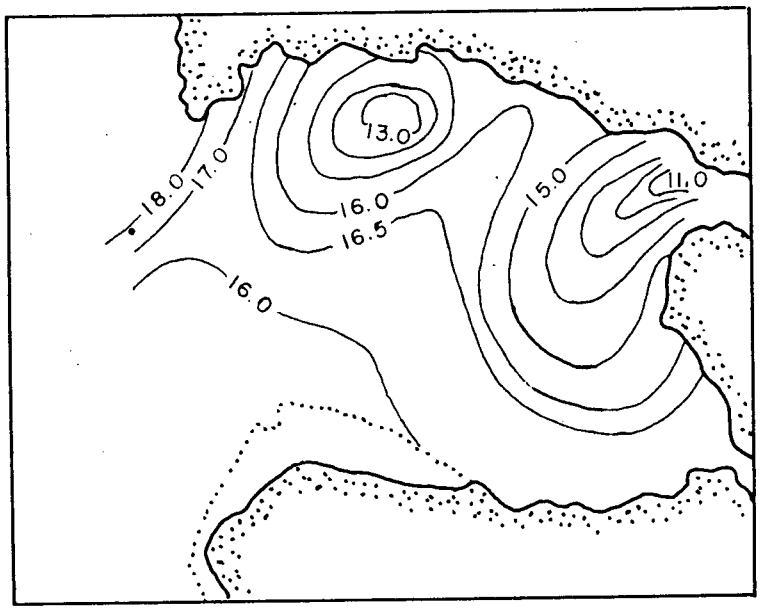


Salinity distribution
6 feet

Figure 39b.

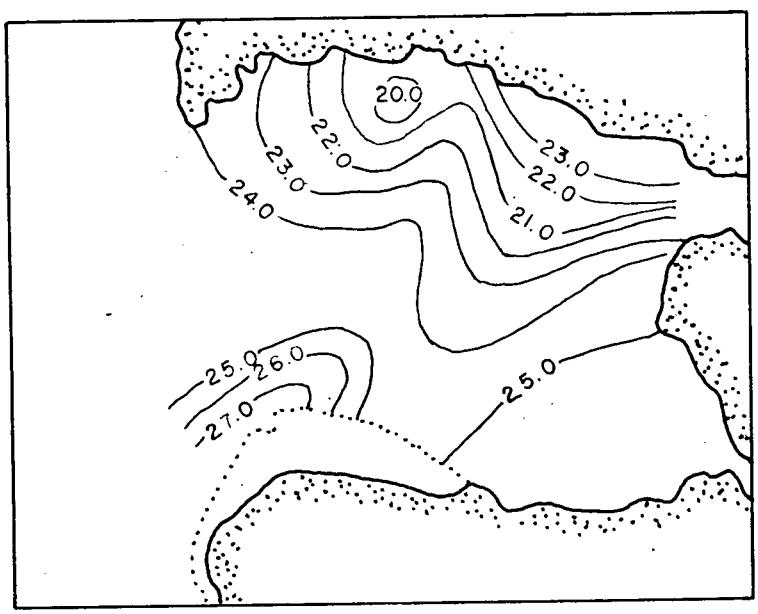


Salinity distribution
18 feet

Figure 39c.

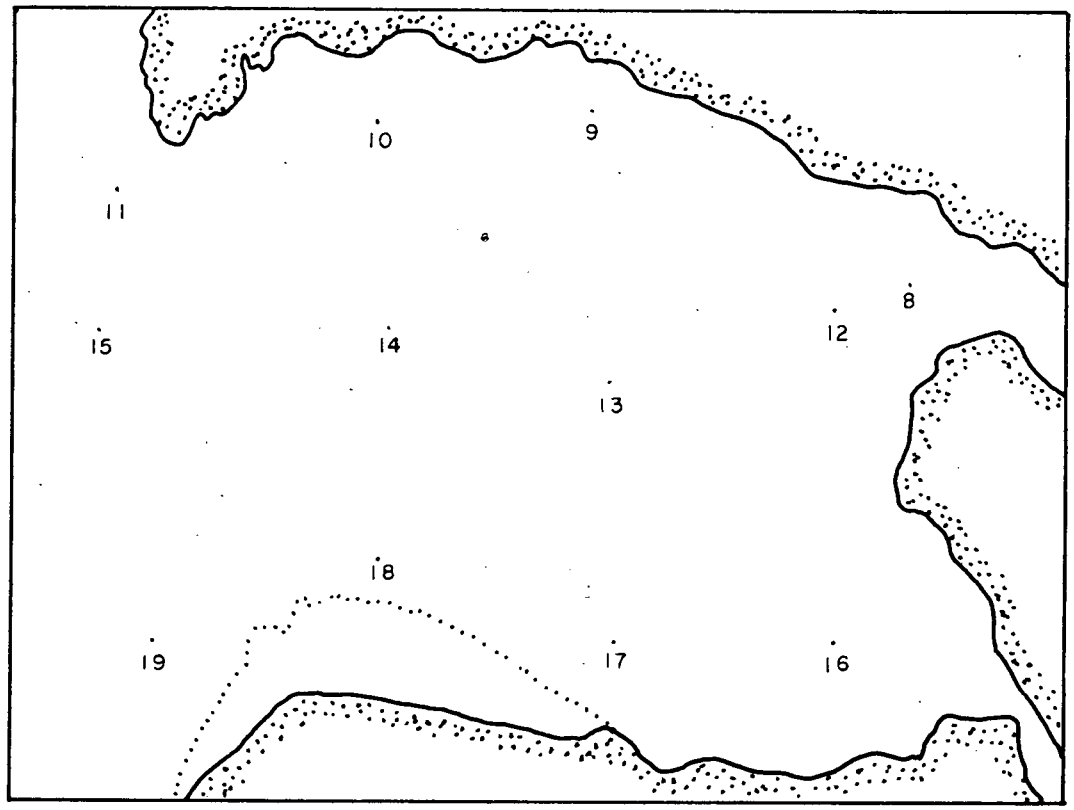


Figure 40. Oceanographic stations
Survey M. 27/ix/50

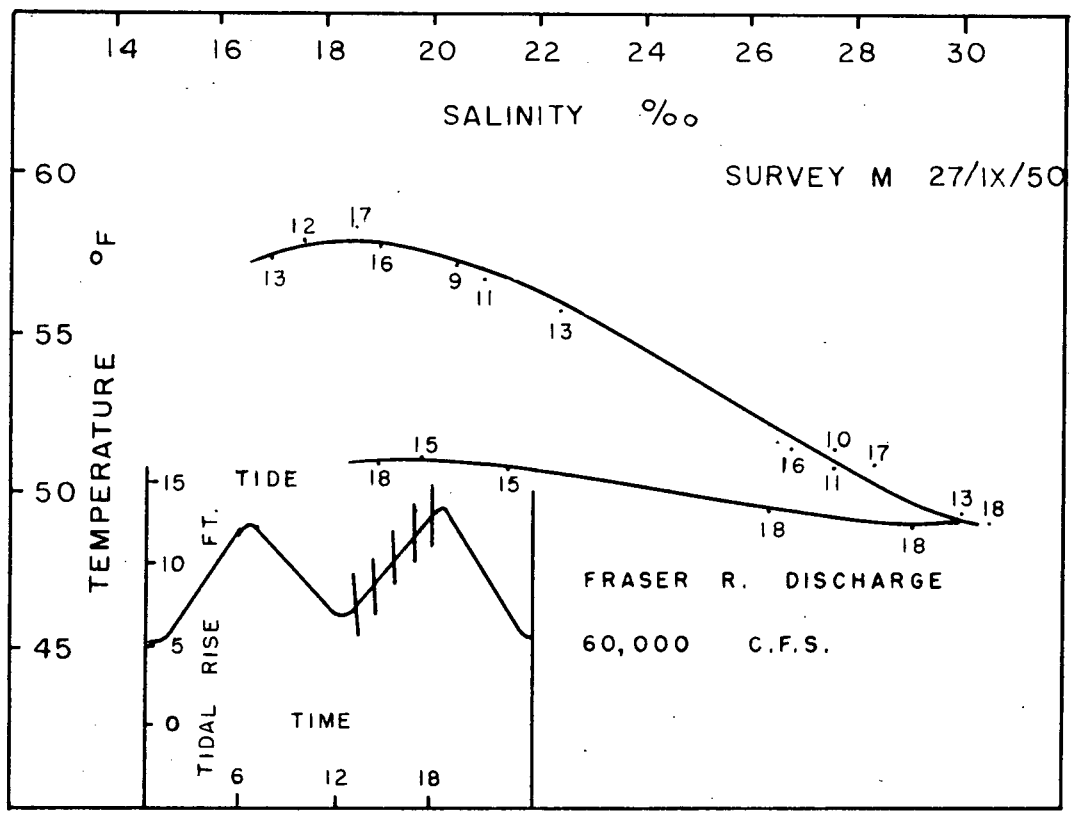


Figure 41. T-S relationships

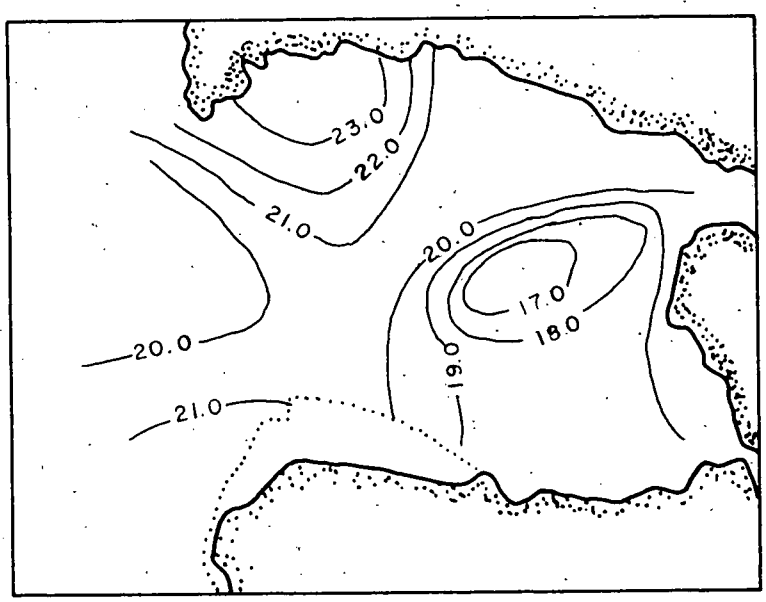


SURVEY M
27/ix/50

Salinity distribution
Surface

Figure 42a.

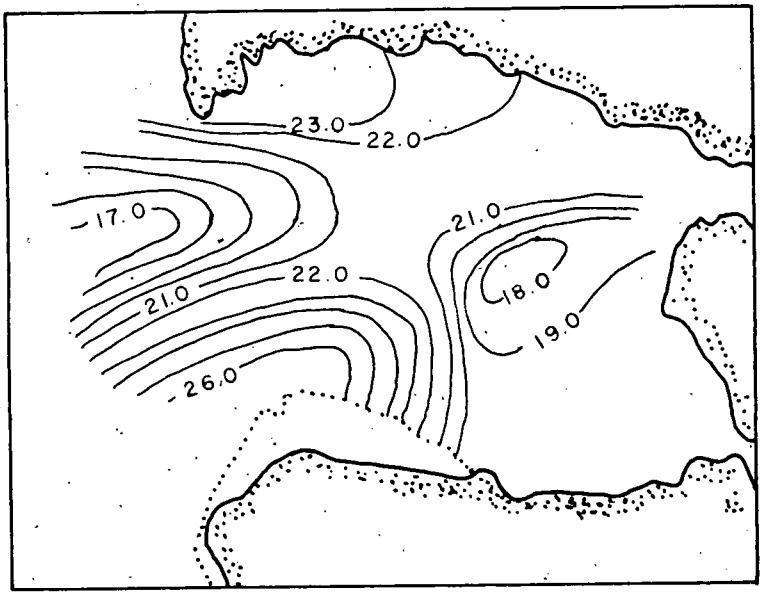


Salinity distribution
6 feet

Figure 42b.

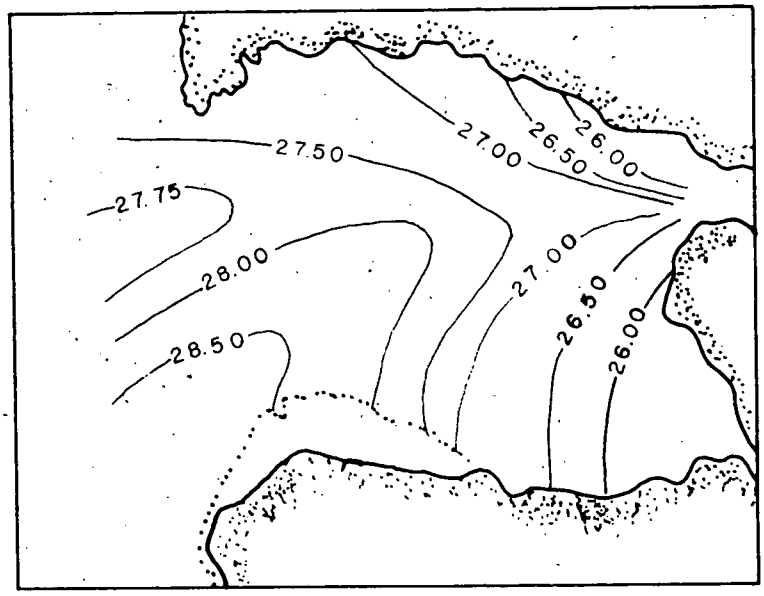


Salinity distribution
18 feet

Figure 42c.

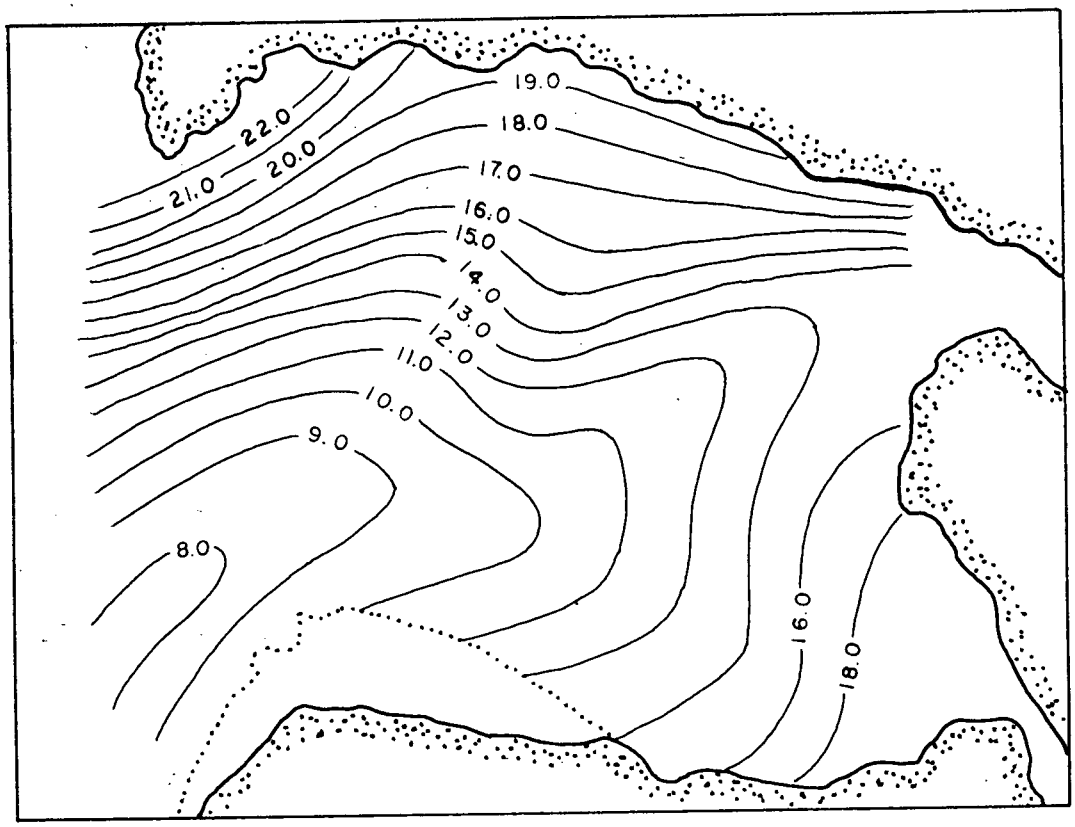


Mean salinity distribution

Burrard Inlet

Figure 43.

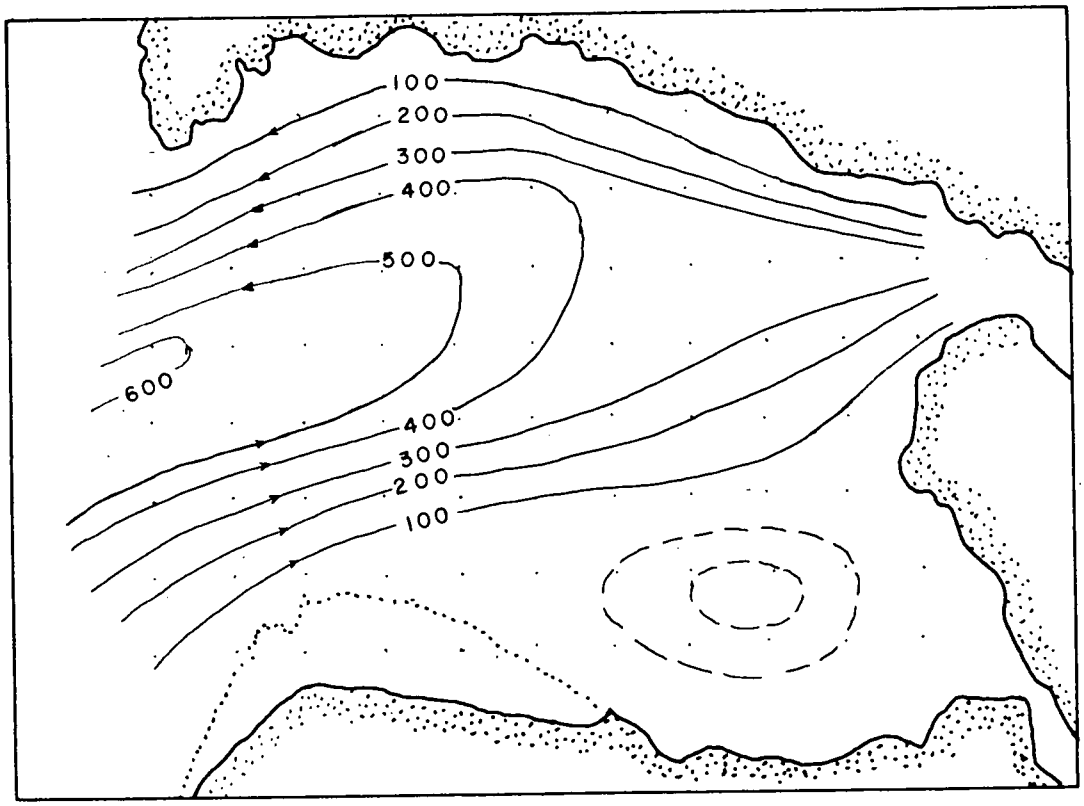


Figure 44. Scalar field of $\Psi$ calculated from the velocity field at 5 feet

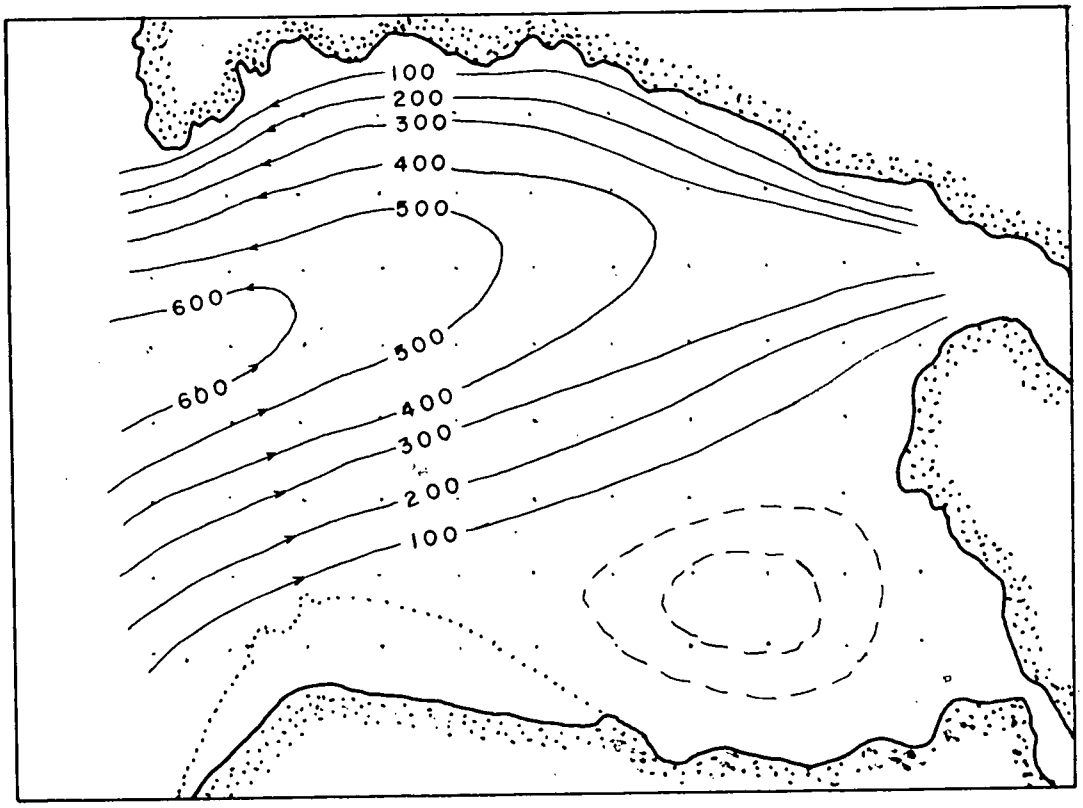


Figure 45. Relaxed scalar field of $\Psi$ , 5 feet, satisfying the differential equation

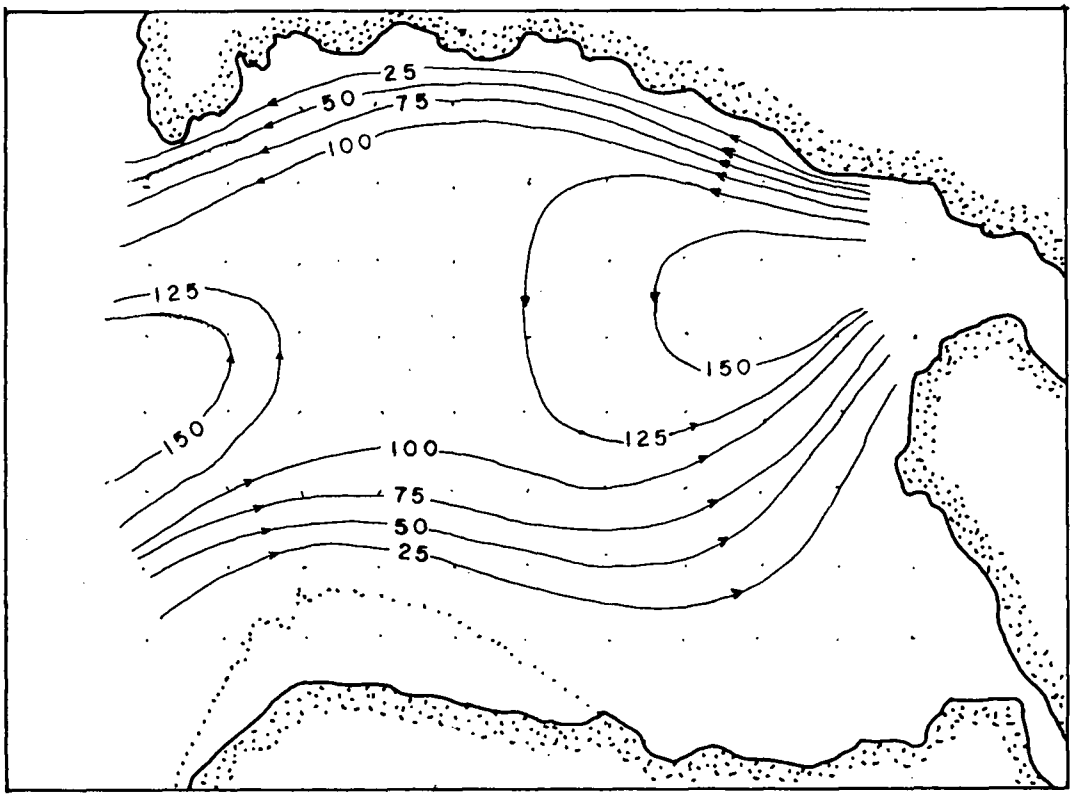


Figure 46. Scalar field of $\Psi$ calculated from the velocity field at 50 feet

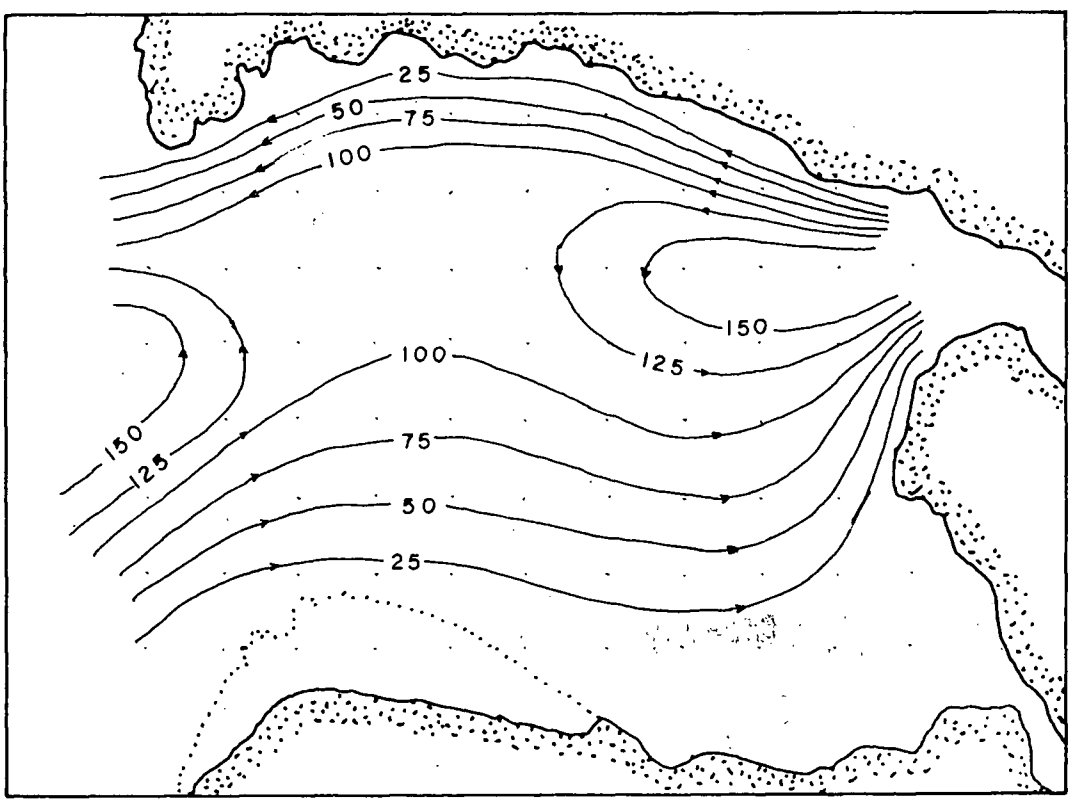


Figure 47. Relaxed scalar field of $\Psi$ satisfying the differential equation at 50 feet

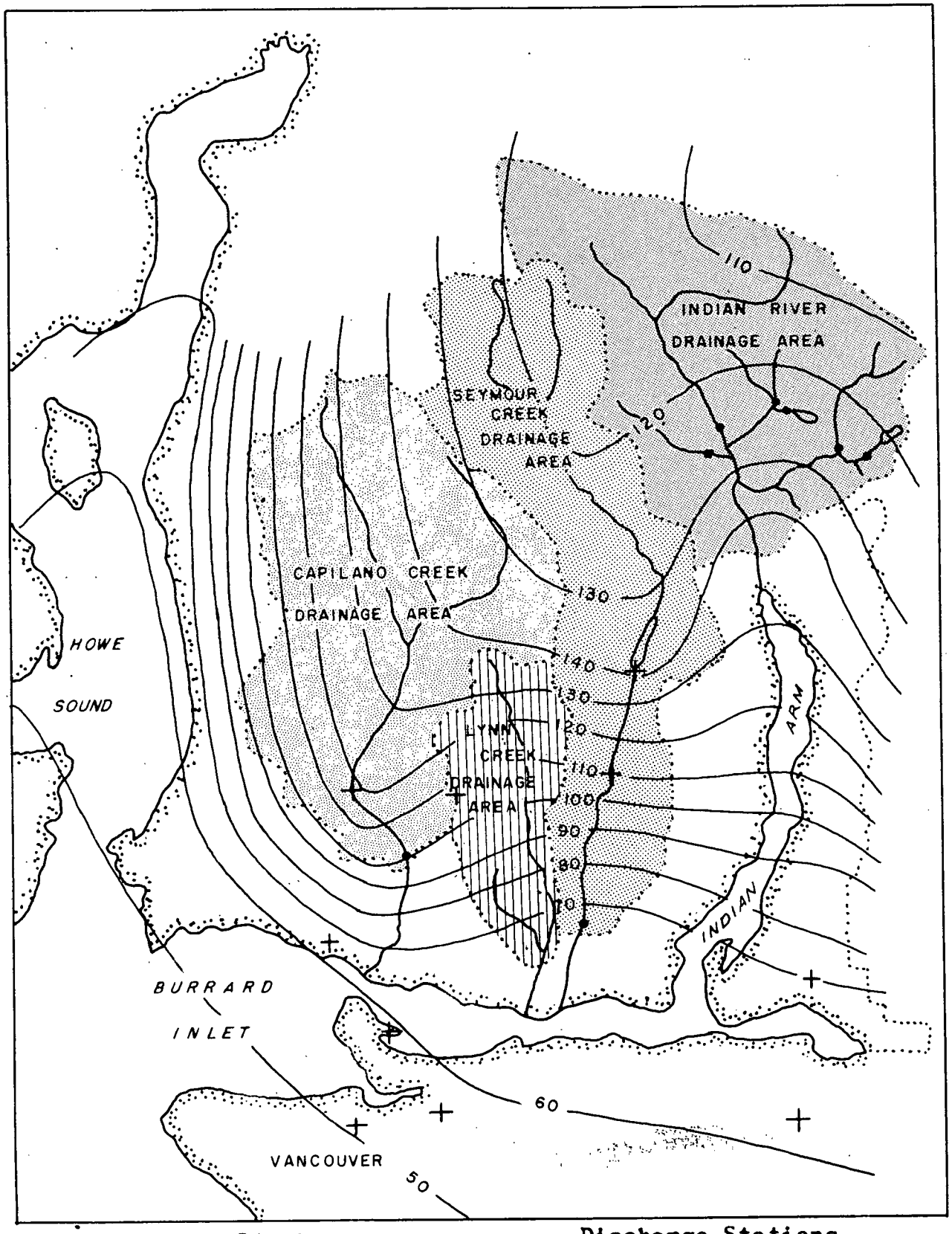


+ Rainfall Stations • Discharge Stations

Average yearly rainfall distribution (inches)
Howe Sound, Burrard Inlet

Figure 48.